

GEORGIA DOT RESEARCH PROJECT 17-14

Final Report

**PRODUCTIVE RE-USE OF SAVANNAH RIVER  
DREDGE MATERIAL**



**OFFICE OF PERFORMANCE-BASED  
MANAGEMENT AND RESEARCH**

**600 WEST PEACHTREE NW  
ATLANTA, GA, 30308**

TECHNICAL REPORT DOCUMENTATION PAGE

1. Report No.: FHWA-GA-20-1714		2. Government Accession No.: N/A		3. Recipient's Catalog No.: N/A	
4. Title and Subtitle: Productive Re-Use of Savannah River Dredge Material			5. Report Date: SEPTEMBER 2020		
			6. Performing Organization Code: N/A		
7. Author(s): Kimberly E. Kurtis ( <a href="https://orcid.org/0000-0002-1252-7323">https://orcid.org/0000-0002-1252-7323</a> ), Susan E. Burns ( <a href="https://orcid.org/0000-0002-3029-7314">https://orcid.org/0000-0002-3029-7314</a> ), Daniel Benkeser, and Hejintao Huang			8. Performing Organ. Report No.: 17-14		
9. Performing Organization Name and Address: Georgia Institute of Technology School of Civil and Environmental Engineering 790 Atlantic Drive NW Atlanta, GA, 30332 (404) 385-0825 <a href="mailto:kkurtis@gatech.edu">kkurtis@gatech.edu</a>			10. Work Unit No.: N/A		
			11. Contract or Grant No.: PI #0000185399		
12. Sponsoring Agency Name and Address: Georgia Department of Transportation Office of Performance-based Management and Research 600 W. Peachtree NW Atlanta, GA, 30308			13. Type of Report and Period Covered: Final; August 2017 - September 2020		
			14. Sponsoring Agency Code: N/A		
15. Supplementary Notes: Prepared in cooperation with the U.S Department of Transportation and Federal Highway Administration					
16. Abstract: <p>Approximately 6 million m<sup>3</sup> of river sediment is dredged from the Savannah River annually in order to keep the river navigable. While this material is currently being stored in facilities located riverside, the long-term viability of these facilities is in question due to changes in planned land use. As an alternative to storing or relocating these materials, investigations were made into the beneficial use of these materials in geotechnical or structural applications. The possible beneficial uses include:</p> <ol style="list-style-type: none"> <li>1. Utilization as a structural/non-structural fill</li> <li>2. Fine aggregates source for concrete mixes</li> <li>3. Lightweight aggregate production for use in concrete mixes</li> <li>4. Production of supplementary cementitious materials</li> <li>5. Ingredient in cement feedstock</li> </ol> <p>This investigation was conducted by comparing these sediments to pre-existing ASTM standards, proof of concept production, or through a comprehensive literature review. It was found that this sediment could be utilized in each of these situations depending on its physical and chemical characteristics. Further economic and life cycle analyses were performed to weigh reuse options. Based on this analysis, from a technical standpoint, all of the sediment stored can be utilized in one of the investigated applications. Due to the broad scope of the current investigation, further study is needed in order to assess and improve the quality in some of these final products.</p>					
17. Key Words: River Dredge, Aggregate, SCM, R <sup>3</sup> Method, Structural Fill			18. Distribution Statement: No Restriction		
19. Security Class (this report): Unclassified		20. Security Class (this page): Unclassified		21. Number of Pages: 158	22. Price: Free

GDOT Research Project No. 17-14

Final Report

PRODUCTIVE RE-USE OF SAVANNAH RIVER DREDGE MATERIAL

By

Kimberly E. Kurtis, Ph.D., P.E

Professor – College of Civil and Environmental Engineering

Susan E. Burns, Ph.D., P.E

Professor – College of Civil and Environmental Engineering

Daniel Benkeser

Graduate Research Assistant

Hejintao Huang

Graduate Research Assistant

Georgia Institute of Technology

Contract with

Georgia Department of Transportation

In Cooperation with

U.S Department of Transportation

Federal Highway Administration

September 2020

The contents of this report reflect the views of the author(s) who are responsible for the facts and the accuracy of the data presented herein. The contents do not necessarily reflect the official views or policies of the Georgia Department of Transportation or the Federal Highway Administration. This report does not constitute a standard, specification, or regulation.

# TABLE OF CONTENTS

<b>CHAPTER 1. INTRODUCTION AND BACKGROUND .....</b>	<b>3</b>
<b>BACKGROUND .....</b>	<b>3</b>
<b>REPORT ORGANIZATION .....</b>	<b>5</b>
<b>CHAPTER 2. MATERIAL COLLECTION AND CHARACTERIZATION .....</b>	<b>7</b>
<b>DREDGE SAMPLING .....</b>	<b>7</b>
<b>SOIL CLASSIFICATION .....</b>	<b>10</b>
<b>SOIL MINERALOGY .....</b>	<b>18</b>
<b>SOIL MORPHOLOGY .....</b>	<b>25</b>
<b>CHAPTER 3. USE AS A STRUCTURAL/NON-STRUCTURAL FILL .....</b>	<b>31</b>
<b>HYDRAULIC CONDUCTIVITY TEST .....</b>	<b>32</b>
<b>COMPACTION TEST .....</b>	<b>35</b>
<b>DISCUSSION .....</b>	<b>37</b>
<b>CHAPTER 4. USE AS AN AGGREGATE .....</b>	<b>40</b>
<b>FINE AGGREGATE TESTING .....</b>	<b>41</b>
Standards for Fine Aggregates .....	41
Particle Size Distribution .....	41
Clay Lumps and Friable Particles .....	43
Deleterious Substances .....	44
Alkali Silica Reactivity .....	45
<b>LIGHTWEIGHT EXPANDED CLAY AGGREGATE .....</b>	<b>47</b>
Literature Review .....	47
Lightweight Aggregate Proof of Concept .....	54
<b>CHAPTER 5. USE AS A SUPPLEMENTARY CEMENTITIOUS MATERIAL ....</b>	<b>60</b>
<b>SOURCES OF POZZOLANIC REACTIVITY .....</b>	<b>61</b>
Kaolinite De-Hydroxylation .....	61
Other Sources of Pozzolanic Reactivity .....	63
<b>SCM PRODUCTION OPTIMIZATION .....</b>	<b>66</b>
Materials .....	66
General SCM Production Process .....	67
Final SCM Production Process .....	68

<b>DREDGE SCM CHARACTERIZATION .....</b>	<b>70</b>
Dredge Testing Procedure.....	70
Particle Size Distribution .....	71
Mineralogical Composition.....	73
Chemical Composition.....	75
<b>POZZOLANIC REACTIVITY OF DREDGE MATERIAL .....</b>	<b>76</b>
Compressive Strength .....	76
Calcium Hydroxide Consumption.....	79
Isothermal Calorimetry .....	82
Alkali Silica Reactivity .....	84
<b>ANALYSIS AND IMPROVEMENTS TO POZZOLANIC REACTIVITY .....</b>	<b>87</b>
Analysis of River Sediment Performance .....	87
Drawbacks and Improvements.....	88
<b>CHAPTER 6. R<sup>3</sup> TEST METHOD .....</b>	<b>92</b>
R <sup>3</sup> TEST METHOD EXPERIMENTAL PROCESS.....	92
BOUND WATER .....	93
ISOTHERMAL CALORIMETRY.....	95
CALCIUM HYDROXIDE CONSUMPTION .....	97
CORRELATIONS AND PERFORMANCE OF R <sup>3</sup> METHOD .....	98
<b>CHAPTER 7. APPLICATION AS A CEMENT FEEDSTOCK.....</b>	<b>101</b>
CEMENT PRODUCTION .....	101
LITERATURE REVIEW.....	103
CEMENT FEEDSTOCK WITH SAVANNAH SEDIMENT.....	105
<b>CHAPTER 8. LIFE CYCLE ANALYSIS.....</b>	<b>108</b>
INTRODUCTION – LCA.....	108
Goal and Scope .....	108
LCA ANALYSIS .....	111
System Boundaries .....	112
Analysis.....	113
<b>CHAPTER 9. RECCOMENDATIONS AND CONCLUSIONS .....</b>	<b>116</b>
RECOMENDATIONS .....	117
Structural/Non-Structural Fill .....	117

<b>Fine Aggregates .....</b>	<b>117</b>
<b>Lightweight Expanded Clay Aggregates .....</b>	<b>118</b>
<b>SCM Assessment through the R<sup>3</sup> Method.....</b>	<b>120</b>
<b>Life Cycle Analysis.....</b>	<b>122</b>
<b>Beneficial Use Decision Making Process.....</b>	<b>124</b>
<b>FUTURE WORK.....</b>	<b>126</b>
<b>CONCLUSIONS .....</b>	<b>127</b>
<b>APPENDIX A.....</b>	<b>131</b>
<b>ACKNOWLEDGEMENTS .....</b>	<b>142</b>
<b>REFERENCES .....</b>	<b>143</b>

## LIST OF TABLES

Table 1. Dredged material containment areas.....	14
Table 2. Relevant soil properties of dredged river sediments.....	16
Table 3. Summary of crystalline phases and amount.....	18
Table 4. Hydraulic conductivity of river sediments.....	33
Table 5. Optimum water content and maximum dry unit weight.....	36
Table 6. Clay lumps and friable particles for 13B-1.....	43
Table 7. Deleterious substances for sample 13B-1.....	45
Table 8. LECA heating processes.....	55
Table 9. Results of LECA production attempts.....	58
Table 10. Sediment LECA physical properties.....	59
Table 11. Chemical oxide composition of cement and metakaolin.....	67
Table 12. Primary particle sizes of heat-treated sediments.....	71
Table 13. XRD phase composition of river sediment.....	73
Table 14. Chemical oxide composition of calcined river sediments.....	76
Table 15. X-ray diffraction of river sediment samples.....	105
Table 16. Predicted chemical oxide composition of river sediments.....	106
Table 17. Predicted cement feedstock composition.....	107
Table 18. Diesel fuel production per 1kg fuel (Adapted from GaBi Database). ....	114
Table 19. Life cycle analysis of non-structural fill in terms of GWP.....	114
Table 20. Life cycle analysis of SCM in terms of GWP.....	115

## LIST OF FIGURES

Figure 1. Photo. Savannah harbor channel disposal areas.....	5
Figure 2. Photo. Sampling locations for material characterization.....	7
Figure 3. Photo. Sample site 12A-2. ....	8
Figure 4. Photo. Sample site 13A. ....	9
Figure 5. Photo. Sample site 13B-2. ....	9
Figure 6. Photo. Samples collected from site 13B-3.....	10
Figure 7. Photo. Sample site 14A-2. ....	10
Figure 8. Photo. Oven-dried samples prior to grinding. ....	11
Figure 9. Graph. Grain size distribution of dredged river sediment.....	12
Figure 10. Graph. Grain size distribution of 12A-1 and 13A using hydrometer and laser PSD for fine grains.....	13
Figure 11. Photo. Savannah harbor dredged material containment areas. ....	15
Figure 12. Photo. Dredged material samples post combustion at 950 °C. Red tint indicates formation of iron oxides during combustion.....	17
Figure 13. Graph. Mass loss measured using LOI and TGA tests, compared with total organic carbon content measured for dredged samples.....	17
Figure 14. Graph. X-ray diffraction scans for sample 12A-1.....	19
Figure 15. Graph. X-ray diffraction scans of sample 13A.....	20
Figure 16. Graph. X-ray diffraction scans for sample 13B-1.....	20
Figure 17. Graph. X-ray diffraction scans for sample 13B-2.....	21
Figure 18. Graph. X-ray diffraction scans for sample 14A-1.....	22
Figure 19. Graph. X-ray diffraction scans for sample 14B-1.....	23
Figure 20. Graph. X-ray diffraction scans for sample 14B-2.....	24
Figure 21. Graph. X-ray diffraction scans for sample 14B-3.....	25
Figure 22. Photos. SEM microscopy of sample 12A-1. ....	26
Figure 23. Photos. SEM microscopy of sample 13A. ....	27
Figure 24. Photo. SEM microscopy of sample 13B-1.....	28
Figure 25. Photo. SEM microscopy of sample 13B-2.....	28
Figure 26. Photo. SEM microscopy of sample 14A-1.....	29
Figure 27. Photo. SEM microscopy for sample 14B-1.....	29
Figure 28. Photo. SEM microscopy of sample 14B-2.....	30
Figure 29. Photo. SEM microscopy of sample 14B-3.....	30
Figure 30. Graph. Hydraulic conductivity for sample 12A-1 under 5, 10, and 15 psi effective stress.....	33
Figure 31. Graph. Hydraulic conductivity of sample 13B-1 under 5, 10, and 15 psi effective stress.....	34
Figure 32. Graph. Hydraulic conductivity of sample 14A-1 under 5, 10, and 15 psi effective stress.....	34
Figure 33. Graph. Hydraulic conductivity of sample 14B-1 under 5, 10, and 15 psi effective stress.....	35
Figure 34. Graph. Standard Proctor test water content V. dry unit weight for sample 12A-1 (zero air void curve shown in red). ....	36

Figure 35. Graph. Standard Proctor test water content V. dry unit weight for sample 13A (zero air void curve shown in red).....	37
Figure 36. Graph. Particle size distribution of sample 13B-1.....	42
Figure 37. Graph. 14 day AMBT test (ASTM C1260).....	46
Figure 38. Photo. Commonly marketed LECA (Rashad, 2018).....	49
Figure 39. Graph. Composition diagram of bloated clays (Riley, 1950).....	50
Figure 40. Photo. VPM-30 vacuum power wedger (pug mill).....	52
Figure 41. Graph. Moisture content for LWA tested sediments.....	53
Figure 42. Photos. LECA initial proof of concept 14A-1 (a), 14A-2 (b), 13A (c), and 13B-2 (d).....	54
Figure 43. Photos. Small scale LECA with (left) and without (right) expanded core.....	56
Figure 44. Photo. Sample 13A with a 2-day (V.2.1) and 7-day (V.2.2) rest time. ....	57
Figure 45. Illustration. Standard crystal structure of kaolinite (Sperinck & Wright, 2010).....	62
Figure 46. Illustration. Simulated kaolinite structure with increasing levels of dehydroxylation (Sperinck & Wright, 2010).....	63
Figure 47. Photo. Microscopy of sample 12A-2 (left), 13A (middle), and 14A-1 (right) after calcination.....	65
Figure 48. Graph. Strength activity index, temperature optimization.....	69
Figure 49. Graph. Particle size distribution of heat-treated river sediments.....	73
Figure 50. Graph. Strength activity index of calcined river sediment.....	78
Figure 51. Graph. Raw compressive strength of calcined river sediments.....	78
Figure 52. Graph. Calcium hydroxide consumed by heat-treated river sediments.....	81
Figure 53. Graph. Consumed calcium hydroxide normalized by sediment kaolin content.....	82
Figure 54. Graph. Normalized evolved heat of calcined river sediments.....	84
Figure 55. Graph. Cumulative heat evolved of calcined river sediment.....	84
Figure 56. Graph. AMBT expansion of heat-treated river sediments.....	86
Figure 57. Graph. Kaolinite correlations between ASR expansion, CH consumption, and SAI.....	89
Figure 58. Graph. Sample 13B-3 strength optimization.....	90
Figure 59. Graph. Bound water content of heat-treated river sediment.....	94
Figure 60. Graph. Normalized heat evolved for R <sup>3</sup> pastes.....	96
Figure 61. Graph. Cumulative heat evolved R <sup>3</sup> pastes.....	96
Figure 62. Graph. Calcium hydroxide consumed in R <sup>3</sup> pastes.....	97
Figure 63. Graph. Correlation for CH consumption of cement paste and bound water in the R <sup>3</sup> paste.....	99
Figure 64. Graph. Correlation between CH content of blended cement paste and CH content of R <sup>3</sup> paste.....	99
Figure 65. Graph. Correlation between CH consumed for blended cement paste and cumulative heat of the R <sup>3</sup> paste.....	100
Figure 66. Illustration. Stages of the ordinary portland cement production process (Carpio, Junior, Coelho, & Silva, 2008).....	103

<b>Figure 67. Illustration. Life cycle flowchart and definitions of the four main phases.</b>	109
<b>Figure 68. Illustration. Main stages, typical inflows and outflows in life cycle assessment.</b>	110
<b>Figure 69. Illustration. The Flow of Work: The life cycle of non-structure fill broken into three main stages: excavation, transportation, and compaction.</b>	112
<b>Figure 70. Illustration. The Flow of Work: The life cycle of supplementary cementitious material is broken into three main stages: excavation &amp; processing, transportation, and manufacturing.</b>	113
<b>Figure 71. Illustration. Comprehensive life cycle flow chart for sediment applications.</b>	123
<b>Figure 72. Illustration. Technical decision tree for sediment application</b>	125
<b>Figure 73. Graph. Raw sediment TGA analysis.</b>	131
<b>Figure 74. Graph. Raw XRD scans for sample 12A-2 raw.</b>	132
<b>Figure 75. Graph. Raw XRD scan for sample 13A raw.</b>	133
<b>Figure 76. Graph. Raw XRD scan for sample 13B-2 raw.</b>	134
<b>Figure 77. Graph. Raw XRD scan for sample 13B-3 raw.</b>	135
<b>Figure 78. Graph. Raw XRD scan for sample 14A-1 raw.</b>	136
<b>Figure 79. Graph. Raw XRD scan for sample 12A-2 800 °C.</b>	137
<b>Figure 80. Graph. Raw XRD scan for sample 13A 800 °C.</b>	138
<b>Figure 81. Graph. Raw XRD scan for sample 13B-2 800 °C.</b>	139
<b>Figure 82. Graph. Raw XRD scan for sample 13B-3 800 °C.</b>	140
<b>Figure 83. Graph. Raw XRD scan for sample 14A-1 800 °C.</b>	141

## SI\* (MODERN METRIC) CONVERSION FACTORS

### APPROXIMATE CONVERSIONS TO SI UNITS

Symbol	When You Know	Multiply By	To Find	Symbol
<b>LENGTH</b>				
in	inches	25.4	millimeters	mm
ft	feet	0.305	meters	m
yd	yards	0.914	meters	m
mi	miles	1.61	kilometers	km
<b>AREA</b>				
in <sup>2</sup>	square inches	645.2	square millimeters	mm <sup>2</sup>
ft <sup>2</sup>	square feet	0.093	square meters	m <sup>2</sup>
yd <sup>2</sup>	square yard	0.836	square meters	m <sup>2</sup>
ac	acres	0.405	hectares	ha
mi <sup>2</sup>	square miles	2.59	square kilometers	km <sup>2</sup>
<b>VOLUME</b>				
fl oz	fluid ounces	29.57	milliliters	mL
gal	gallons	3.785	liters	L
ft <sup>3</sup>	cubic feet	0.028	cubic meters	m <sup>3</sup>
yd <sup>3</sup>	cubic yards	0.765	cubic meters	m <sup>3</sup>
NOTE: volumes greater than 1000 L shall be shown in m <sup>3</sup>				
<b>MASS</b>				
oz	ounces	28.35	grams	g
lb	pounds	0.454	kilograms	kg
T	short tons (2000 lb)	0.907	megagrams (or "metric ton")	Mg (or "t")
<b>TEMPERATURE (exact degrees)</b>				
°F	Fahrenheit	5 (F-32)/9 or (F-32)/1.8	Celsius	°C
<b>ILLUMINATION</b>				
fc	foot-candles	10.76	lux	lx
fl	foot-Lamberts	3.426	candela/m <sup>2</sup>	cd/m <sup>2</sup>
<b>FORCE and PRESSURE or STRESS</b>				
lbf	poundforce	4.45	newtons	N
lbf/in <sup>2</sup>	poundforce per square inch	6.89	kilopascals	kPa

### APPROXIMATE CONVERSIONS FROM SI UNITS

Symbol	When You Know	Multiply By	To Find	Symbol
<b>LENGTH</b>				
mm	millimeters	0.039	inches	in
m	meters	3.28	feet	ft
m	meters	1.09	yards	yd
km	kilometers	0.621	miles	mi
<b>AREA</b>				
mm <sup>2</sup>	square millimeters	0.0016	square inches	in <sup>2</sup>
m <sup>2</sup>	square meters	10.764	square feet	ft <sup>2</sup>
m <sup>2</sup>	square meters	1.195	square yards	yd <sup>2</sup>
ha	hectares	2.47	acres	ac
km <sup>2</sup>	square kilometers	0.386	square miles	mi <sup>2</sup>
<b>VOLUME</b>				
mL	milliliters	0.034	fluid ounces	fl oz
L	liters	0.264	gallons	gal
m <sup>3</sup>	cubic meters	35.314	cubic feet	ft <sup>3</sup>
m <sup>3</sup>	cubic meters	1.307	cubic yards	yd <sup>3</sup>
<b>MASS</b>				
g	grams	0.035	ounces	oz
kg	kilograms	2.202	pounds	lb
Mg (or "t")	megagrams (or "metric ton")	1.103	short tons (2000 lb)	T
<b>TEMPERATURE (exact degrees)</b>				
°C	Celsius	1.8C+32	Fahrenheit	°F
<b>ILLUMINATION</b>				
lx	lux	0.0929	foot-candles	fc
cd/m <sup>2</sup>	candela/m <sup>2</sup>	0.2919	foot-Lamberts	fl
<b>FORCE and PRESSURE or STRESS</b>				
N	newtons	0.225	poundforce	lbf
kPa	kilopascals	0.145	poundforce per square inch	lbf/in <sup>2</sup>

## **Executive Summary**

Approximately 6 million m<sup>3</sup> of river sediment is dredged from the Savannah River annually in order to maintain navigability of the river. This sediment is stored in facilities located riverside. Unfortunately, planned development in this region puts these facilities at risk, and necessitates the removal of up to 11.5 million m<sup>3</sup> of this stored sediment (USACE, 2012). The work described in this report investigates the possibility of beneficially utilizing this material instead of the costly endeavor of relocating the material to a new location. Possible reuse options include applications as a structural/non-structural fill, fine/lightweight aggregates for use in concrete mixes, supplementary cementitious materials, and feedstock for cement production.

To investigate these possible applications, samples were collected from eleven sites and were selectively chosen for testing in these applications. Eight samples were chosen for testing as structural/non-structural fill. These sediments were characterized via the USCS soil classification system. Samples were then exposed to hydraulic conductivity and compaction tests. Possible fine aggregate sources (sample 13B-1) were tested for particle size, the effects of impurities, and for their susceptibility to the alkali aggregate reaction (ASTM C33 and ASTM C1260). Lightweight aggregates were produced through the sintering (1150 °C) of five sediment samples and were tested for their physical properties in accordance with ASTM C330. Five sediment samples were processed into supplementary cementitious materials via calcination (600-900 °C). They were then tested against ASTM C618 standards for natural pozzolans; additional tests were performed to

assess their ability to mitigate alkali silica reaction (ASTM C1567). Lastly, a literature review was conducted on the viability of utilizing the river sediments as a cement feedstock.

Results indicate that, upon meeting certain physical and chemical requirements, dredged sediments perform adequately in the majority of the applications presented. The only exception being their potential use as a fine aggregate in concrete, as the sediments typically contain unacceptable quantities of organics and fines in order to be properly utilized without extensive processing. Additional environmental and economic life cycle analysis was conducted in order to help determine in which application certain sediments should be used. It can be concluded from this work that all sediment samples can be effectively utilized in one of the presented applications regardless of composition or heavy metal/alkali contamination. This allows for the beneficial utilization of the entire stored river sediments including those contaminated with heavy metals. A decision tree framework is presented to guide in assessing sediments for these various applications.

## CHAPTER 1. INTRODUCTION AND BACKGROUND

### BACKGROUND

Approximately 6 million m<sup>3</sup> of river sediment is dredged from the Savannah River annually by the Army Corps of Engineers in order to keep the river navigable. This dredged river sediment is usually stored in facilities located along the riverside (seen in figure 1). While this storage option is an acceptable option in the short term, the long-term viability of these facilities is questionable. The construction of a deep water container port is planned in this region, necessitating the relocation of up to 11.5 million m<sup>3</sup> of this stored material. This process will be excessively expensive and time consuming due to the large volume and high water weight of the overall material. In order to mitigate this cost, a number of beneficiation techniques should be applied to this dredged material in order to allow for the processing and subsequent marketing of the product.

Prior analysis showed that the dredge material composition and physical characteristics varied, with samples from different locations containing varying amounts of sands, silts, and clays (Mezencevova, Yeboah, Burns, & Kahn, 2012) (Yeboah, Mezencevova, Phillips, Burns, & Kurtis, 2011). Such materials can typically be processed into a wide variety of geotechnical and structural applications, such as:

1. Structural/non-structural fill, useful for structural support or on embankments
2. Fine aggregates, which can be utilized to replace sand in mortar and concrete mixes
3. The production of lightweight expanded clay aggregates (LECA), which can be utilized in landscaping and to produce lightweight concrete mixes
4. The production of pozzolanic supplementary cementitious materials (SCMs)
5. The partial replacement of raw materials in cement feedstock

This report will investigate the viability of these beneficial reuse options based on overall performance, in consideration of economic and environmental assessments. Additional recommendations will be made with the purpose of advising which dredged materials can be used in those situations.

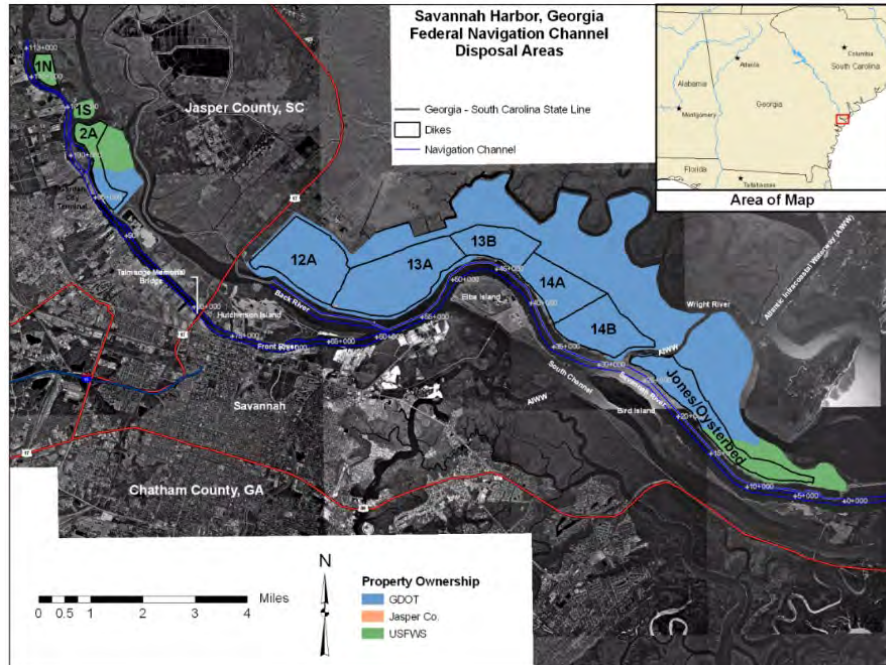


**FIGURE 1. PHOTO. SAVANNAH HARBOR CHANNEL DISPOSAL AREAS.**

## REPORT ORGANIZATION

This report is organized into eleven chapters:

Chapter 2 covers the collection and characterization of the dredge material samples, including their soil classification in terms of ASTM D2487.

Chapter 3 covers the dredge material's potential use as a non-structural fill.

Chapter 4 covers the dredge material's use as a concrete aggregate, including its use as a fine aggregate (sand fill) and its production into a lightweight expanded clay aggregate (LECA).

Chapter 5 covers the production and performance of the dredge material into a supplementary cementitious material.

Chapter 6 explores the viability of the new  $R^3$  test method for measuring pozzolanic reactivity (Avet, Snellings, Diaz, Haha, & Scrivener, 2016).

Chapter 7 covers the possibility of utilizing Savannah River sediment as a cement feedstock.

Chapter 8 presents the economic and life cycle assessment of the dredge material with the purpose of investigating the economic and environmental aspects of producing the dredge material into SCMs.

Chapter 9 draws main conclusions, and contributions of this work are summarized. Additionally, recommendations for implementation and potential future work are summarized.

## CHAPTER 2. MATERIAL COLLECTION AND CHARACTERIZATION

### DREDGE SAMPLING

Samples were collected from on-site collections disposal areas (seen in figure 1) on two separate occasions. Several five-gallon buckets of river sediment were collected at surface level from each location. Samples were named primarily based on their storage location, listed in Figure 2.

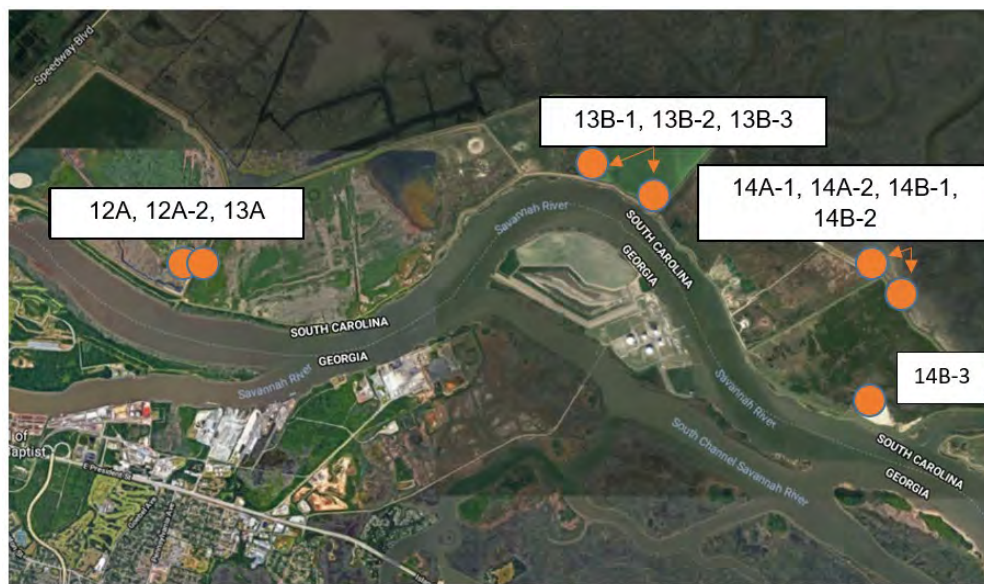


**FIGURE 2. PHOTO. SAMPLING LOCATIONS FOR MATERIAL CHARACTERIZATION.**

Samples 12A-1, 13A, 13B-1, 13B-2, 14A-1, 14A-2, 14B-1, 14B-2, and 14B-3 were collected in January 2018. Samples 12A-2 and 13B-3 were collected later in August 2018, at the exact same locations as 12A-1 and 13B-2 respectively.

Once collected, the samples were dried in an oven at 110 °C overnight in order to remove excess quantities of water. Samples were then broken apart by a standard soil crusher before further analysis. Not all soil samples were assessed by all of the experimental tests, with testing performed based upon initial assessment and judicious use of resources.



**FIGURE 3. PHOTO. SAMPLE SITE 12A-2.**



**FIGURE 4. PHOTO. SAMPLE SITE 13A.**



**FIGURE 5. PHOTO. SAMPLE SITE 13B-2.**



**FIGURE 6. PHOTO. SAMPLES COLLECTED FROM SITE 13B-3.**



**FIGURE 7. PHOTO. SAMPLE SITE 14A-2.**

## **SOIL CLASSIFICATION**

All samples were received in a wet state. Each was composed primarily of fine-grained soils, including silt and clay with the exception of the sample obtained at

the third location (14B), which was primarily sand. The pH values of all samples ranged from 6 ~ 7, as measured by a pH indicator in the field. After oven-drying, the sample color ranged from light brown to black (Figure 8). Larger particles were broken apart into fine particles with mortar and pestle. In the field, the soil would be classified as predominantly sand and silt with a very small number of aggregated particles. All experiments in Chapter 2 and Chapter 3 are performed after the soil was oven-dried and crushed.



**FIGURE 8. PHOTO. OVEN-DRIED SAMPLES PRIOR TO GRINDING.**

Grain size distributions were determined on the dried and crushed samples according to ASTM D422 and by laser particle size analysis with a refractive index of 1.511 (Malvern 3000 Hydro Eve), and the results were combined to yield the overall particle distribution (Figure 9 and Figure 10). For each sieve test, a soil sample weighing approximately 500 grams was shaken through sieve Nos. 4, 10, 20, 40, 60, 140, 200 with opening sizes of 0.1870 inch (4.760 mm), 0.0787 inch (2.000 mm), 0.0331 inch (0.841 mm), 0.0165 inch (0.420 mm), 0.0098 inch (0.250

mm), 0.0041 inch (0.105 mm) and 0.0029 inch (0.0074 mm) respectively. All material passing the No. 200 sieve was retained in the pan and kept for hydrometer (sedimentation) testing (ASTM D7928-17).

Comparing the results from the hydrometer with the results obtained from the laser diffraction tests (PSA) demonstrated that the grain size curves diverge. This is believed to be due to different assumptions for calculating particle size in each method (Figure 10). The hydrometer analysis relies on Stokes's Law, with the assumption that all particles are spherical, while the PSA is primarily useful when particle size distributions are uniform, resulting in deviations in the resulting grain size analysis curves.

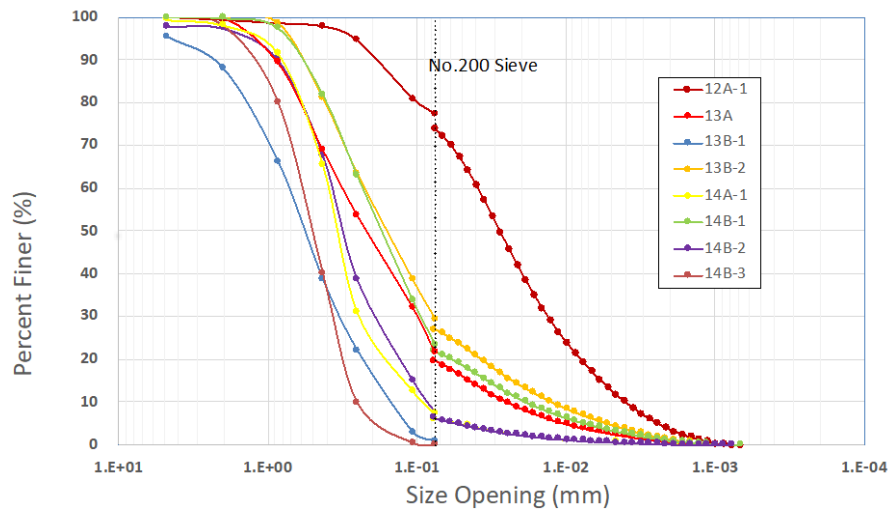


**FIGURE 9. GRAPH. GRAIN SIZE DISTRIBUTION OF DREDGED RIVER SEDIMENT.**

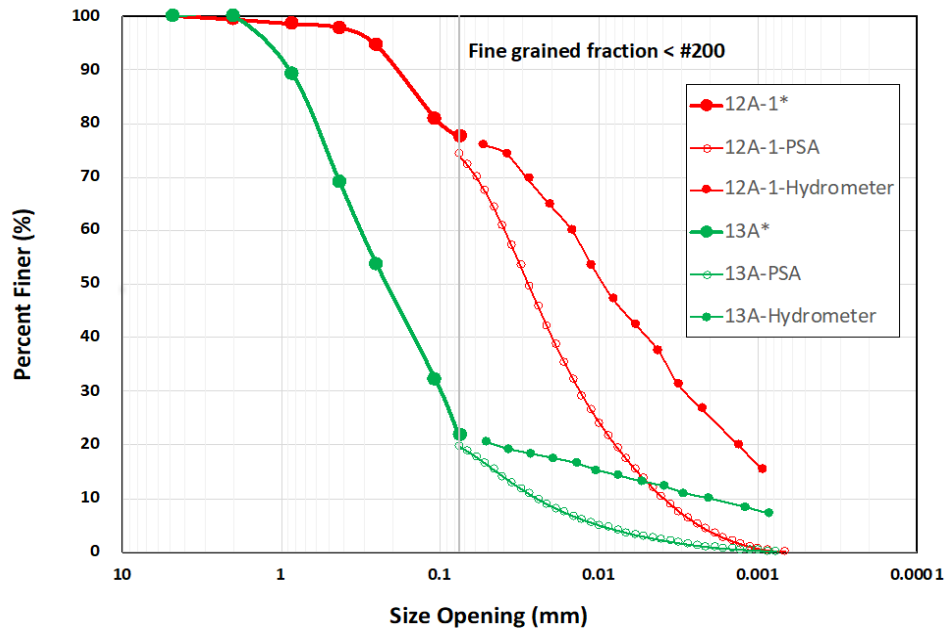


**FIGURE 10. GRAPH. GRAIN SIZE DISTRIBUTION OF 12A-1 AND 13A USING HYDROMETER AND LASER PSD FOR FINE GRAINS.**

With the change in locations, the soil classification varies widely from fine-grain soil to very coarse-grained soil. Though gravity may have influence on the variations soil type distributions, more importantly, it is caused by the rotations of disposal of dredged sediments. Based on GDOT Savannah Harbor Expansion Project Dredged Material Management Plan Update, soil dredged from the lower and upper reaches of the project are mainly composed of sand, while the main constituents removed from the middle harbor and sediment basin are silt. The dredged material containment areas (DMCA) are shown in Figure 11, with the areas and stations shown listed in Table 1. Based on the plan, 12A-1 and 13A are primarily silts and clays. 13B, 14A, and 14B are transitional reaches that have a higher percentage of sand. From 14B to the mouth of the Savannah River is primarily sand, which indicates that the source of sediment is offshore. Our findings

are consistent with what is stated in the plan, with 12A-1 as the largest fine contents. 13A, 13B-2, and 14B-1 have a substantial combination of fines and sands (about 25% fines on average). 14A-1 and 14B-2 are mostly composed of sands with less than 10 percent fines. 14B-3, the closest to the mouth of harbor, is purely coarse sand. The only deviation from the plan is that 13B-1 is mostly sandy (barely no fines).

**TABLE 1. DREDGED MATERIAL CONTAINMENT AREAS.**

<b>DMCA</b>	<b>Location(Station)</b>	<b>Acreage</b>
2A	93+000 to 103+000	240
12A	6+500BR to 10+500BR*	1040
13A	47+800 to 57+000 (2+000BR)	1307
13B	42+000 to 47+800	540
14A	37+000 to 42+000	647
14B	28+000 to 37+000	703
Jones/Oysterbed (JOI)	10+000 to 27+000	890

\*BR refers to Back River or that portion of the channel located in the Back River



**FIGURE 11. PHOTO. SAVANNAH HARBOR DREDGED MATERIAL CONTAINMENT AREAS.**

Samples, along with their relevant physical properties (including the Atterberg limit result and specific gravity), are denoted based on their USCS soil classification (Table 2). Atterberg limits tests were performed according to ASTM Standard D4318. The USCS soil classification system is a soil classification system used in engineering and geology to describe the texture and grain size of the soil. Based on the system, three soils can be classified as clayed sand (SC); two soils are classified as poorly graded sand (SP); two soils are classified as poorly graded sand combined with silty sand (SP-SM); one soil is classified as fat clay (CH). The plastic index of the four soils tested is relatively high. Soils with a high PI tend to be clay while those with low PI tend to be silt. The total organic content for all soil samples is relatively low. The specific gravity was tested for each sample following ASTM D-854. Each procedure was repeated two times, and the

average reading was reported. The specific gravity of eight soil samples ranged from 2.51 to 2.70. The specific gravity for quartz is 2.65, for reference.

**TABLE 2. RELEVANT SOIL PROPERTIES OF DREDGED RIVER SEDIMENTS.**

<b>Sample ID</b>	<b>USCS SOIL CLASSIFICATION</b>	<b>LL (%)</b>	<b>PL (%)</b>	<b>PI (%)</b>	<b>Specific Gravity</b>	<b>D50 (mm)</b>
12A-1	CH	69	47	22	2.51	0.029
13 A	SC	70	38	32	2.68	0.2
13 B-1	SP	( - )	( - )	( - )	2.7	0.55
13 B-2	SC	67	43	24	2.64	0.16
14 A-1	SP-SM	( - )	( - )	( - )	2.74	0.33
14 B-1	SC	56	32	24	2.65	0.17
14 B-2	SP-SM	( - )	( - )	( - )	2.67	0.21
14 B-3	SP	( - )	( - )	( - )	2.67	0.5

The total organic carbon content for the dredged materials was quantified using a Shimadzu TOC-V analyzer fitted with a solid sample module (SSM-5000A). Inorganic and total carbon contents were measured by acidification with 85% nitric acid at 200 °C, and combustion at 900 °C, respectively. Total organic carbon content (TOC) was determined by subtraction. This method measures the amount of CO<sub>2</sub> produced during the combustion process, so the mass loss of other mineral phases is not quantified using this measurement. Consequently, the loss on ignition (LOI) method, in accordance with ASTM D7348-13, and dual-atmosphere thermogravimetric analysis (TGA) method were also applied to the samples to help identify mass loss. LOI was determined by heating dredge material to 750 °C in a muffle furnace. Eight samples of dredge material (12A-1, 13A, 13B-1, 13B-2, 14A-1, 14B-1, 14B-2, and 14B-3) were tested to a maximum temperature of 950 °C. During combustion, iron present in the mineral structures' oxides changes to iron oxide phases, such as hematite. The presence of the reddish color is an

indicator of structural iron that was transformed from kaolinite particles into iron oxides at high combustion temperatures. The mass loss quantified by the LOI and TGA methods were in close agreement, while the TOC method yielded smaller values because it only quantified loss of organic carbon.

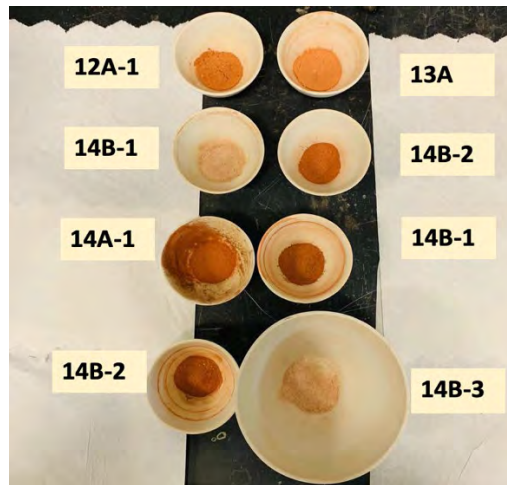


**FIGURE 12. PHOTO. DREDGED MATERIAL SAMPLES POST COMBUSTION AT 950 °C. RED TINT INDICATES FORMATION OF IRON OXIDES DURING COMBUSTION.**

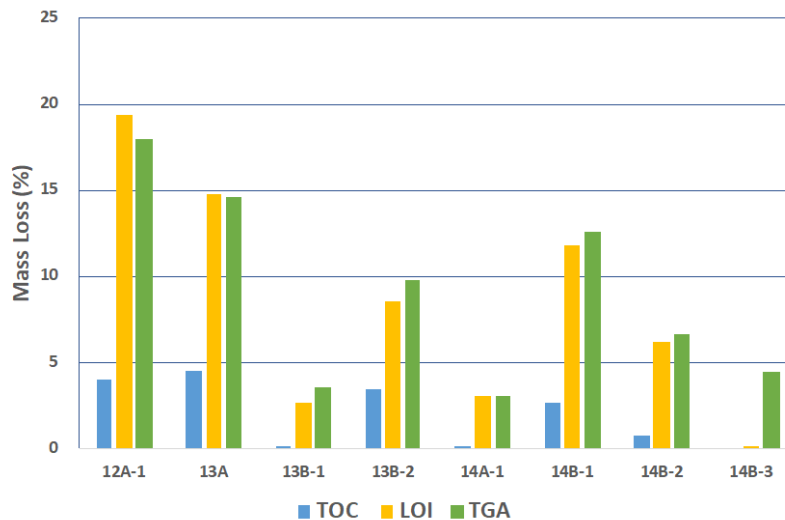


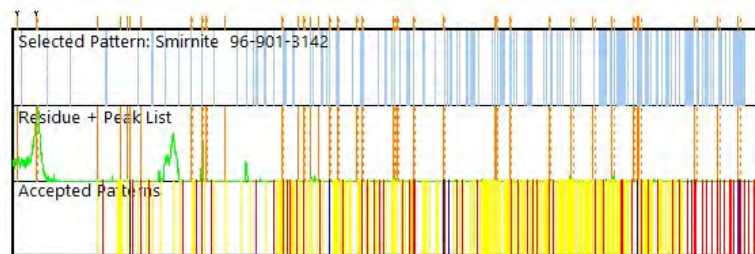
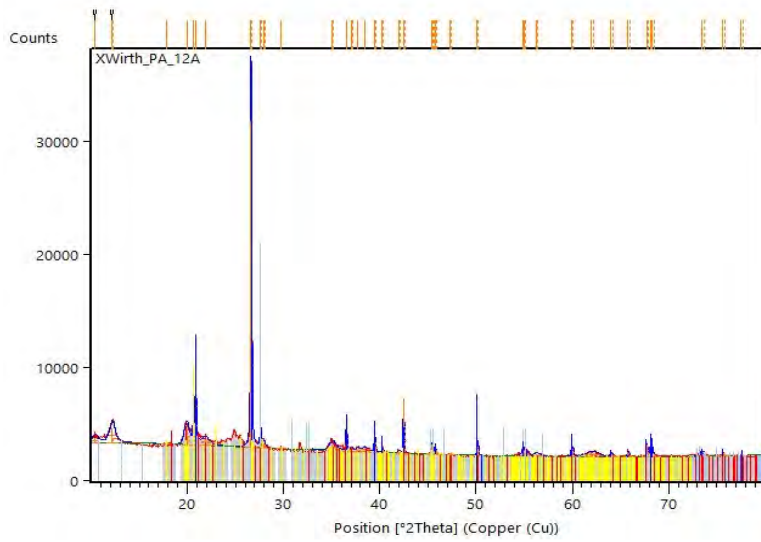
**Figure 13. Graph. Mass loss measured using LOI and TGA tests, compared with total organic carbon content measured for dredged samples.**

## SOIL MINERALOGY

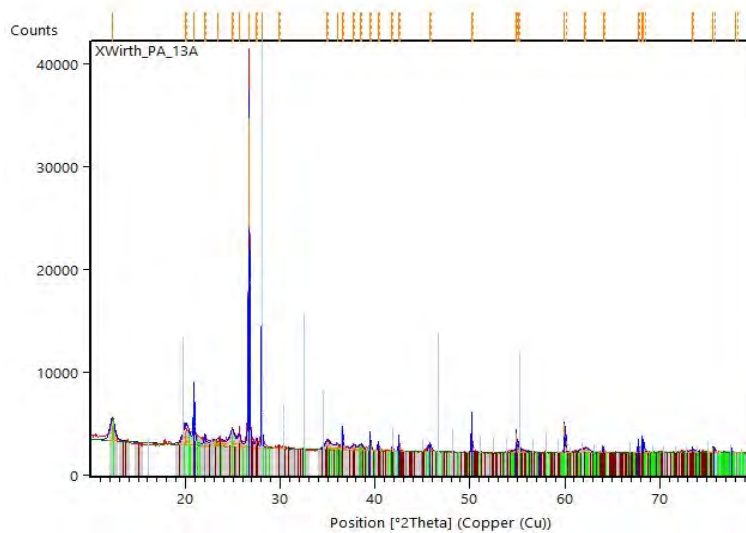
The samples were characterized by x-ray diffraction (XRD) (PANalytical Empyrean) under Cu-K $\alpha$  radiation in the range of 10 to 80  $^{\circ}2\theta$  at a scan rate of 0.04  $^{\circ}/s$ . The collected data was used for the identification of crystalline phases and was analyzed using the software HighScore Plus to provide a semi-quantitative assessment of composition. The chemical composition for each sample, as determined by XRD, is shown in Figures 14, 15, 16, 17, 18, 19, 20 and 21. The XRD evaluation provides semi-quantitative analysis of the crystalline components. These results are also summarized in Table 3. From this, quartz and kaolinite are the two main crystallite phases present in the dredged materials, but some samples also contain calcite, muscovite, and other phases.

**TABLE 3. SUMMARY OF CRYSTALLINE PHASES AND AMOUNT.**

<b>Sample Name</b>	<b>Main Components with Percentages</b>			
12A-1	Quartz (74%)	Montmorillonite (11%)	Muscovite 2M1 (15%)	
13A	Quartz (68%)	Kaolinite (20%)	Cristobalite low (1%)	Orthoclase (11%)
13B-1	Quartz (83%)	Calcite (5%)	Cristobalite (1%)	Muscovite 2M1 (12%)
13B-2	Quartz (40%)	Orthoclase (7%)	Cristobalite (--)	Muscovite-2M1 (52%)
14A-1	Quartz (92%)	Muscovite 2M1 (2%)	Cristobalite (--)	Calcite (1)
14B-1	Quartz (68%)	Kaolinite (11%)	Calcite/ Dolomite (2%)	Muscovite 2M1 (15%)
14B-2	Quartz (34%)	Dolomite (2%)	Muscovite (62%)	Lime (2%)
14B-3	Quartz (97%)	Lime (3%)		



**FIGURE 14. GRAPH. X-RAY DIFFRACTION SCANS FOR SAMPLE 12A-1.**



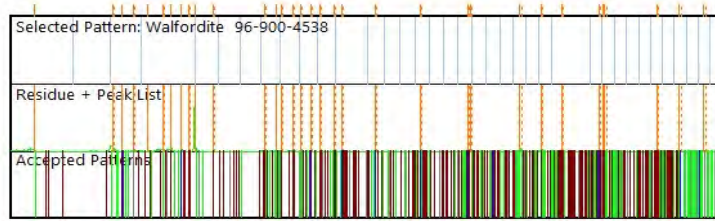


**FIGURE 15. GRAPH. X-RAY DIFFRACTION SCANS OF SAMPLE 13A.**

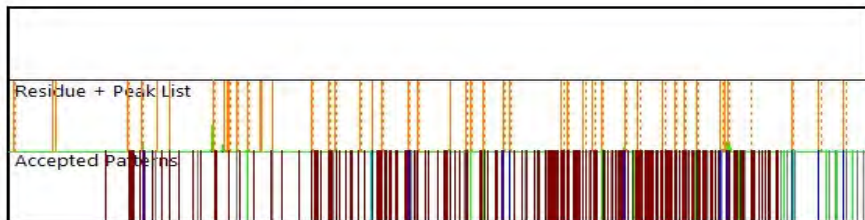
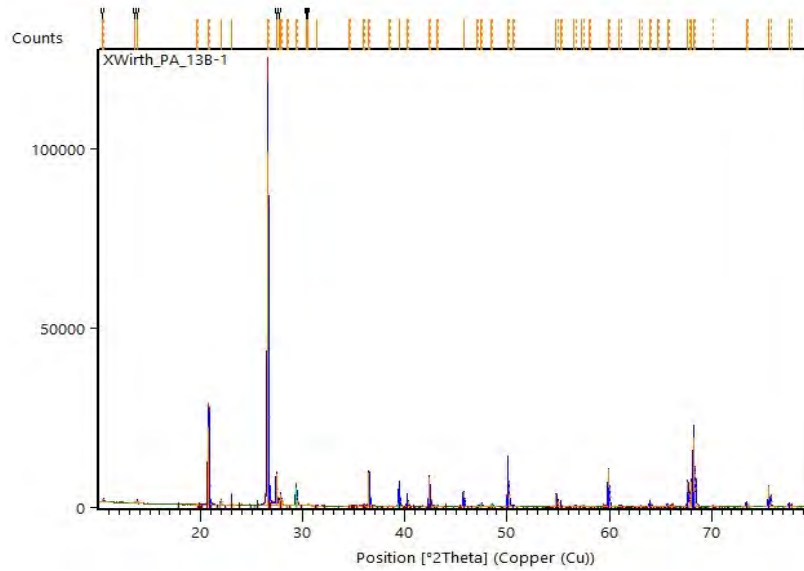


**FIGURE 16. GRAPH. X-RAY DIFFRACTION SCANS FOR SAMPLE 13B-1.**

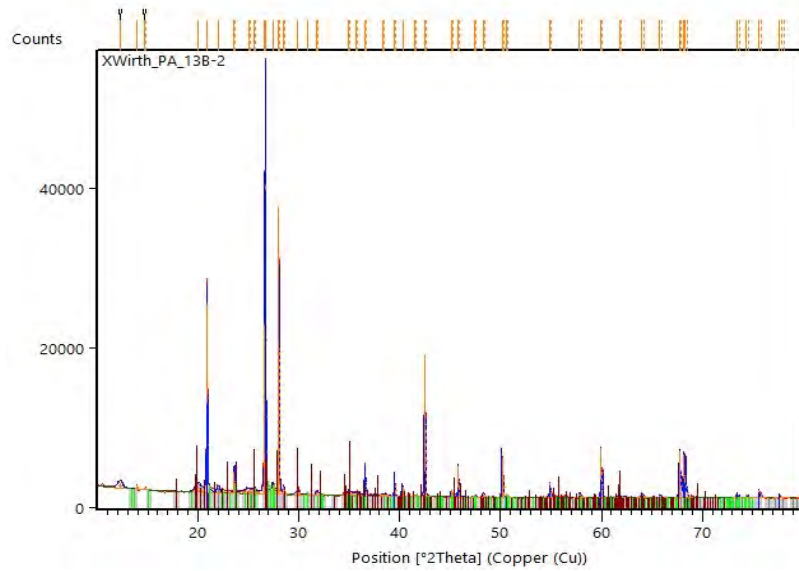


**FIGURE 17. GRAPH. X-RAY DIFFRACTION SCANS FOR SAMPLE 13B-2.**

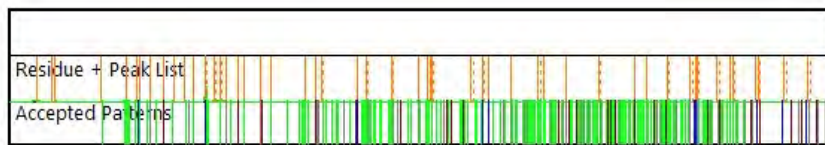
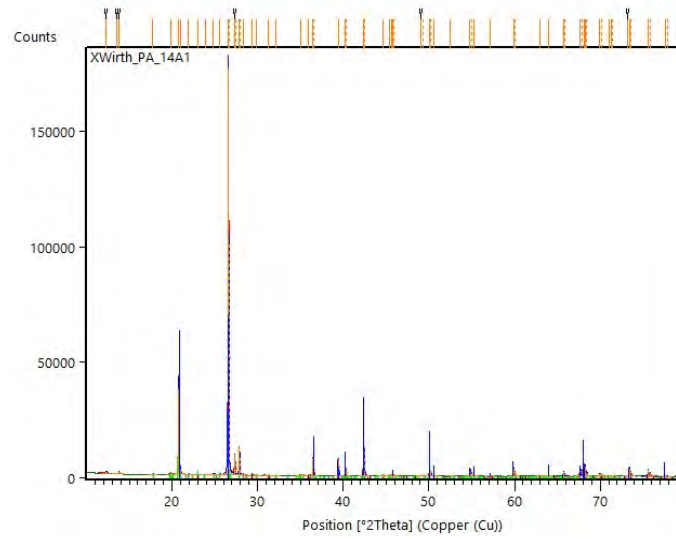


**FIGURE 18. GRAPH. X-RAY DIFFRACTION SCANS FOR SAMPLE 14A-1.**

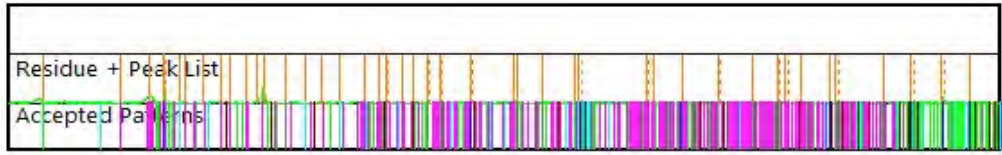
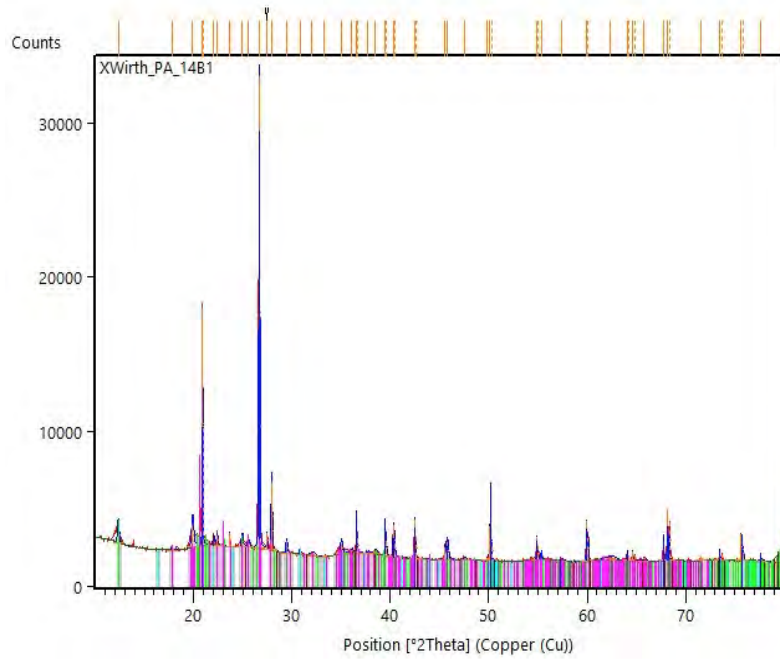


**FIGURE 19. GRAPH. X-RAY DIFFRACTION SCANS FOR SAMPLE 14B-1.**

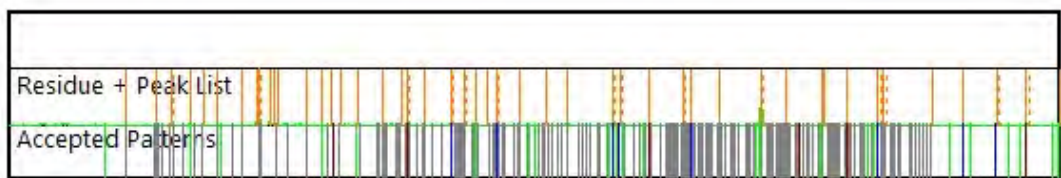
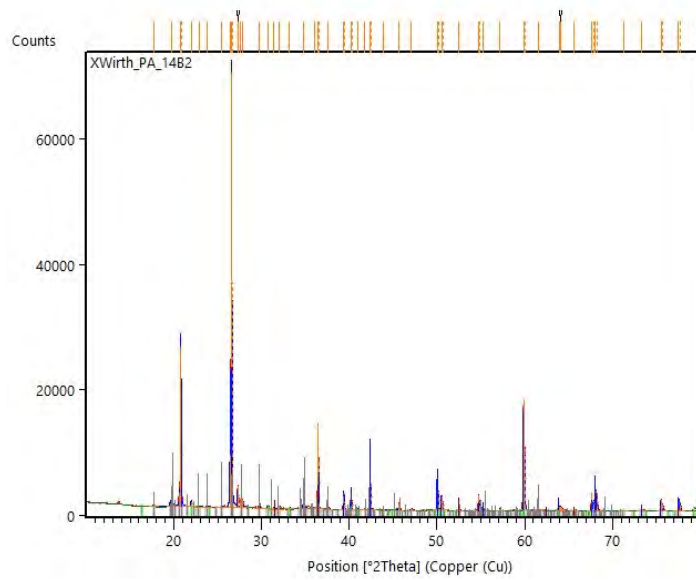


**FIGURE 20. GRAPH. X-RAY DIFFRACTION SCANS FOR SAMPLE 14B-2.**

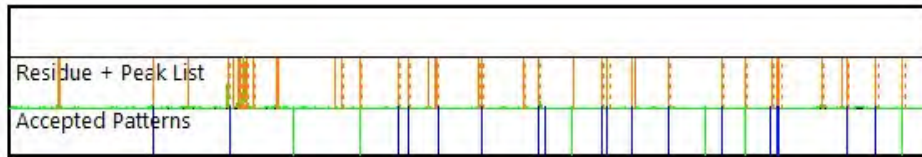
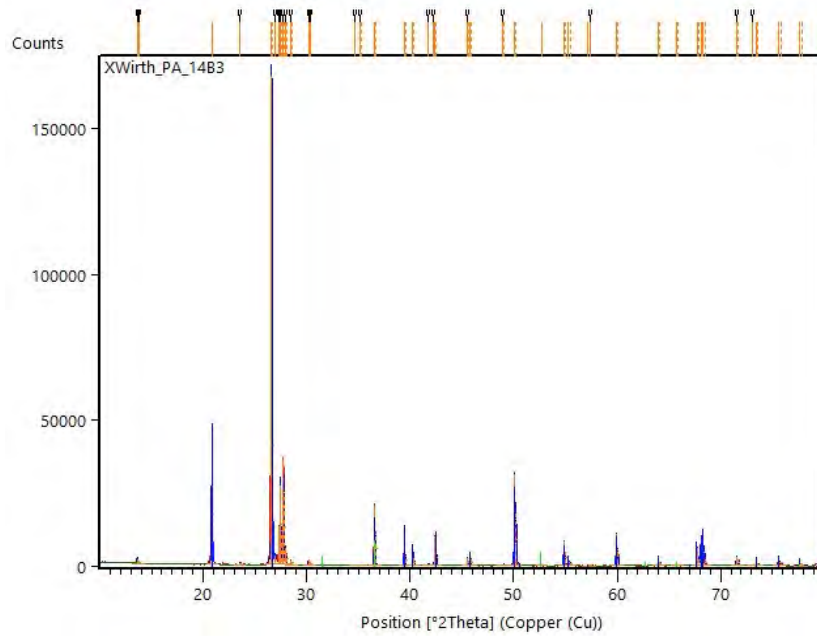


**FIGURE 21. GRAPH. X-RAY DIFFRACTION SCANS FOR SAMPLE 14B-3.**

## SOIL MORPHOLOGY

A scanning electron microscope (SEM) (Hitachi SU8010) was used to characterize morphology, which aids in soil identification. The SEM results show the flaky, angular structures of the dredged materials. Some of them contain diatoms, stemming from their previous river environment. The samples with more

fine contents have small crystalline structures and are flakier and more angular, while the course material is less flaky and more spherical.

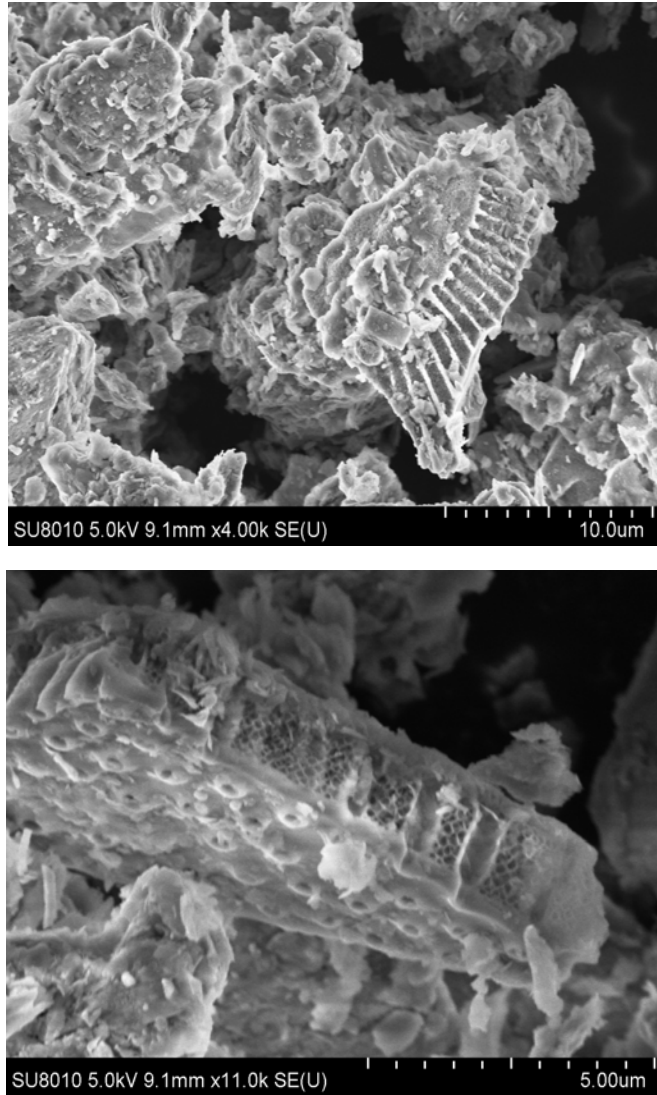


**FIGURE 22. PHOTOS. SEM MICROSCOPY OF SAMPLE 12A-1.**

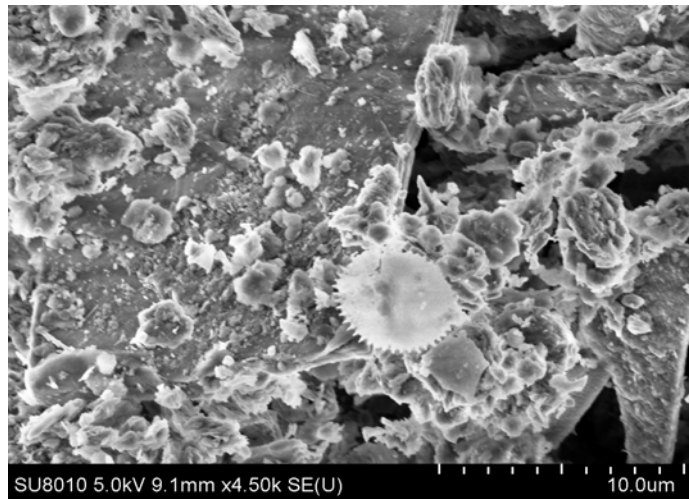
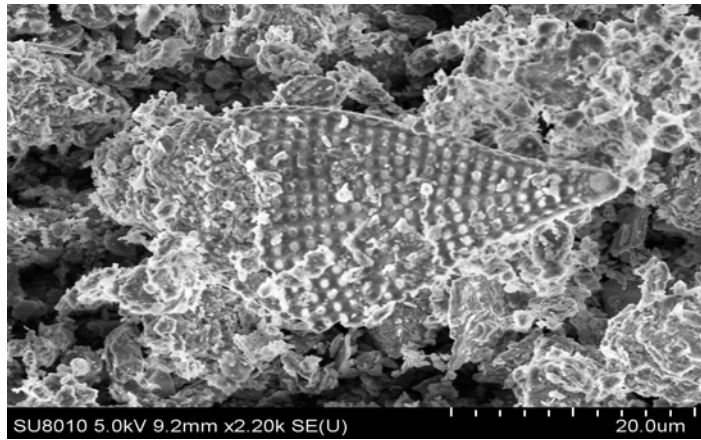


**FIGURE 23. PHOTOS. SEM MICROSCOPY OF SAMPLE 13A.**

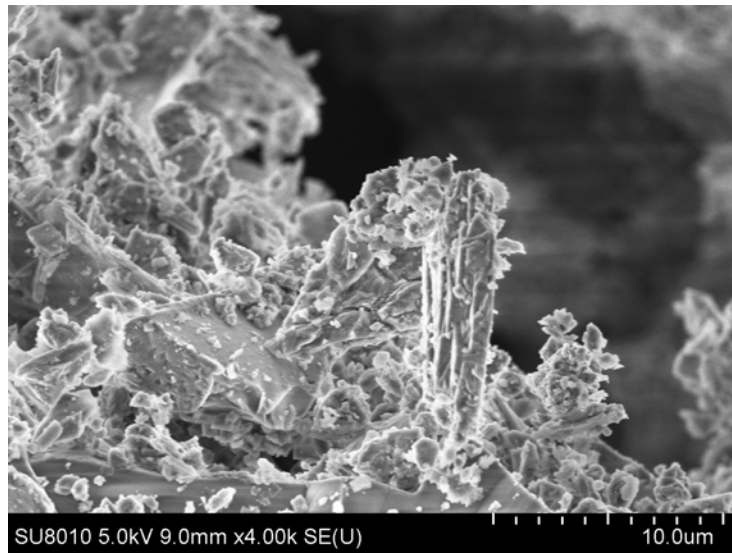


**FIGURE 24. PHOTO. SEM MICROSCOPY OF SAMPLE 13B-1.**

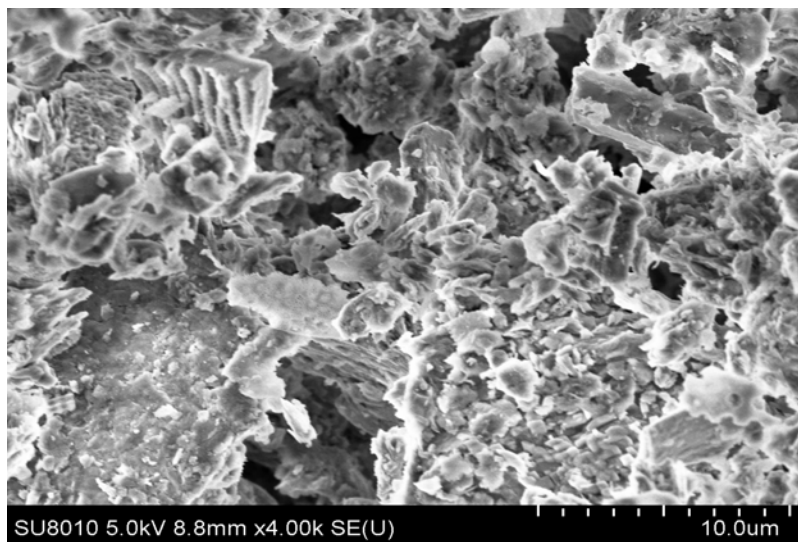


**FIGURE 25. PHOTO. SEM MICROSCOPY OF SAMPLE 13B-2.**

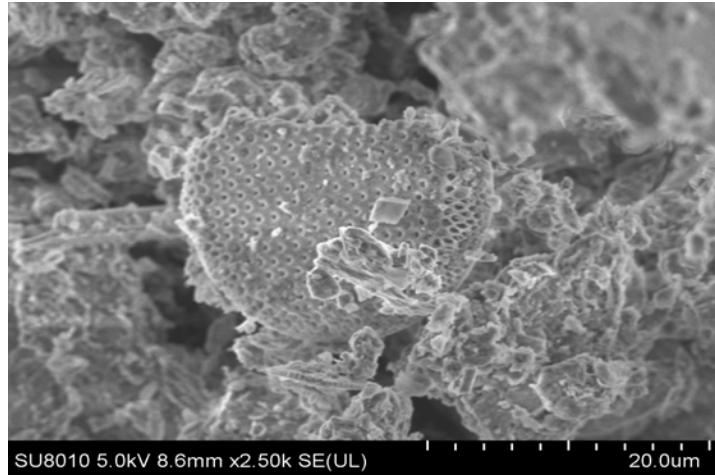


**FIGURE 26. PHOTO. SEM MICROSCOPY OF SAMPLE 14A-1.**

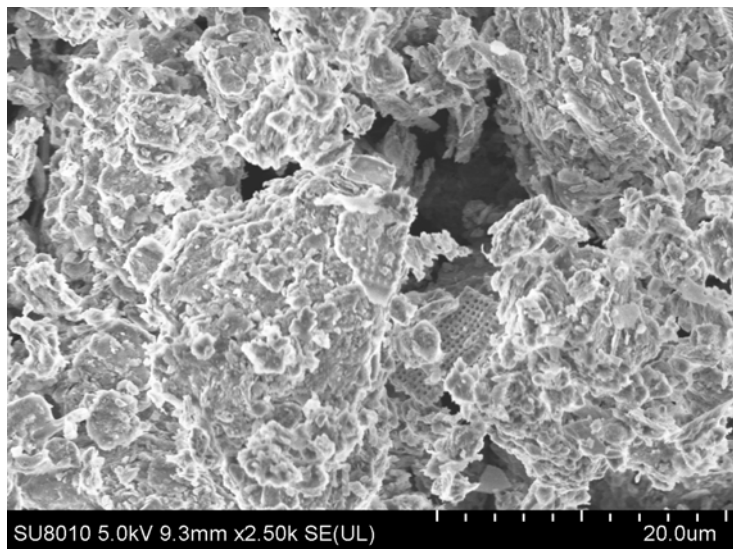


**FIGURE 27. PHOTO. SEM MICROSCOPY FOR SAMPLE 14B-1.**

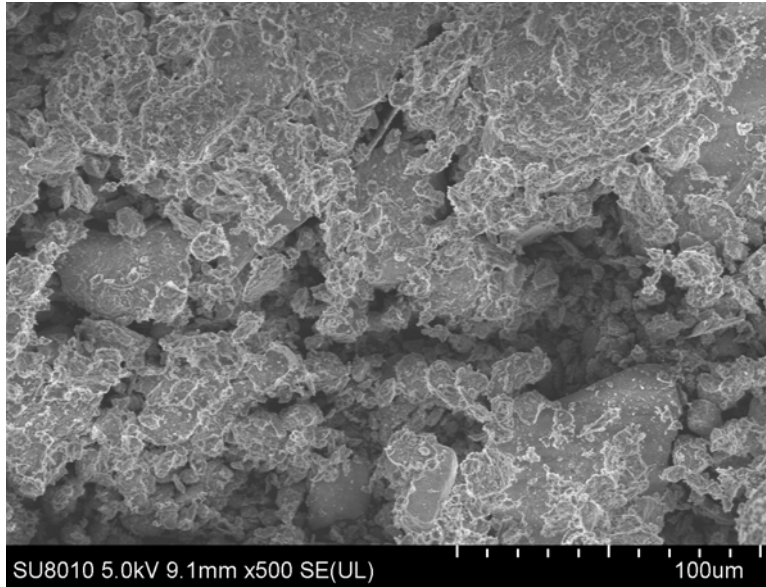


**FIGURE 28. PHOTO. SEM MICROSCOPY OF SAMPLE 14B-2.**

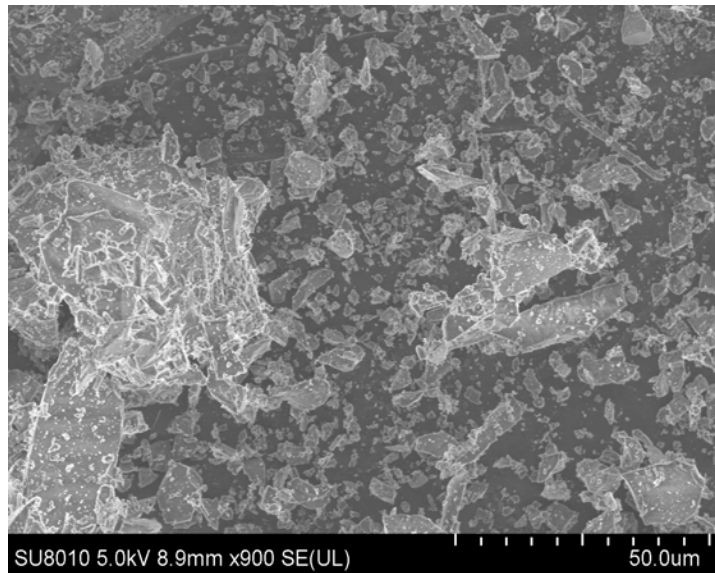


**Figure 29. Photo. SEM microscopy of sample 14B-3.**

### **CHAPTER 3. USE AS A STRUCTURAL/NON-STRUCTURAL FILL**

Fill is earthy material used to fill a depression or hole in the ground or otherwise change the grade or elevation of property. Usually constituted of subsoil (soil from beneath the topsoil) obtained from cuttings, borrow pits or excavation sites, fill has little organic content, such that little biological activity could occur. Once the organic material decomposes, it will cause pockets of space within the fill material which could result in settling. Uneven or excessive settling may lead to damages to any structure built on the soil.

Types of fill include select fill, general fill (structure fill) and non-structure fill. Select fill is at the highest standards and is usually used for the applications where “non-permeable” is required, for example, fill placed adjacent to retaining walls and reinforced soil embankments. General (structural) fill is a medium quality material that usually consists of inorganic, non-plastic, granular soils containing less than 10 percent of material passing No. 200 mesh sieve, with a Unified Soil Classification of GP, GW, SP, SPGM, SW-SM or SP-SM.

Non-structure material is a lower quality material which does not meet the requirements of general fill. For example, non-structure fill can be utilized as the fill for non-structure zones of embankments. The specifications by the transportation authorities is relatively relaxed, and do not have to meet the strict bearing capacity requirements (Arulrajah et al., 2014). In other words, any

material (usually any clay or silt) that is non-structural, ranging from clean and dry to clean and mixed, can be applied to this category.

## **HYDRAULIC CONDUCTIVITY TEST**

Flexible wall hydraulic conductivity tests following ASTM D5084 were conducted to investigate the hydraulic performance of dredged materials under different confining pressures (5, 10 and 15 psi). The samples that underwent the hydraulic conductivity test include 12A-1, 13B-1, 14A-1 and 14B-1, as shown in Figure 30 to Figure 33. They represent CH, SP, SP-SM and SC soil, respectively. The hydraulic conductivity ranged from  $10^{-7}$  cm/sec for the fine-grained soils to  $10^{-3}$  cm/sec for the coarse-grained soils (Table 4). The very low hydraulic conductivity values measured for the fines may be a concern in applications that require drainage and dewatering, as  $10^{-7}$  cm/sec is on the order of conductivity values used in barrier applications. However, the conductivity values measured in the coarser soil samples indicate relatively free draining materials, suitable for fills. It was noted that diatoms were present in the samples, which may have some impact on the results of hydraulic conductivity. Diagenetic bonding of diatomaceous fabric may reduce the well-connected pore spaces significantly, which would also alter the tortuosity and increase the length of drainage path (Masters and Christian, 1990).

**TABLE 4. HYDRAULIC CONDUCTIVITY OF RIVER SEDIMENTS.**

Confining Pressure (kPa)	12A-1 (cm/s)	13B-1 (cm/s)	14A-1 (cm/s)	14B-1 (cm/s)
34.5	7.5E-07	7.8E-03	1.2E-03	3.1E-05
68.9	6.7E-07	5.3E-03	8.2E-04	2.5E-05
103.4	4.3E-07	2.5E-03	4.3E-04	1.8E-05

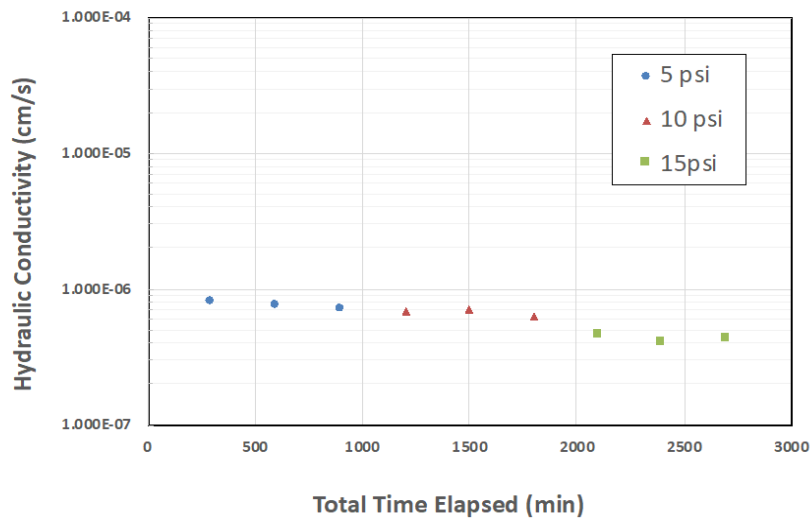


**FIGURE 30. GRAPH. HYDRAULIC CONDUCTIVITY FOR SAMPLE 12A-1 UNDER 5, 10, AND 15 PSI EFFECTIVE STRESS.**

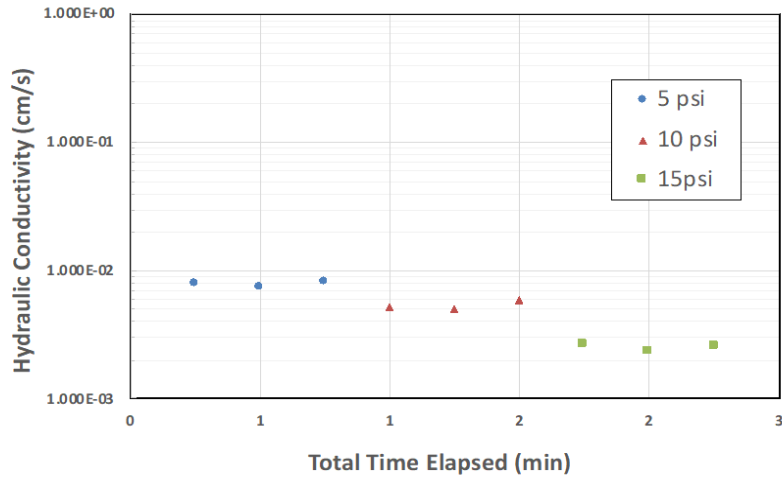


**FIGURE 31. GRAPH. HYDRAULIC CONDUCTIVITY OF SAMPLE 13B-1 UNDER 5, 10, AND 15 PSI EFFECTIVE STRESS.**

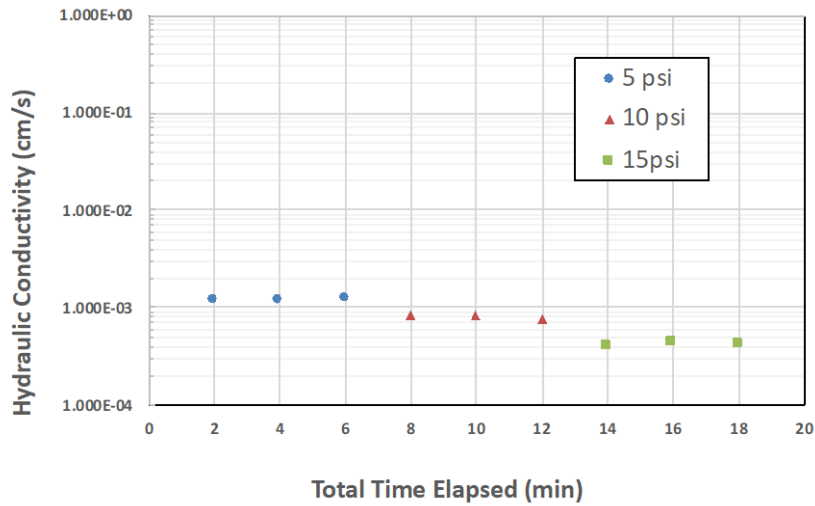


**FIGURE 32. GRAPH. HYDRAULIC CONDUCTIVITY OF SAMPLE 14A-1 UNDER 5, 10, AND 15 PSI EFFECTIVE STRESS.**

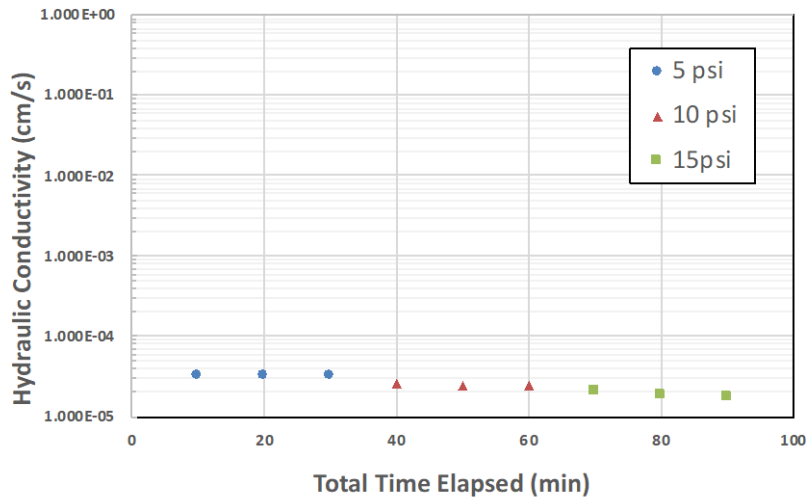


**FIGURE 33. GRAPH. HYDRAULIC CONDUCTIVITY OF SAMPLE 14B-1 UNDER 5, 10, AND 15 PSI EFFECTIVE STRESS.**

### COMPACTION TEST

Dredged material samples (12A-1 and 13A) were tested to determine maximum dry unit weight according to ASTM D698, using standard effort. The soil was added to the Proctor mold in three layers, and each layer was compacted with 25 blows from a 5.5 lb hammer. As listed in Table 5, the optimum water content of sample 12A-1 was 35.8%, and the maximum dry unit weight was 79.6 lb/ft<sup>3</sup> (12.4 kN/m<sup>3</sup>). The optimum water content of sample 13A was 38.0%, and the maximum dry unit weight was 75.4 lb/ft<sup>3</sup> (11.8 kN/m<sup>3</sup>). The results of the optimum water content tests of the two dredged samples are slightly higher than what has been found from the literature for dredged sediments, which typically ranges between 19.5 and 30% (Yu et.al, 2016; Baxter et al, 2005), and is likely caused by

the high organic content or the presence of diatoms in the soil (Figure 34 and Figure 35). For use as a fill material, the soil will have highest unit weight when the water content is wet of the optimum. The fill soil will exhibit the lowest deformability but will have highest strength when the water content is dry of the optimum.

**TABLE 5. OPTIMUM WATER CONTENT AND MAXIMUM DRY UNIT WEIGHT.**

Sample Number	Optimum Water Content (%)	Maximum Dry Unit Weight (lb/ft <sup>3</sup> )
12A-1	35.8	79.6
13A	38	75.4

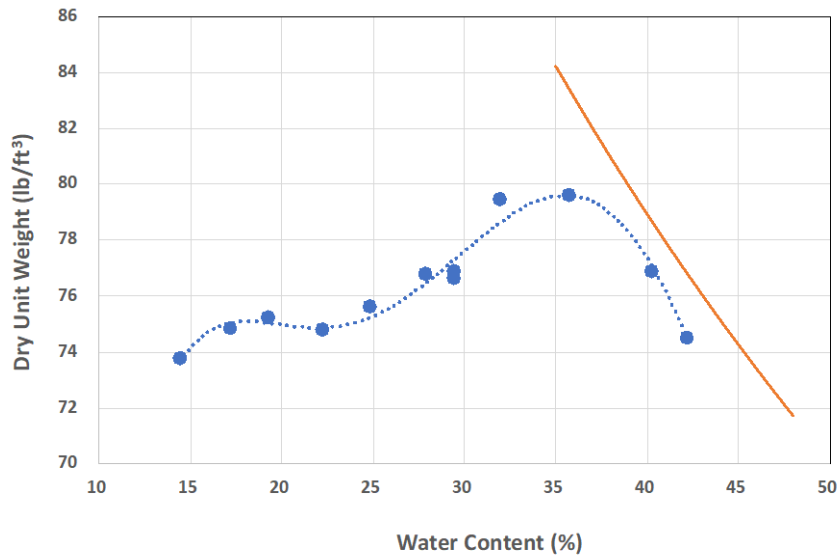


**FIGURE 34. GRAPH. STANDARD PROCTOR TEST WATER CONTENT V. DRY UNIT WEIGHT FOR SAMPLE 12A-1 (ZERO AIR VOID CURVE SHOWN IN RED).**

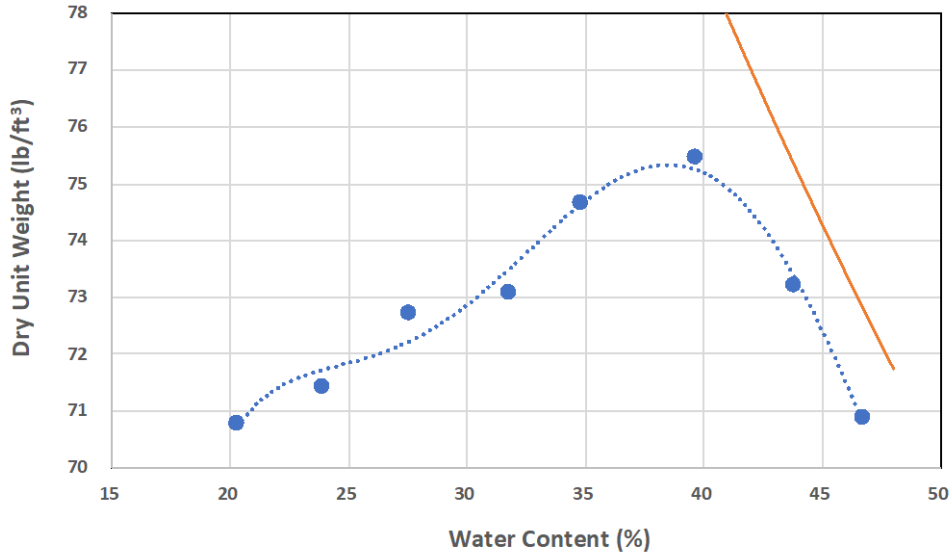


**FIGURE 35. GRAPH. STANDARD PROCTOR TEST WATER CONTENT V. DRY UNIT WEIGHT FOR SAMPLE 13A (ZERO AIR VOID CURVE SHOWN IN RED).**

## DISCUSSION

Results from the characterization tests demonstrated that the soils segregate in relation to disposal practices. In general, the coarse-grained dredge sediments have commercial value and are disposed in isolated containment dikes where they can be harvested for beneficial use. Finer grained dredged sediments are sluiced to containment dikes where they are allowed to gravity settle and consolidate under self-weight. Significant differences were measured as a function of disposal location, with significant differences quantified in all physical characteristics. The total organic contents of the fine-grained soils (12A-1, 13A) are approximately 4%

higher than the TOC of the coarse-grained soils, which will impact the mechanical properties of dredged soils, including strength and deformability. Additionally, the organic matter in the soils will increase chemical activity, as well as physiochemical and microbiological processes (Malkawi et al., 1999).

While the TOC method measured the amount of CO<sub>2</sub> produced during the combustion process, the mass loss of other mineral phases was not quantified using this technique. Consequently, the loss on ignition (LOI) method, and dual atmosphere Thermogravimetric analysis (TGA) method were also applied to the samples to help identify other sources of mass loss as a function of mineralogy. During combustion, iron present in the mineral structures is oxidized to iron oxide phases, such as hematite. The reddish color is an indicator of structural iron that was transformed into iron oxides at high combustion temperatures. XRD tests are in process to confirm the mineral phases that were involved in the transformation to iron oxide. The mass loss quantified by the LOI and TGA methods were in close agreement and yielded approximately 15 to 20% in fine-grained soils, compared to approximately 3% in coarse-grained soils.

For the dredged sediments tested in this study, increasing organic matter content resulted in increased optimum water content and decreased maximum dry unit weight (Hamouche and Zentar, 2020). Organic material absorbs water, resulting in a sponge-like and soft consistency, thus reducing the soil's compatibility by increasing the stability of the soil and also by retaining more water that absorbs energy during compaction (Malkawi et al., 1999). For use as a fill material, the soil will have highest unit weight when the water content is at

optimum, where the fill soil will exhibit the lowest deformability.

From an engineering perspective, the high organic content, low maximum dry densities, and high optimum moisture contents of CH and SC would restrict the usage to non-structural fill applications. In general, the presence of high organic content in the soils may lead to long-term decomposition settlements attributable to biodegradation. However, this would not affect the usage of CH and SC in non-structural fill applications, for example, on a road embankment where the material does not have to sustain high loads. SP and SP-SM soils can be used as materials for structural fill. In other words, dredged soils with high-strength, low-organic content and less than 10% of fines can be used as structure fill while the soils with high-organic, low-strength and high fine contents (more than 10%) will serve as non-structural fill.

## CHAPTER 4. USE AS AN AGGREGATE

This chapter covers the possibility of processing river sediment samples for use as aggregate in concrete. This will include their use as a fine aggregate and as a lightweight aggregate (LWA). Fine aggregate testing will be conducted for their use in structural concrete mixes, in accordance with ASTM C33 (C33, 2018). Additional sediment samples will be processed into lightweight aggregates. The general requirements for lightweight aggregates are based on bulk density ( $<1120 \text{ kg/m}^3$ ). In order for these aggregates to be utilized in concrete mixes, additional data on gradation and compressive strength will be needed. There is a specific sub-category of LWA called lightweight expanded clay aggregates (LECA). This material possesses a porous core and is generally more valuable since it tends to possess a lower density and can be used in a wider range of applications.

## **FINE AGGREGATE TESTING**

### **Standards for Fine Aggregates**

The river sediment was tested for fine concrete aggregates, following standard test methods listed in ASTM C33 (C33, 2018). Should these samples pass ASTM C33 it would mean that untreated river sediments might be able to be marketed as a fine aggregate mixture for standard use concrete. Among all of the river sediment samples collected, sample 13B-1 was chosen for this purpose due to its high sand content. Before testing, samples were first dried in a 110 °C oven overnight and then screened with a No. 4 and No. 200 sieve to remove over/undersized aggregates and shells.

### **Particle Size Distribution**

The particle size distribution of sample 13B-1 after being screened was conducted in accordance with ASTM C136 (C136, 2020) which specifies standard sieve analysis. Analysis was conducted utilizing 1/2 in, Nos. 4, 8, 16, 30, 50, and 100 sized sieves. A full particle size distribution of sample 13B-1 can be seen in

Figure 36 which is plotted alongside the maximum and minimum size for fine concrete aggregates classification listed by ASTM C33.

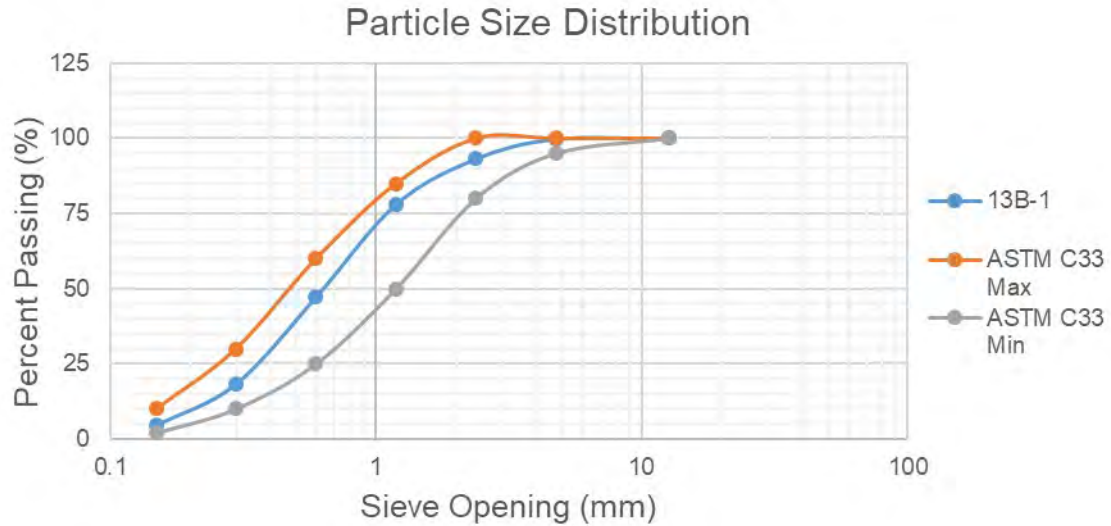


**FIGURE 36. GRAPH. PARTICLE SIZE DISTRIBUTION OF SAMPLE 13B-1.**

Figure 36 shows that sample 13B-1 passes ASTM C33 standards for particle size distribution and therefore can be classified as concrete fine aggregate. Additionally, in the event that the river sediment does not pass ASTM C33, it may still be utilized as a mortar or masonry sand. Those standards require a finer particle size distribution than what is listed here. In addition, the particle size distribution is generally dense (or continuous) which is ideal for particle packing. Other particle size distributions generally allow for more void space, which would lead to lower end strengths.

## Clay Lumps and Friable Particles

Since clay can clump together into large agglomerations, it can be accidentally measured in the particle size distribution as a sand particle. This can create issues with workability and strength of concrete as clays can absorb a large amount of water and break apart upon wetting. As such, limiting the quantity of clay lumps and friable particles is necessary for the use of these materials as concrete aggregate. This clay quantity is measured via ASTM C142 (C142, 2017) by allowing the aggregate to soak for 24 hours before wet sieving it and determining the mass difference before and after the sieve. These results are then reported as a percentage weight change as seen in Table 6. It can be seen that sample 13B-1 passes experimental tests for clay lumps and friable particles.

**TABLE 6. CLAY LUMPS AND FRIABLE PARTICLES FOR 13B-1.**

Wt. %	
Percent Clay Lumps and friable Particles	0.8%
Maximum ASTM C33 limit	3%

## Deleterious Substances

The deleterious substances test is a measurement of how organic substances and other deleterious substances affect the performance of concrete mixes. Organic substances essentially behave as void space and as such, they may significantly affect compressive strength. Standard test methods for testing deleterious substances are described in ASTM C40 (C40, 2020). For this test, 2 in mortar cubes were prepared and tested in accordance with ASTM C109 (C109, 2020), using the river sediment in its natural form, while a second set is cast using cleaned dredge material. The dredge material was cleaned by wetting the sample with a 3% NaOH solution which was then steadily drained and diluted with DI water until the pH of the solution reached the same pH of ordinary DI water (~7). The cleaned river sediment should then possess a negligible amount of deleterious substances. All tested mortar cubes were then cured in a 100% humidity hydration chamber for 24 hours at 23 °C (room temperature). Cubes were then submerged in a saturated calcium hydroxide (CH) solution at 23 °C until compression testing was performed at 7 days. The cleaned river sediment should possess a greater compressive strength compared to the uncleaned samples. If the cleaning increases the compressive strength by more than 5% then the deleterious substances significantly affect sand performance and cannot be utilized. The results for this test method are listed in Table 7.

**TABLE 7. DELETERIOUS SUBSTANCES FOR SAMPLE 13B-1.**

Deleterious Substances	
% Difference	76%
Minimum ASTM C33	95%
Confirmed (Y/N)	N

It can be seen in Table 7 that the river sediment contains a significant amount of deleterious substances which affects the compressive strength of the resulting mortar. Therefore, if a Savannah River sediment is to be used as a fine concrete aggregate, it will need to be cleaned of organic substances first.

### **Alkali Silica Reactivity**

The screened river sediment was also tested for its alkali silica reactivity (ASR) potential, utilizing the accelerated mortar bar expansion test (AMBT). Mortar mixes were made in accordance with ASTM C1260 (C1260, 2014) and cast into 1x1x11.25 in molds, utilizing both the tested river sediment (13B-1) and a standard sand that passes ASTM C33. Mortars were cured in a 100% hydration chamber for 24 hours at 23 °C before being demolded. Samples were then submerged into a water container at 80 °C for 24 hours in order to allow for any already present alkalis to dissolve into the water. The water was then drained, and zero-day length measurements were taken. The samples were then submerged in a 1M NaOH solution at 80 °C for the full duration of the test. Samples length was measured

periodically until Day 14. According to ASTM C1778 (C1778, 2020) an AMBT expansion of  $>0.1\%$  at 14 days may be at risk of potentially damaging ASR expansions. Results for these AMBT tests can be seen in Figure 37.

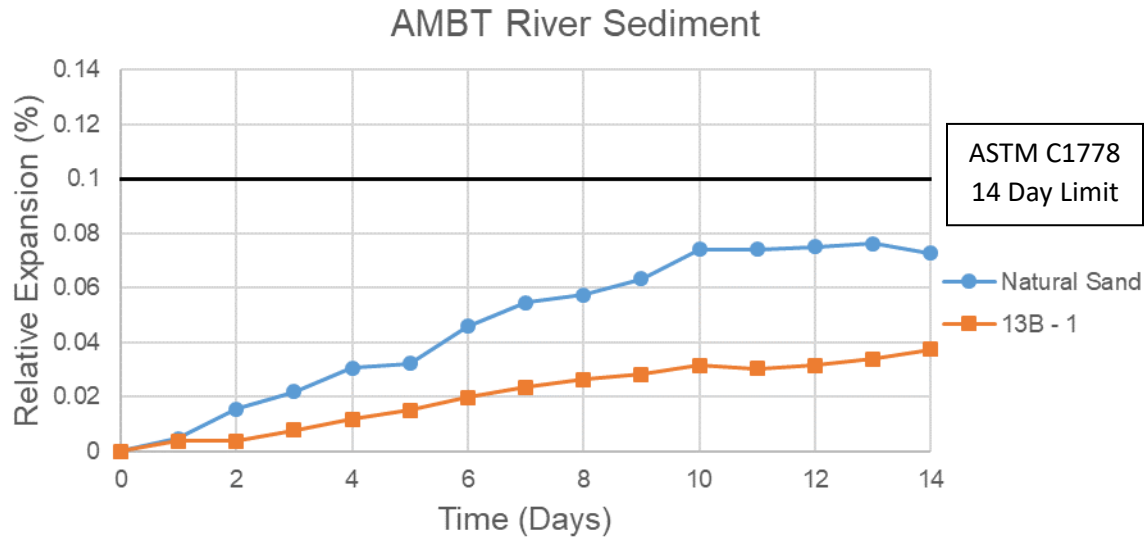


**FIGURE 37. GRAPH. 14 DAY AMBT TEST (ASTM C1260).**

Results for the AMBT test shows that the 13B-1 river sediment sample passes the standards listed by ASTM C1778 for alkali aggregate reactivity. The river sediment sample also performs better than the natural sand that is typically used for mortar/concrete mixes.

## **LIGHTWEIGHT EXPANDED CLAY AGGREGATE**

Lightweight expanded clay aggregates are typically produced from clay sources to create aggregates with porous cores. The samples used for fine aggregates possessed little clay content and could not be utilized in this application. Larger quantities of clay contents are required for the aggregates to be a binder. In this section, these sediments will be processed utilizing traditional lightweight aggregate production methods and are measured for physical properties.

### **Literature Review**

Lightweight expanded clay aggregate (LECA) is usually a gravel-sized aggregate (> No. 4 Sieve) which possesses a density of < 75% of normal weight aggregates (or a bulk density of < 1120 kg/m<sup>3</sup>) (C330, 2017). These aggregates typically present similar properties (compressive strengths, conductivity, etc.) as normal weight aggregates, but the lowered density contributes to a lower unit weight of the resulting concrete mix. This reduces the dead load of the resulting concrete mixes, leading to lower labor costs. Additionally, the low weight allows for more flexibility in design. The high porosity characteristic of lightweight aggregates

may allow for internal curing and for improved thermal insulation properties. In addition to their use in concrete mixes, they can also be marketed for a number of other applications (Rashad, 2018). These alternative applications include: 1) structural backfill for geotechnical applications, especially for retaining walls, foundations, etc.; 2) use as a wastewater filter in water treatment facilities, especially for drinking water, industrial wastewater, and farm water; 3) use as a growing medium in hydroponics. In addition to this, lightweight aggregates possess a greater capacity for fire resistance in comparison to normal weight aggregates, which allows them to retain strength at 300-600 °C (the temperature wood burns at).

Lightweight aggregates can be produced with a number of different raw materials including clays, shales, and slates. Other materials, such as blast slag, can be used as a substitution, but clays, shales and slates are the most common. Despite the variety of raw materials, all lightweight aggregates are produced through very similar processes.

The normal production process is started by grinding and screening the raw material. The material is then usually formed into spherical or oblong shapes utilizing a pelletizer or hoppers. Formed material is then fed into a rotary kiln at 1100-1300 °C before being rapidly cooled, and the final product should have a volume of between 5-6 times that of the raw material (Rashad, 2018). During the heating process, most components are liquefied, and any combustible materials such as organics, evaporating water, and mineral oxidation, are gasified. The liquefied combustion product is then rapidly cooled down in order to allow the

gasified materials to be entrapped in its structure. This leads to two distinct sections for lightweight expanded clay aggregates: an expanded, low density porous core (due to the entrapped air created from gasified solids in the structure) and an outer edge characterized by a thin, solid ceramic shell which provides strength in the aggregates. A commonly marketed LECA can be seen in Figure 38, where the shell and expanded porous core can be distinguished.



**FIGURE 38. PHOTO. COMMONLY MARKETED LECA (RASHAD, 2018).**

In order to determine whether a sediment sample qualifies for use as a lightweight aggregate feed-stock, it must first contain a proper chemical composition as defined by Charles Riley in 1950. In his study, he classified the chemical composition of various types of bloating (expanding) or non-bloating clays as shown in Figure 39 (Riley, 1950). Through this figure it can be seen that bloating clays typically possesses a chemical composition of 48-80%  $\text{SiO}_2$ , 8-25%  $\text{Al}_2\text{O}_3$ , and 5-25% miscellaneous oxides (Wei, Yang, lin, Chuang, & Wang, 2008).

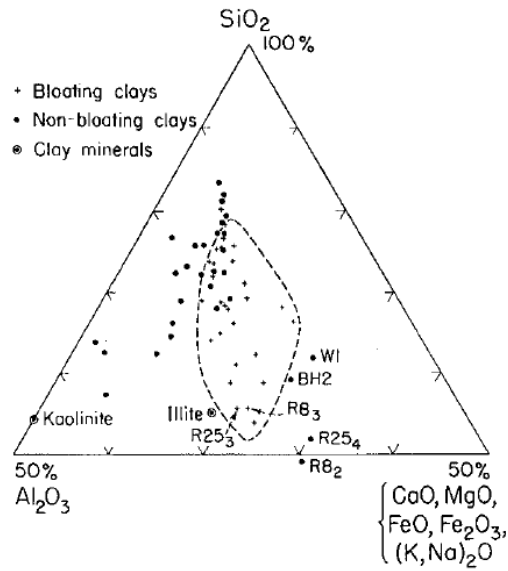


**FIGURE 39. GRAPH. COMPOSITION DIAGRAM OF BLOATED CLAYS (RILEY, 1950).**

These river sediments can be plotted onto Figure 39 in order to determine if they behave like a bloating clay. It can also be seen in this figure that kaolinite does not typically behave as a bloating clay, likely associated with the early temperatures it de-hydroxylate's at. In contrast, the clay mineral Illite (chemically similar to muscovite) is very close to the composition of bloating clays and would only require small additions of silica and miscellaneous elements to be considered a bloating clay. Additionally, a sediment containing carbonates or iron-bearing elements would actually be beneficial as a bloating clay, as those materials will release carbon dioxide or oxygen at relatively higher temperatures.

Yu-Ling Wei already completed processing river sediments into lightweight expanded clay aggregates in 2008 (Wei, Yang, lin, Chuang, & Wang, 2008). In this research, he successfully creates lightweight aggregates from harbor sediments

which pass density and strength measurements. While the chemical composition of our material and his does differ to some degree (Savannah River sediments possess more silica on average), his work shows promising results and can be considered a reference for the production of LECA from river sediments for this specific case.

### **Production of Lightweight Expanded Clay Aggregates**

In our situation, a sediment with a non-ideal chemical composition may still work as river sediments can contain a significant organic content, which will gasify upon exposure to high temperatures. Conversely, most samples measured possess large amounts of quartz, which may disqualify it for use as a LECA. However, it may be possible to process this material into a bloating clay through a simple screening to remove excess silica. Four dredge samples were chosen for LECA production testing based on sand content of the dredge. Samples 14A-1 and 14A-2 were chosen due to their excessively high sand content (>95%), sample 13A was chosen due to its kaolinite content (~20% by weight), and 13B-2 was chosen due to its muscovite content (~50% muscovite). The purpose of this was to determine if these materials can be properly processed into lightweight aggregates, even with the variety in composition. These samples were dried and

crushed but not screened, as it was necessary to determine if the original material could be successful without additional processing. Dredge samples were mixed into a VPM-30 Vacuum Power Wedger (Figure 40) with enough water to put the dredge into a plastic state. This generally led to a water content of approximately 50%, which is, on average, slightly greater than what the sediments possess in their natural state (Figure 41).



**FIGURE 40. PHOTO. VPM-30 VACUUM POWER WEDGER (PUG MILL).**

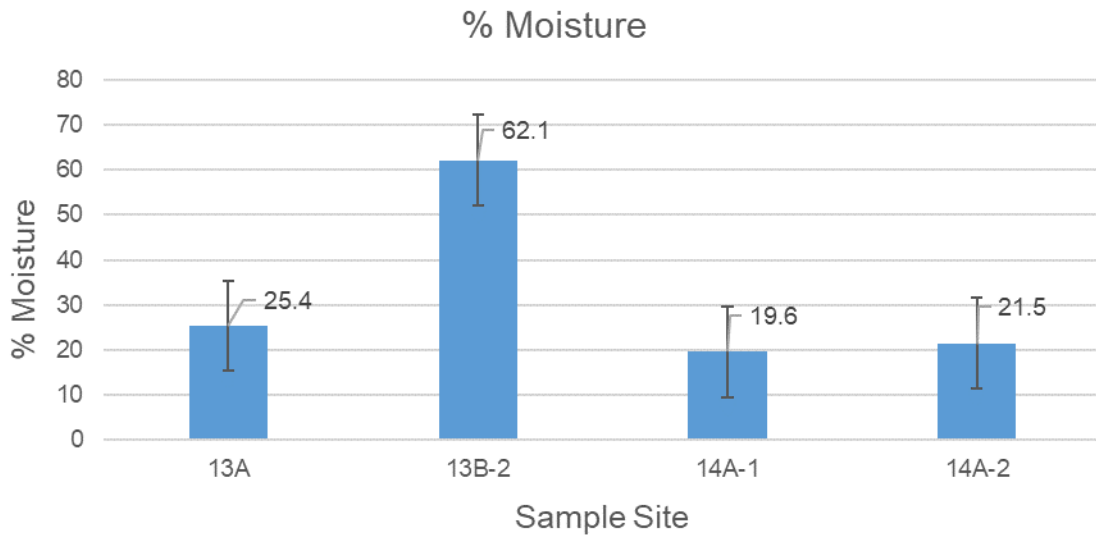


**FIGURE 41. GRAPH. MOISTURE CONTENT FOR LWA TESTED SEDIMENTS.**

The dredge was then extruded at various shapes and sizes before being shaped into either spherical or cylindrical shapes. Samples were then placed into a muffle furnace and heated at a rate of 5 °C/min until they reached 1150 °C and were held for a period before being air-dried. Variables tested include the heating pretreatment, rest time, sample size, and sample shape.

Tested sample shapes and sizes include a sphere with a 1.25" diameter, and cylinders with 0.5" and 3/8" diameters. In addition to variations in sample size, variations on a sample's thermal pretreatment were studied including holding the samples at 110 °C and at 830 °C. Additionally, the materials were tested for variations in rest time after the raw sediment was molded.

## Lightweight Aggregate Proof of Concept

The initial screening of the material was completed with 1.25" diameter spheres. Samples 14A-1 and 14A-2 contained too much sand to properly bond and fell apart soon after heating. These samples were not included in future proof of concept tests as they cannot be improved upon. Sample 13A properly bonded but did not bloat (no porous core), resulting in a homogenous brick-like aggregate. Sample 13B-2 bonded properly and contained the expanded porous core and ceramic shell characteristic of commercially available LECA (Figure 42).

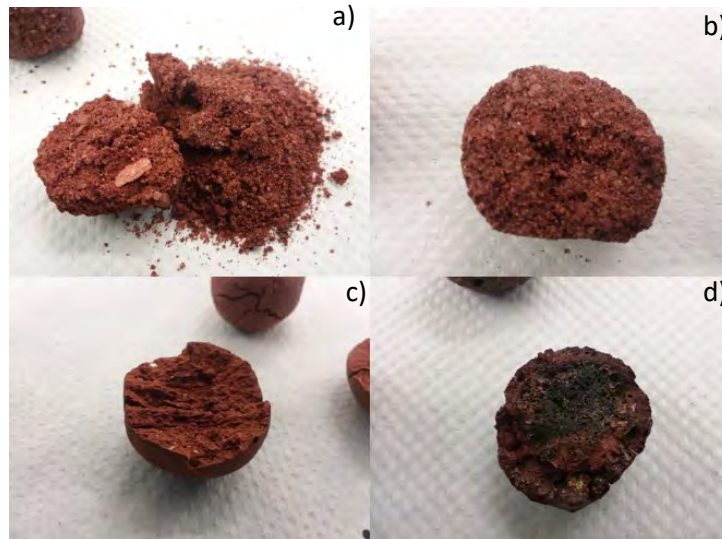


**FIGURE 42. PHOTOS. LECA INITIAL PROOF OF CONCEPT 14A-1 (A), 14A-2 (B), 13A (C), AND 13B-2 (D).**

Smaller cylindrical samples (1/2" and 3/8" diameter) were created with sample 13B-2 and were tested in a variety of ways in order to create a porous core. Samples were extruded using a pug mill at the same water content as in previous

cases. These series of tests measured: 1) preheating temperatures, 2) maximum temperature holding times, 3) cooling times, and 4) resting Times. A full write-up of all the heating schemes tested is listed in Table 8.

**TABLE 8. LECA HEATING PROCESSES.**

Heating Methods					
Heating Id. No.	Resting Time	Pretreatment (°C)	Max Temp (°C)	Hold Time (Min)	Cooling
V.1	None	None	1150	60	Left Overnight
V.2	None	None		60	Air Cooled
V.3	None	110 and 830		60	
V.4	None	110		60	
V.5	None	110 and 830		10	
V.6	None	None		10	
V.2.1	2 Days	None		60	
V.2.2	7 Days	None		60	

Small-scale aggregates sintered with original method (V.1) failed to create a porous core. As such, from here on, the samples were removed from the muffle furnace in order to allow for a quicker cooling time (V.2). Samples created utilizing this method contained a porous core characteristic of LECA, as seen in Figure 43 (left picture), though some samples did shatter later due to the expansion. Preparation method V.3 pretreated samples at 110 °C and 830 °C before heating the samples at 1150 °C similar to how Wei prepared his harbor sediments in the production of LECA (Wei, Yang, Lin, Chuang, & Wang, 2008). Resulting samples did not possess an expanded core and did not shatter. As such, most of the gasification likely occurs around 800 °C before the samples solidify. In this regard, the 830 °C pretreatment is removed for treatment V.4. In these samples, shattering once again occurs in the expanded core aggregate. In an attempt to increase the size of the expanded core and to reduce possible cost, the samples were held at 1150 °C for 10 minutes instead of 1 hour. For test method V.5, the samples were

pretreated at 110 °C and 830 °C before holding samples at 1150 °C for 10 minutes. Samples once again did not contain any expanded core; reasons for this are attributed to the 830 °C pretreatment (Figure 43, right). Heating method V.6 involved no preheating at 1150 °C and the samples were held for 10 minutes before being removed from the furnace and air-cooled. These samples also contained expanded cores characteristic of commercially available LECA.



**Figure 43. Photos. Small scale LECA with (left) and without (right) expanded core.**

It was determined through the tests that heating method V.6 is the most useful for small-scale tests, although pretreatment at 110 °C will likely be necessary for large scale production. This pretreatment will counteract the high water content characteristic of river sediment. This is because the plastic state of the raw material will likely cause the feedstock to breakdown with the agitation present in rotary kilns.

The next LECA preparation method to be tested is resting time. The raw dredge material was initially dried at 110 °C for storage purposes. This means that any hydrated phases would have lost their structural water. It takes some time for

these elements to rehydrate so the water would likely be considered free water if prepared right away, which might vaporize at lower temperatures (Grim & Bradley, 1948). Allowing the sediments to rest after wetting them may allow these phases to rehydrate, which leads to water release at higher temperatures. In order to test this, sample 13A was blended and allowed to rest for 2 and 7 days before being tested in accordance with the V.6 heating method. Images for the resulting aggregates can be seen in Figure 44. Samples allowed to rest for 2 days did not contain a core, but the aggregates tested at 7 days contained a distinctive core with a different coloration (black core with an orange shell).



**FIGURE 44. PHOTO. SAMPLE 13A WITH A 2-DAY (V.2.1) AND 7-DAY (V.2.2) REST TIME.**

The core does not seem to be very porous; however, the additional resting time may cause the sediment to bloat. Mezencevova observed similar cores in their production of bricks from similar materials (Mezencevova, Yeboah, Burns, & Kahn, 2012). This is an important aspect to note, as the river sediment may need

to be dewatered before being transported. Depending on how these materials are dewatered, these hydrated phases may need to be reformed in order for proper bloating to occur. A full summary on the results of the proof of concept LECA tests can be seen in Table 9.

**TABLE 9. RESULTS OF LECA PRODUCTION ATTEMPTS.**

Sample Tests				
Sediment Sample	Heating Method	Aggregate Shape	Results	Success (Yes/No/Partial)
13A	V.1	1.25" Sphere	Successful Bond, No expanded Core	Partial
13B-2			Successful Bond with expanded Core	Yes
14A-1			No Bond	No
14A-2			No Bond	No
13B-2	V.1	0.375-0.5" Cylinder	No Expanded Core	No
	V.2		Expanded Core but Shattered	Yes
	V.3		No Expanded Core	No
	V.4		Expanded Core but Shattered	Yes
	V.5		No Expanded Core	No
	V.6		Expanded Core but Shattered	Yes
13B-2	V.6	1.25" Sphere	Expanded Core	Yes
13A	V.2.1		No Expanded Core	Partial
13A	V.2.2		With Core	Yes

ASTM C330 specifies the standards used for the production of structural lightweight aggregates. These standards describe requirements for particle size, bulk density, and concrete strength. To measure this, samples 13A and 13B-2 were produced with the spherical aggregates in accordance with heating method V.6.2 and V.6 respectively. In this scenario, producing the quantities of aggregates necessary for C330 testing is not practical due to the need to hand shape every aggregate. As such, only the dry density and specific gravity were determined via water displacement (determining lightweight concrete strengths should be determined in future works). These results can be seen in Table 10. Both dredge materials possess specific gravities and dry densities of ~1 and ~1000 kg/m<sup>3</sup> respectively. While this data cannot be directly compared to standards listed in

ASTM C330, it can be utilized to predict the performance of the final aggregate. ASTM C330 defines lightweight aggregates as any aggregate possessing a bulk density of  $<1120 \text{ kg/m}^3$  (C330, 2017). Samples measured for bulk density will typically contain greater quantities of void space. As such, the bulk density would be even lower than the dry density. Since the dry density for both samples already passes the ASTM standard, the bulk density should also pass.

**TABLE 10. SEDIMENT LECA PHYSICAL PROPERTIES.**

LECA Physical Properties	LECA	
	13A	13B-2
S.G. (-)	1.07	1
Dry Density ( $\text{kg/m}^3$ )	1062	998.6

While both samples (13A and 13B-2) would technically qualify as lightweight aggregates, only sample 13B-2 bloats and possesses a porous core, (see Figure 42). The porous core is not necessarily required for the samples to qualify as lightweight aggregates, but these samples generally perform better as they possess lower density and greater thermal qualities while retaining compressive strengths. The main difference between 13A and 13B-2 is that sample 13B-2 is collected from a sediment feedstock with a majority of muscovite and other 2:1 clays (described in chapter 5.1.2). Therefore, while it may be possible for any sediment samples to be produced into LECA as long as the sand content is low enough, it is preferable to utilize sediment feedstock with similar or greater quantities of muscovite than that of sample 13B-2. Samples with large amounts of kaolinite (such as 13A) may be better utilized as a supplementary cementitious material as described in chapter 5.

## CHAPTER 5. USE AS A SUPPLEMENTARY CEMENTITIOUS MATERIAL

Supplementary cementitious materials (SCMs) are a group of materials that, when ground to a fine powder, can replace a percentage of ordinary portland cement (OPC) in a cementitious material mix. Such mixes can possess improved strength, workability, and durability depending on what material is utilized. SCMs are separated into two distinct categories: hydraulic or pozzolanic materials. The primary difference between the two is in how they produce calcium silicate hydrate gel (C-S-H gel), which is the primary strength-giving phase in cement paste. Hydraulic materials react directly with water to form C-S-H similarly to cement and tend to possess large quantities of CaO in their chemical makeup. Pozzolans are primarily constituted of amorphous silica or aluminate-silicate powders. Such materials react with calcium hydroxide, produced as a byproduct of cement hydration, and water to form additional C-S-H (Mehta, 1987). Due to this dependence on the formation of cement hydration byproducts, pozzolans as a whole tend to react more slowly than hydraulic materials but tend to create more durable cementitious mixes.

In the case of Savannah River sediment, most samples contain some quantity of clay, primarily kaolinite and muscovite. These materials can be produced into pozzolanically active materials (described in section 5.1.2 and 5.1.3) and possess relatively little quantities of calcium-bearing minerals. As such, processed sediment will be tested as a Class N (or natural) pozzolan in accordance with

ASTM C618 (C618, 2019). Pozzolanic reactivity is traditionally measured with thermogravimetric analysis and isothermal calorimetry (section 5.4). These methods are indirect, however, and are heavily dependent on the types of cement used in the mix.

## **SOURCES OF POZZOLANIC REACTIVITY**

### **Kaolinite De-Hydroxylation**

Most clays are, by definition, some type of alumina silicate powder (Fernandez, Martirena, & Scrivener, 2011). Typically, clays are composed of layers of tetrahedral silica sheets and octahedral alumina sheets with some form of ion bonded between them. Clays are classified as 1:1 with one sheet of silica per sheet of alumina or 2:1 clays with two layers of silica sheets per layer of alumina. Therefore, when the clay is amorphous, it can be considered a natural pozzolan. However, most clays are highly structured crystalline materials in their natural state, which disallows ions from dispersing into pore solutions and reacting with calcium hydroxide. As such, they need to be processed in order to become amorphous. This can be accomplished in a number of ways, but the simplest and most common method is calcination (or heat treatment). Clays typically incorporate

hydroxyl groups in their crystal structure, as seen in the crystal structure of kaolinite in Figure 45, which is a 1:1 clay with no interlayer ions.

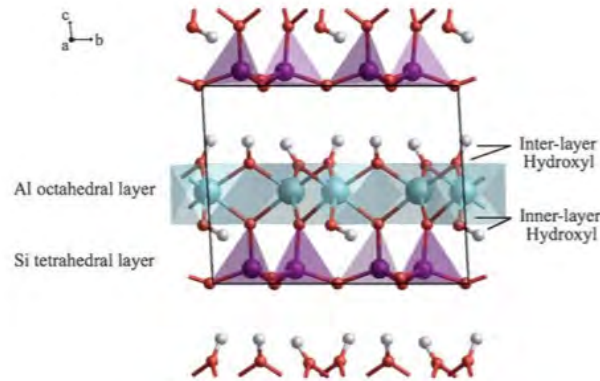


**FIGURE 45. ILLUSTRATION. STANDARD CRYSTAL STRUCTURE OF KAOLINITE (SPERINCK & WRIGHT, 2010).**

When heated up to 400-600 °C clay kaolinite goes through a process called de-hydroxylation (Snellings, Horckmans, Bunderen, Vandewalle, & Cizer, 2017). In this process, the hydroxyl groups leave the structure in the form of water. The crystal structure of the clay restructures itself and the structure becomes amorphous. When kaolinite de-hydroxylates it converts into metakaolin, which is already considered a very highly reactive pozzolan (this process can be seen in Figure 46). Higher levels of heat, typically between 600-900 °C, make these hydroxyl groups release more violently increasing levels of disorder and create more reactivity (Hollanders, 2016). Since kaolinite is a common element present in the Savannah River sediment, it can be considered the primary reactive phase in sediment samples. When heating kaolinite to levels between 925-950 °C, metakaolinite recrystallizes and forms Spinel. At temperatures above 950 °C, the

spinel will reform into crystalline mullite. This means that temperatures above 900 °C leads to a drop in pozzolanic reactivity due to the loss in structural disorder.

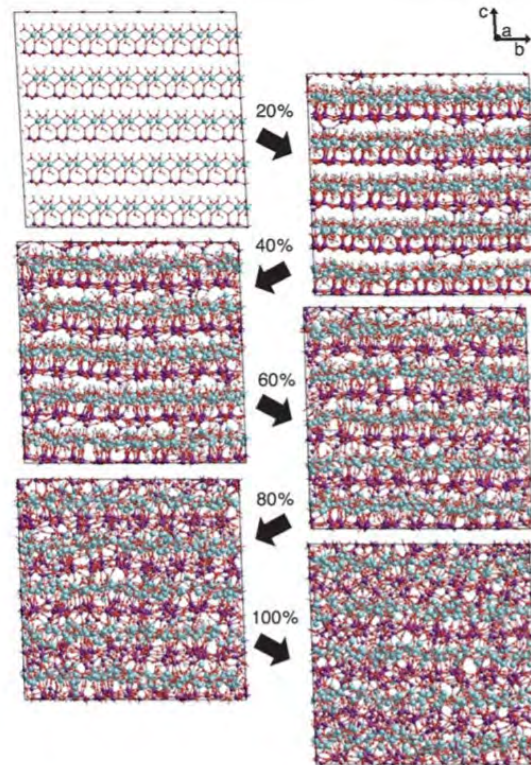


**FIGURE 46. ILLUSTRATION. SIMULATED KAOLINITE STRUCTURE WITH INCREASING LEVELS OF DE-HYDROXYLATION (SPERINCK & WRIGHT, 2010).**

### **Other Sources of Pozzolanic Reactivity**

Another common clay mineral present in large quantities in Savannah River dredge sediments is muscovite. Muscovite, while technically classified as a type of mica, is characterized by the chemical composition and crystalline structure

characteristic of clay minerals. This material possesses the structure and composition of a 2:1 clay with potassium present as interlayer ions (He, Bjarne, & Makovicky, 1995) (He, Makovicky, & Osbaeck, 1995). The exact definition of clay can vary depending on the industry. Most geotechnical engineers define clays as soil materials smaller than 2  $\mu\text{m}$ . Silts are defined as a soil material between 2-75  $\mu\text{m}$  with sands and gravels possessing larger particle sizes. Since muscovite can exist in larger particle sizes, it is frequently considered to be a type of mineral, despite its chemical composition. This material is structurally and chemically similar to illite with the only difference being the morphology of the material. Illite can therefore be used as a comparison when determining the possible pozzolanic reactivity of muscovite. Studies completed by Rodrigo Fernandez investigate the de-hydroxylation of various clay minerals, including illite. He determined that the de-hydroxylation of clay minerals depend on the amount and location of hydroxyl groups in the clay structure (Fernandez, Martirena, & Scrivener, 2011). While muscovite can de-hydroxylate, it does so at higher temperatures (500-700  $^{\circ}\text{C}$ ) compared to kaolinite. In addition, due to the relatively low amount of hydroxyl groups present in muscovite, the overall degree of disorder is lower as well (Bernal, 2017) (Fernandez, Martirena, & Scrivener, 2011). The pozzolanic reactivity of muscovite has been measured in the past, and it was discovered that it possesses a small degree of pozzolanic reactivity fit for non-structural applications. For the sake of practicality, most researchers consider muscovite entirely non-reactive.

Most river sediments typically contain amorphous silica in their coarser aggregates due in part to the presence of shells from marine life. While in most

cases such as amorphous silica will behave like reactive aggregates, when such aggregates are smaller than 100  $\mu\text{m}$  they behave like pozzolans. As such, this can likely be considered to be a source of pozzolanic reactivity.

Diatoms are a type of single celled algae, which typically exist in marine or aquatic environments. Diatoms are composed of approximately 90% amorphous silica with minor amounts of alumina and ferric oxide. This chemical composition, accompanied by the diatoms' relatively small particle size (2-200  $\mu\text{m}$ ), may lead to their classification as a Class N pozzolan (Sierra, Miller, Sakulich, MacKenzie, & Barsoum, 2010). In our case, the river sediment will be screened so that particles larger than 90  $\mu\text{m}$  will be removed from the material. The existence of diatoms was previously confirmed in the raw material (Section 2.4). Scanning electron microscopy was used to confirm that the diatoms continue to exist even after calcination (Figure 47).

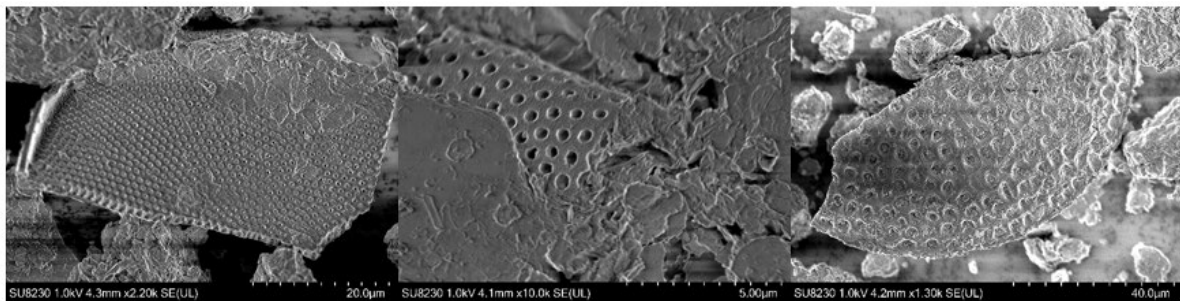


**FIGURE 47. PHOTO. MICROSCOPY OF SAMPLE 12A-2 (LEFT), 13A (MIDDLE), AND 14A-1 (RIGHT) AFTER CALCINATION.**

## SCM PRODUCTION OPTIMIZATION

### Materials

All experimental mixes tested in Chapter 5 utilized the Type I/II cement produced by Argos. A commercially available metakaolinite was utilized as a reference material. This metakaolin possesses a >99% purity and was purchased from the Burgess Pigment Company. The elemental composition of the cement and metakaolin can be seen in Table 11. Commercially available polycrystalline quartz was used as a reference in the form of a non-reactive SCM. This quartz was purchased from U.S Research Nanomaterials Incorporated and possesses an average particle size of 45  $\mu\text{m}$  at >99% purity. Please note that if portland cement, metakaolin, or nonreactive quartz is referred to in future sections of chapter 5 that it is referring to the materials in this section.

**TABLE 11. CHEMICAL OXIDE COMPOSITION OF CEMENT AND METAKAOLIN.**

Oxide Content (Wt. %)	Type I/II Cement	Metakaolin
SiO <sub>2</sub>	20.41	51.4
Al <sub>2</sub> O <sub>3</sub>	4.82	44.8
Fe <sub>2</sub> O <sub>3</sub>	3.19	0.4
Sum of Oxides	28.42	96.6
CaO	63.01	0
SO <sub>3</sub>	2.79	0
Na <sub>2</sub> O	0.05	0
K <sub>2</sub> O	0.54	0
TiO <sub>2</sub>	0.22	1.5
MgO	3.22	0
P <sub>2</sub> O <sub>5</sub>	0.06	0
LOI	1.57	1.1
D <sub>50</sub> (µm)	15.7	1.4

### General SCM Production Process

Since kaolinite is the most reactive component, the Savannah River sediments were processed similarly to the production of metakaolin (Fernandez, Martirena, & Scrivener, 2011) (Hollanders, Adriaens, Skibsted, Cizer, & Elsen, Pozzolanic reactivity of pure calcined clays, 2016). Dredge samples were dried in an oven at 110 °C overnight in order to remove moisture. Samples were then crushed and passed through a No. 170 (90 µm) sieve in order to separate fines from the material. In ordinary circumstances, SCMs produced in this manner would be passed through a No. 200 (75 µm) sieve; however, since amorphous silica with a particle size below 100 µm acts like pozzolan, a coarser sieve was utilized to allow for a greater quantity of pozzolans to be included in the final product. The

sieved powders were then placed in a muffle furnace and heated at a rate of 5 °C/min until the calcination temperature was reached (ideal temperature to be determined). Samples were held at that temperature for one hour before being removed from the furnace and allowed to air cool to room temperature. Since kaolinite completely de-hydroxylates at 600 °C and additional degrees of disorder occur between 600-900 °C, the ideal calcination temperature will be determined between these temperatures (Fernandez, Martirena, & Scrivener, 2011).

## **Final SCM Production Process**

Sample 14A-1 was processed at 600, 800, and 900 °C with the assumption that similar results would be obtained for other samples. The reactivity of the resulting SCM was tested via strength activity index (relative strength of an SCM+OPC mortar mix compared to a 100% OPC mortar mix).

All experiments conducted in Chapter 5 utilized this cement. Three mortar samples were prepared for each product by replacing 20% of OPC weight with the processed clay. Mortars were mixed in accordance with ASTM C109 (C109, 2020) and molded into 2 in (50 mm) cubes. The samples were then cured in a 100% hydration chamber at 23 °C for 24 hours prior to demolding. Once demolded, the cubes were submerged in a saturated calcium hydroxide solution at 23 °C.

Samples were then removed at 7 and 28 days and tested for their strength activity index (SAI). Results can be seen in Figure 48.

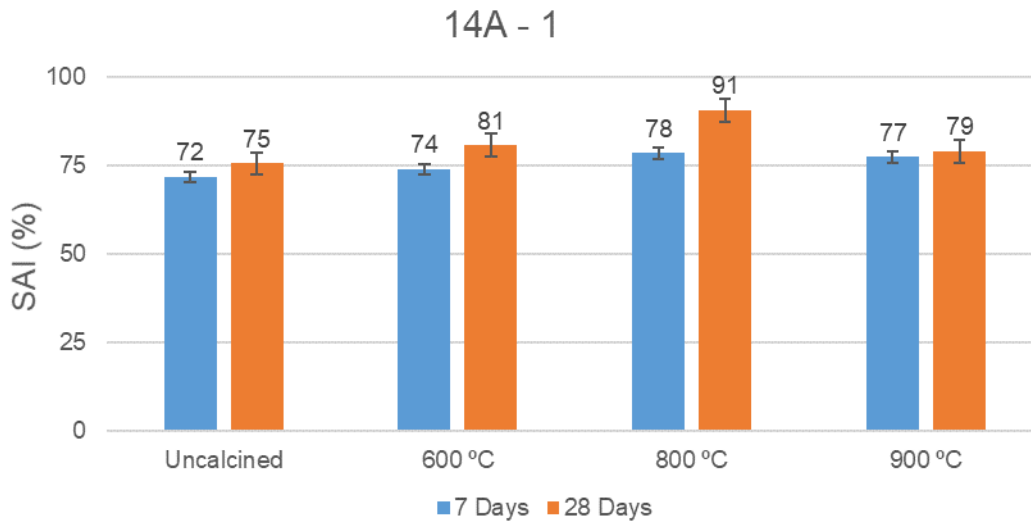


**FIGURE 48. GRAPH. STRENGTH ACTIVITY INDEX, TEMPERATURE OPTIMIZATION.**

It should be noted that ASTM C618 states that a strength activity index greater than or equal to 75% at either 7 or 28 days meets standards for Class N pozzolans. In this scenario, all of the samples tested, including the raw samples, meet these standards. Whether or not an engineer desires to actually utilize an SCM that passes ASTM C618 in this method is up to the individual. However, it can be seen that the sample calcined at 800 °C reaches the highest compressive strength both at 7 and 28 days. A possible explanation might be that calcination at temperatures 600 °C and below does not allow high levels of disorder to be reached, and the sample calcined at 900 °C likely recrystallizes leading to lower

compressive strengths. Additionally, even certain uncalcined or non-reactive SCMs may pass the strength activity index if fine enough (seen in Figure 48). It can be seen through this that the strength activity index is an unreliable method for measuring the pozzolanic reactivity. For this reason, even if all the samples passed the SAI test, additional measurements for reactivity and durability will be conducted at 800 °C. Characterization tests will specify non-calcined and calcined materials. When not specified, the calcination temperature should be assumed to be 800 °C.

## **DREDGE SCM CHARACTERIZATION**

### **Dredge Testing Procedure**

Five dredge sediment samples (12A-2, 13A, 13B-2, 13B-3, and 14A-1) were chosen for SCM testing from a wide collection area. These samples were chosen based on their mineralogical variation and on their sand content (Section 2.3). For example, sample 14A-1 was chosen in particular because of its excessive sand content as it was necessary to determine if such a material can be processed into a SCM of acceptable quality. All samples were calcined at 800 °C utilizing the procedure described in section 5.2.1. These samples were characterized by their

particle size distribution, chemical oxide composition, and mineralogical composition. Pozzolanic reactivity was determined by measuring the heat evolution during cement hydration and through the calcium hydroxide consumptions of cement paste. SCM performance was measured through the strength activity index and through ASR expansion.

## Particle Size Distribution

The particle size distribution of these sediments was determined using the same equipment and methods described in Chapter 2. The material was considered non-spherical and the refraction angle of kaolinite was used as a material constant. Samples were dispersed in ethanol and ultra-sonicated for 30 seconds before scans were taken. The results of these scans can be seen in Figure 49. The primary particle sizes (D10, D50, and D90) of the powders along with the estimated fineness of the material can be seen in Table 12.

**TABLE 12. PRIMARY PARTICLE SIZES OF HEAT-TREATED SEDIMENTS.**

	D <sub>10</sub> (μm)	D <sub>50</sub> (μm)	D <sub>90</sub> (μm)	Fineness (%)
12A-2	6.22	31.8	75.5	28.2
13A	6.29	35.7	83.3	34.4
13B-2	4.68	29.5	72.7	26.4
13B-3	5.74	31.3	61.9	22.0
14A-1	6.44	36.3	71.3	31.3

It can be seen from these figures that the treated sediments are relatively coarse. The average particle size of each element varies from 30-40  $\mu\text{m}$  with a fineness varying from 20-35%. If the particle size of a material is small enough, it can create a stronger overall concrete mix. This is caused in part by densification of the overall material, which happens when the SCM fits itself into void space between cement and aggregate grains. The other improvement caused by fine SCMs is created through nucleation effects. Having smaller particle sizes increases the surface area of the SCM thus increasing the number of “nucleation sites” available for hydration products to form on. Formation on such sites is easier than forming in solution; this increases the hydration rate of the overall material. However, these improvements are only notable when the average particle size of the material is less than 10  $\mu\text{m}$ . As such, we can expect there to be a minimal amount of particle packing or nucleation effects from the heat-treated river sediments.

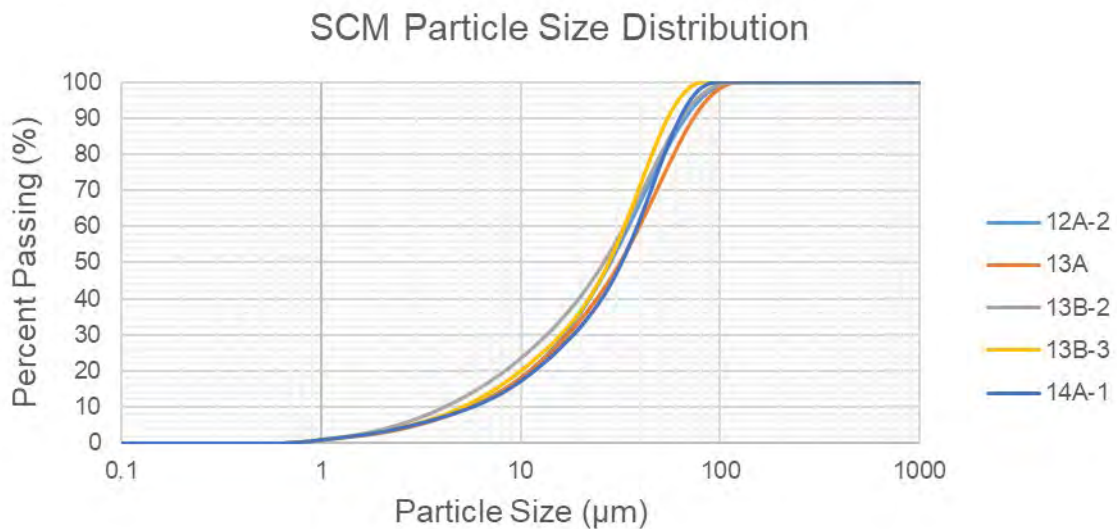


**FIGURE 49. GRAPH. PARTICLE SIZE DISTRIBUTION OF HEAT-TREATED RIVER SEDIMENTS.**

The results obtained with these scans are slightly coarser than the particle size distribution measured for the sediment fines in Chapter 2. This may be attributed to agglomerations created during the calcination process.

### **Mineralogical Composition**

The mineralogical composition of the screened river sediment samples was determined utilizing X-Ray Diffraction (XRD), using an X'Pert PRO Alpha-1 diffraction system. The samples were first screened with a No. 170 (90  $\mu\text{m}$ ) sieve before being scanned. These samples were then calcined at 800 °C and scanned again. A portion of lanthanum hexaboride (LaB<sub>6</sub>) was blended into the sediment samples at 5% wt. replacement. The LaB<sub>6</sub> acted as a reference material in order to quantify amorphous content. The results of this quantification can be seen in Table 13.

**TABLE 13. XRD PHASE COMPOSITION OF RIVER SEDIMENT.**

Phases (Wt. %)	Raw					Calcined 800 °C				
	12A-2	13A	13B-2	13B-3	14A-1	12A-2	13A	13B-2	13B-3	14A-1
Quartz	30%	18%	17%	30%	27%	37%	39%	24%	50%	43%
Kaolinite	28%	40%	38%	31%	27%	0%	2%	1%	0%	0%
Gibbsite	1%	4%	1%	0%	1%	0%	1%	0%	0%	0%
Goethite	0%	0%	0%	1%	0%	1%	0%	0%	0%	0%
Hematite	0%	0%	0%	0%	0%	2%	1%	5%	3%	2%
Calcite	0%	0%	1%	0%	1%	0%	0%	0%	0%	0%
Muscovite	40%	38%	44%	38%	45%	9%	33%	10%	14%	19%
Amorphous	0%					51%	24%	59%	32%	35%

The results of this analysis show that the raw material is composed of relatively consistent quantities of quartz (17-30%), kaolinite (27-40%), and muscovite (38-45%). Small quantities of iron bearing elements (such as hematite or goethite) are also commonly found in these elements. These compositions vary greatly in comparison with similar scans observed in Chapter 2. This is attributed to the large quantity of coarse elements in the soil, which were removed in this case. As such, the presence of certain finely-grained materials (like kaolinite) may not be a significant portion of the overall material.

After calcination, the sediment was composed of 29-59% amorphous content. This amorphous material was primarily created from the de-hydroxylation of the kaolinite and muscovite content, which was reduced to >1% and >35% after calcination respectively. The kaolinite reliably decomposed almost completely, while the decomposition of the muscovite was more variable. Despite this variability, the resulting amorphous content did not strongly correlate with either kaolinite nor muscovite content. The remaining elements also received a slight boost in their weight percentage. This was likely caused by the high loss on ignition characteristic of clays, as opposed to any increasing quantities in these elements.

## Chemical Composition

The chemical oxide content of the heat-treated dredge material was determined via X-Ray Fluorescence (see Table 14). This analysis was completed externally by Boral Resources. As requested, samples were ignited at 750 °C and passed through a No. 200 (75 µm) sieve before being sent out. Despite the relatively large variation in the mineralogy of the raw materials, the chemical composition of the overall dredge material remained relatively consistent with no elements varying by more than 5%. All of these elements possessed a primary oxide content ( $\text{SiO}_2 + \text{Al}_2\text{O}_3 + \text{Fe}_2\text{O}_3$ ) of 87-92% for all of the dredge samples. Each sediment sample possessed a sulfate content of less than 3% and an alkali ( $\text{Na}_2\text{O}_e$ ) content of less than 3.5%. While there are not any specific requirements for total alkali content for natural pozzolans, ASTM C1778 does recommend an alkali content of less than 3% to properly control the alkali aggregate reaction. Of the sediments tested, only one sample actually surpasses that limit. This does not limit the possibility of using this sample so long as the alkali aggregate reaction is properly mitigated. The LOI for each sediment (after calcination) remained  $\leq 1.1\%$ . Each of these results meets the standards listed by ASTM C618 for Class N pozzolans. It should also be noted that, while the raw material contains a significant

quantity of muscovite (a potassium-based clay) the total alkali content of the final product was still only ~3% for all samples, which limits the sediments susceptibility for the alkali aggregate reaction.

**TABLE 14. CHEMICAL OXIDE COMPOSITION OF CALCINED RIVER SEDIMENTS.**

Primary Oxide Composition						
Wt. %	ASTM C618	12A-2	13A	13B-2	13B-3	14A-1
SiO <sub>2</sub>	-	60.65	65.99	64.2	65.25	64.45
Al <sub>2</sub> O <sub>3</sub>	-	19.33	17.51	19.75	15.74	16.87
Fe <sub>2</sub> O <sub>3</sub>	-	7.42	6.99	7.69	6.32	6.58
Sum of Oxides	>70%	87.4	90.49	91.64	87.31	87.9
SO <sub>3</sub>	<4%	2.28	0.78	0.24	2.03	1.05
CaO	Report Only	2.3	1.03	0.77	3.29	3.04
Na <sub>2</sub> O	-	2.25	1.25	0.57	1.83	1.03
MgO	-	2.05	1.41	1.27	1.71	1.45
K <sub>2</sub> O	-	1.63	1.85	1.7	1.81	1.97
P <sub>2</sub> O <sub>5</sub>	-	0.37	0.45	0.48	0.38	0.79
TiO <sub>2</sub>	-	1.03	1.14	1.14	1.09	1.2
Total	-	99.31	98.4	97.81	99.45	98.43
Na <sub>2</sub> O <sub>e</sub>	Report Only	3.3	2.5	1.7	3.0	2.3
LOI (%)	<10%	1.09%	1.07%	0.99%	0.66%	0.53%

## POZZOLANIC REACTIVITY OF DREDGE MATERIAL

### Compressive Strength

Compressive strength was assessed through the determination of strength activity index of three, 2 in (50 mm) mortar cubes at 7, 28, and 56 days. These mortars were mixed and tested in accordance with ASTM C109 and C305 (C109, 2020) with a constant water-to-binder ratio of 0.485. The strength activity index is determined through the relative strength between OPC and SCM (at 20% wt. replacement) mix and a 100% OPC mix. These mixes were set in a hydration chamber at 100% humidity at 23 °C for 24 hours before demolding. Mortar cubes were then submerged in a saturated calcium hydroxide solution at 23 °C until the material was tested. The results for the strength activity index can be seen Figure 50 with its raw strength in Figure 51. These blended mortar mixes reached an average of 90% SAI by 56 days, which should remain constant for future values. The raw compressive strength of all of the mortar mixes exceeded 6 ksi (50 MPa) by 28 days. These results are respectable given the coarse nature of the dredge material, which implies a lack of benefits from particle packing or nucleation effects (Berodier & Scrivener, 2014). Additionally, the majority of the dredge material contains large quantities of crystalline, and therefore non-reactive, materials. Despite this, these materials reach relatively high compressive strengths within 85-95% of the control by 56 days. The improvements to compressive strength tend to be more significant at early ages before reaching a relatively constant value.

Ruben Snellings prepared flash calcined river dredged sediments at 865 °C (Snellings, Horckmans, Bunderen, Vandewalle, & Cizer, 2017). These sediments contained a slightly elevated alumina content and a finer particle size. However, the overall material is similar to the Savannah River sediments. Mortars mixed with

these river sediments reach relative strengths between 80 and 100% in the same time frame, similar to the strength achieved with the Savannah River sediments.

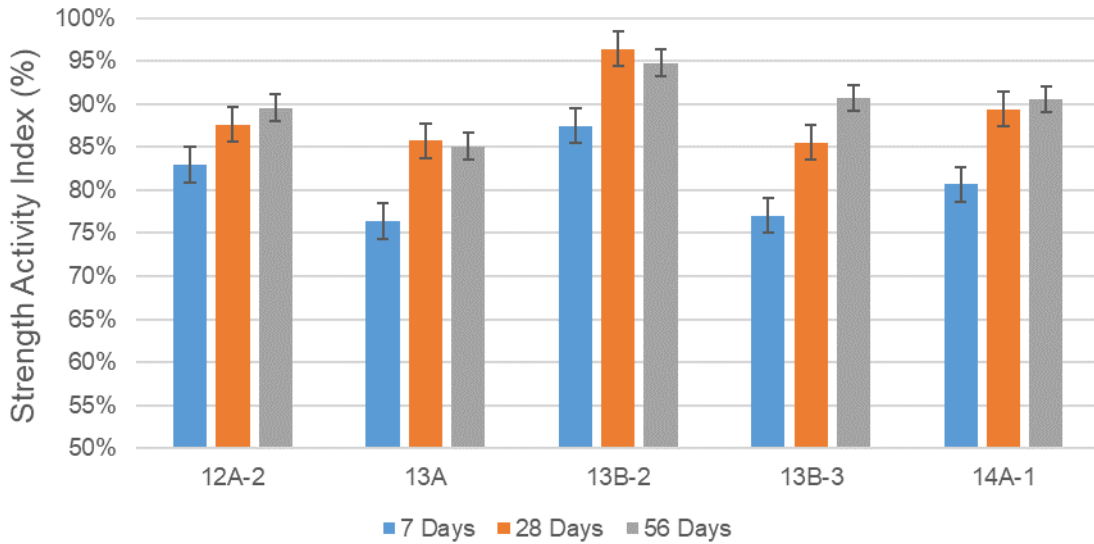


**FIGURE 50. GRAPH. STRENGTH ACTIVITY INDEX OF CALCINED RIVER SEDIMENT.**

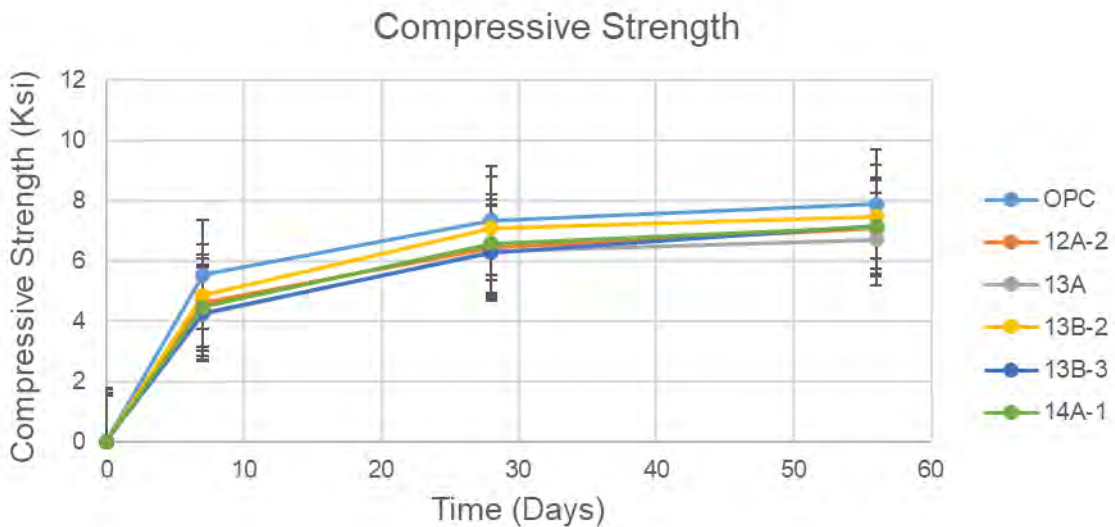


**FIGURE 51. GRAPH. RAW COMPRESSIVE STRENGTH OF CALCINED RIVER SEDIMENTS.**

## Calcium Hydroxide Consumption

The pozzolanic nature of the calcined river sediment means that the degree of reactivity can be indirectly measured via the calcium hydroxide consumption. This is accomplished through the measure of blended cement pastes using thermogravimetric analysis (TGA) in accordance with ASTM E1131. With thermogravimetric analysis, sample mass is measured with increasing temperature. Based on where samples lose mass, the composition of the sample can then be estimated.

In these mixes, blended cement pastes were mixed with a 0.4 water-to-binder ratio and a 20% weight replacement. These blended pastes were double-bagged in sample containers at 23 °C until tested at 7, 28, and 56 days. When tested, the cement paste is ground and passed through a no. 200 sieve. Then samples are loaded into the TGA where they are held in a nitrogen atmosphere. The samples are then held at 40 °C for 90 minutes to release all of the free water. This temperature was chosen because CSH gel will begin to lose bound water above this temperature (Alizadeh & Beaudoin, 2009). Samples are then heated at a rate of 10 °C/min until they reached 1000 °C. Calcium hydroxide decomposes into water and calcium oxide between 380-460 °C. The mass loss within this section is generally associated with the evaporation of the water released from

calcium hydroxide. Mass loss above this point is associated with decomposition of carbonates and remaining clay. Carbonation of calcium hydroxide was not considered during the course of this study due to the variety of mass loss sources. Once this mass drop was converted to calcium hydroxide, it was normalized by the sample mass collected after the loss of all free water. These results were then compared to mixes with cement paste blended with unreactive quartz in order to estimate the total quantity of calcium hydroxide consumed. The calcined river sediments were also compared to commercially available metakaolin prepared at a similar calcination temperature.

The results of this analysis can be seen in Figure 52. Through this analysis, we can see that the river sediments consume ~4% of the total calcium hydroxide by 56 days while metakaolin consumes ~9% by the same time. This implies that the river sediment performs at a rate of 40-45% in comparison to the commercially available metakaolin. While this result is good, what is more important to note is that the amount of calcium hydroxide consumed increases over time. This is indicative of the presence of pozzolanic reactivity in these heat-treated river sediments. The level of calcium hydroxide is strongly influenced by kaolinite purity and is mostly independent of muscovite and the overall amorphous content. If the calcium hydroxide consumed by those materials are normalized by the overall kaolinite content of the sediment, the overall influence of the miscellaneous pozzolanic elements can be seen. These datasets can be seen in Figure 53. It can be seen that the sediment SCMs consume up to 5% more calcium hydroxide kaolin

content. This improvement can be attributed to the additional pozzolanic elements listed in section 5.1.

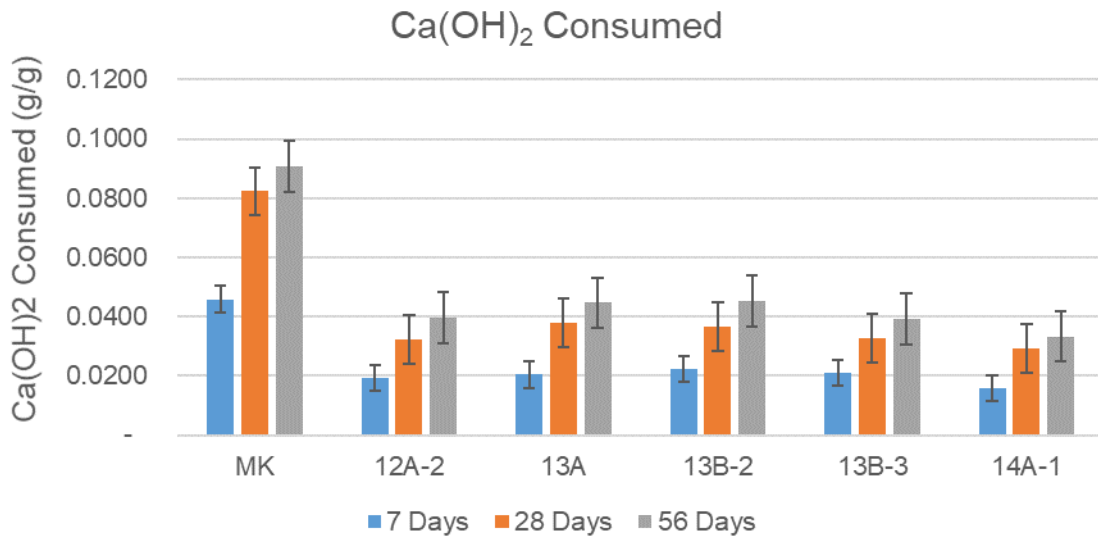


**FIGURE 52. GRAPH. CALCIUM HYDROXIDE CONSUMED BY HEAT-TREATED RIVER SEDIMENTS.**

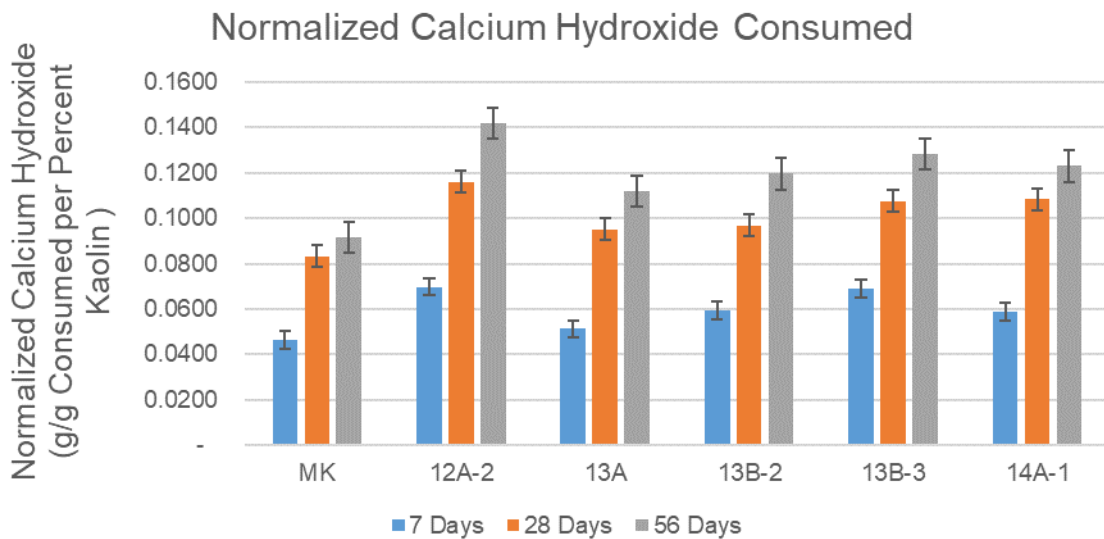


**FIGURE 53. GRAPH. CONSUMED CALCIUM HYDROXIDE NORMALIZED BY SEDIMENT KAOLIN CONTENT.**

## **Isothermal Calorimetry**

The hydraulic reactions of cement are exothermic in nature. Meaning that one can indirectly measure reactivity based on the heat released over time. The pozzolanic reaction is generally very slow and releases heat over time. As such, pozzolans are usually considered to be filler when considering the heat released over time. The only pozzolans that are an exception are silica fume and metakaolin, which actually enhance the heat released over time. Pozzolanic reactivity can be indirectly measured with an isothermal calorimeter.

With this test, blended cement pastes are mixed and measured out into ampules and loaded into isolated chambers. In isothermal calorimetry, the insides of these chambers are held at a constant temperature, and the equipment measures how much energy is needed to maintain that temperature. The mixes are kept in these chambers for a specified amount of time, which varies based on what material is being tested.

The blended cement paste samples were mixed with a constant water-to-binder ratio of 0.4 and a 20% weight replacement of the given SCM. These blended cement pastes were then loaded into the calorimeter at a constant temperature of

23 °C for 48 hours. In addition to the heat-treated river sediment samples, a 100% OPC paste and a mix with 20% nonreactive quartz were also included in the test. The results of these experiments can be seen in Figure 54 and Figure 55 in their normalized (by binder mass) and cumulative forms. The river sediment's results show that they evolve an amount of heat somewhere in between the non-reactive quartz and the 100% OPC mixes. The OPC mix released 270 J/g by 48 hours while the quartz released 222 J/g at the same time, which indicates a drop of ~18%. The heat-treated river sediments dropped by 10-15% in comparison to the OPC mix (228-243 J/g). While these results do correlate with a slightly pozzolanic SCM, they do not correlate with results of commercially available metakaolin as seen in the work completed by M. Frias (Frias, de Rojas, & Cabrera, 2000). Similar results were achieved by Celine Bunderen, when the cumulative heat evolved for heat-treated river sediments were measured (Bunderen, et al., 2018). While isothermal calorimetry is a decent method to compare individual SCMs to each other, it is not a decent comparison to pre-existing tests and parameters. Compressive strength, calcium hydroxide, and particle size do not directly correlate with the amount of heat evolved. Kaolinite also cannot be directly compared to the heat evolved as nonreactive elements can still increase reactivity based on dilution effects; wherein, non-reactive materials do not absorb any water allowing them to react with other elements. Certain properties such as set time may indirectly correlate with the heat evolved, but the accuracy is not guaranteed. It can be inferred that the SCM blends will set more quickly than OPC due to the leftward shift we see in Figure 54, but the exact set time is typically inaccurate (Hu, Ge, & Wang, 2014).

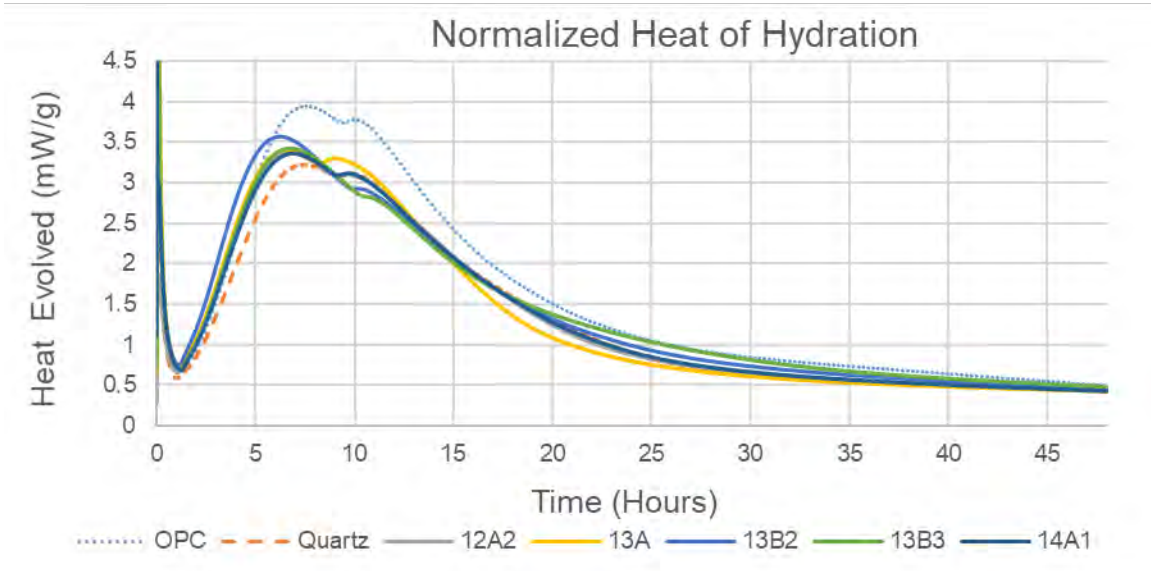


**FIGURE 54. GRAPH. NORMALIZED EVOLVED HEAT OF CALCINED RIVER SEDIMENTS.**

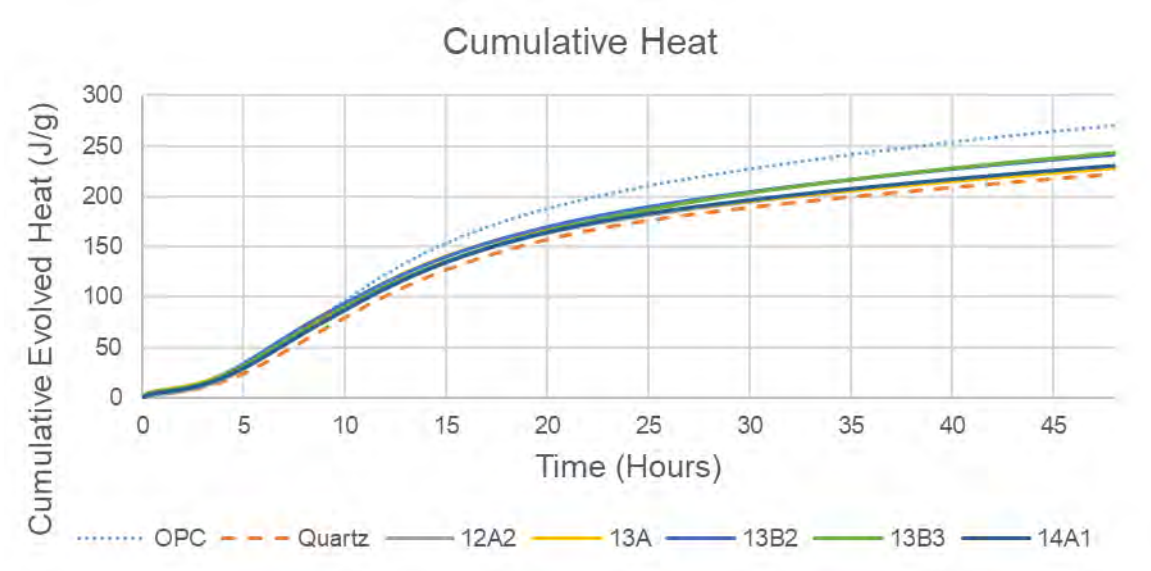


**FIGURE 55. GRAPH. CUMULATIVE HEAT EVOLVED OF CALCINED RIVER SEDIMENT.**

**Alkali Silica Reactivity**

The alkali silica reaction is an expansive chemical reaction that occurs between alkalis, present from cement content or from external sources, and amorphous silica present in certain coarser aggregates. This reaction forms a gel-like material around and through the aggregates which take in water and expand. The gel then applies tensile stresses in the surrounding matrix, eventually leading to crack propagation. These cracks lead to a decrease in ultimate strength and an increase in chemical attack susceptibility. Due to the wide availability of the reactant materials, this is one of the more widespread durability issues associated with concrete and is a major barrier to the long-term viability of concrete structures. To counter this, SCMs, especially pozzolans, are widely utilized to mitigate the ASR reaction. There are a variety of tests utilized to measure ASR susceptibility. However, the most common (and quickest) test used is the accelerated mortar bar test (AMBT) specified with ASTM C1567 (C1567, 2013).

In this test, mortars are mixed with a high amorphous silica reactive aggregate, sourced from Gold Hills, with a constant water-to-binder ratio of 0.47 and a 20% SCM replacement by weight. Mortars are mixed in accordance with ASTM C305 and set in a 100% hydration chamber for 24 hours at 23 °C. Once demolded, the bars are submerged in deionized water at 80 °C for 24 hours. Afterwards, zero-day measurements are taken and the bars are submerged in a 1N NaOH solution at 80 °C. The bars are taken out for periodic measurements until 28 days is reached (modified from 14 days).

These experiments were completed with a 100% OPC, metakaolin, and the calcined river sediments (prepared with the method described in section 5.2.3). Results for these tests can be seen in Figure 56. ASTM C1567 and C1778 report that an expansion less than 0.1% at 14 days is sufficient to confirm that the concrete mix is non-reactive. In our case, all of the river sediment tested passed this limit at 14 days, while two of the five-river sediments passed the 0.1% expansion limit at 28 days. Additionally, it should be noted that the commercially available metakaolin mix performs just as well as the two passing sediment samples at the 28-day mark, indicating that the river sediment is a material highly capable of mitigating the ASR expansion. This performance is primarily dependent on the overall kaolinite content of the sediment, as opposed to the muscovite or amorphous content.

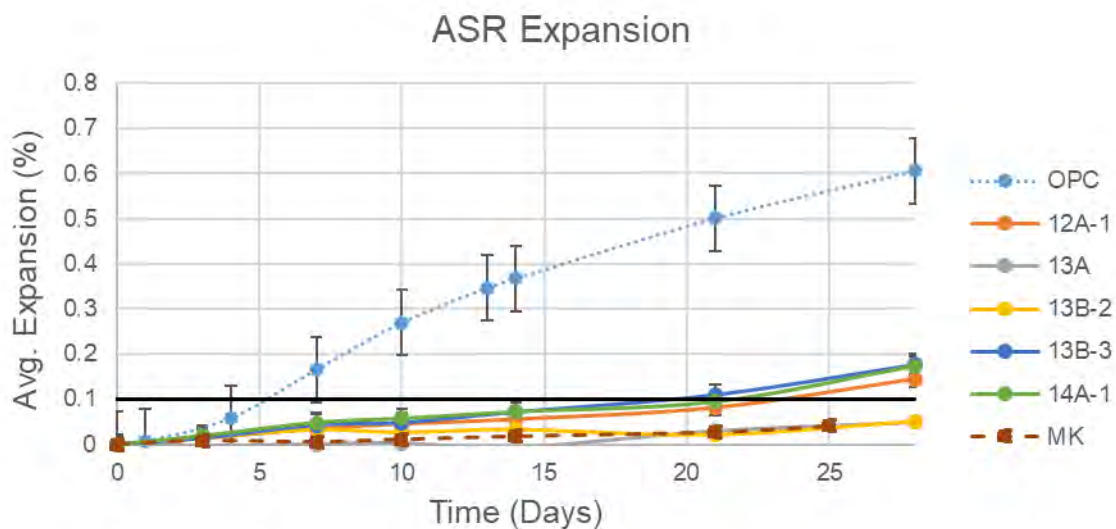


**FIGURE 56. GRAPH. AMBT EXPANSION OF HEAT-TREATED RIVER SEDIMENTS.**

## **ANALYSIS AND IMPROVEMENTS TO POZZOLANIC REACTIVITY**

### **Analysis of River Sediment Performance**

Three general mineralogical quantities can be used to correlate the performance of the heat-treated river sediment: amorphous, muscovite, and kaolinite content. In general, muscovite does not correlate much with the overall performance of the heat-treated river sediment. This reflects the accepted literature, which states that, while heat-treated muscovite is technically an amorphous alumina silicate, it does not exhibit much pozzolanic reactivity at all. The amorphous content also does not correlate very well with the performance of the river sediment. This is likely due to the fact that this quantity also accounts for the disordered muscovite content, which was previously shown to not correlate with performance. In contrast to this, the kaolinite content of the river sediment correlates relatively well with the performance of the material. This means that deciding which materials should be utilized as an SCM is relatively simple. Since the muscovite and amorphous content of the sediment does not beneficially affect the performance of the product, they should not be considered as a factor. Instead, the materials chosen for production into an SCM should instead simply contain a large percentage of kaolinite. In general, it is accepted that a minimum of 40% kaolinite is necessary for use as a relatively highly reactive pozzolan (Avet, Snellings, Diaz, Haha, & Scrivener, 2016). While only one of the sediment samples

meets this limit, the majority of the sediment samples perform well. This is likely due to the presence of muscovite, diatoms, and amorphous silica in the material. While the presence of these materials should not be depended on, it will allow for a greater degree of flexibility in implementation.

## **Drawbacks and Improvements**

The previous experiments suggest that the heat-treated river sediments possess a pozzolanic reactivity of between 40-45% compared to the commercially available metakaolin (>99% purity). The dilution in pozzolanic reactivity is primarily caused by the low kaolinite content. Despite this dilution, certain performance applications are comparable to the referenced metakaolin, which can lead to a lower required purity. The influence of kaolinite content can be seen in Figure 57 which correlates kaolin content of the sediments to ASR expansion (28 Days), calcium hydroxide consumed (56 Days), and the strength activity index (56 Days). It can be seen that there is a relatively strong correlation between kaolinite content and the CH consumed and the ASR expansion. The strength activity index, however, does not vary significantly.

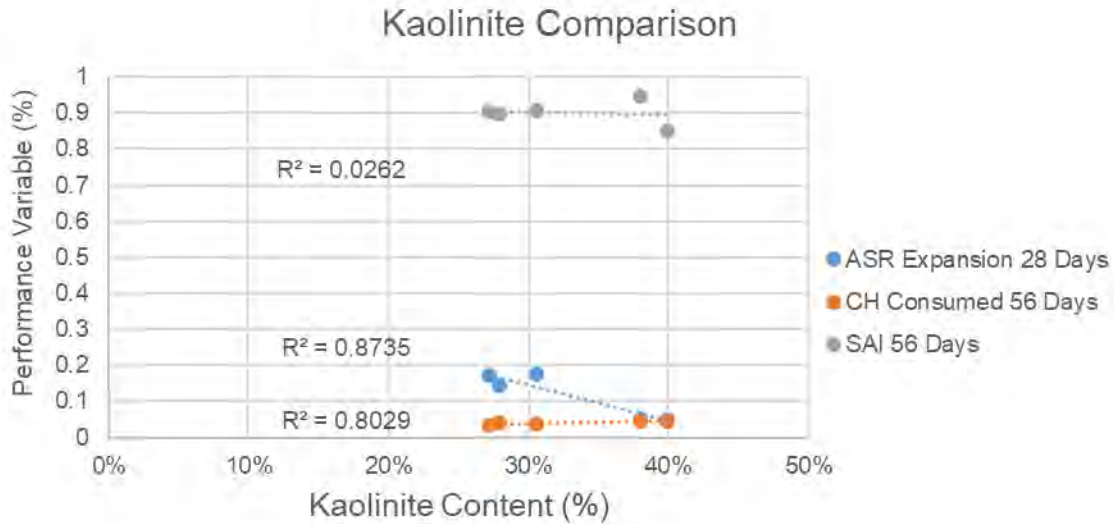


**FIGURE 57. GRAPH. KAOLINITE CORRELATIONS BETWEEN ASR EXPANSION, CH CONSUMPTION, AND SAI.**

A secondary cause of this low level of reactivity is attributed to the coarse nature of the processed river sediment. Currently, the average particle size of these river sediments is between 20-30 microns for each material. This means that these SCMs do not possess the capacity for particle packing or the nucleation effects that commercially available metakaolin has. Particle packing refers to the densification effects that small particle size powders can possess. These small particles will fill in the void spaces between coarser elements of a concrete mix. Nucleation effects occur as an effect of large surface areas, which is directly related to particle size. A large surface area creates larger numbers of nucleation sites where cement products can form more easily. These elements are only noticeable when the SCMs are smaller than 10 microns. If a more aggressive

grinder is used, then the particle packing and nucleation effects can be implemented.

Additionally, there is some evidence that utilizing a muffle furnace for SCM testing is not optimal. To test this, similar feedstock materials (Sample 13B-3) were tested in a muffle furnace at various temperatures as well as samples prepared in a rotary kiln at 800 °C for 1 and 3 hours. These samples were mixed and tested for their strength activity index using the methods described in section 5.4.1. It was found that the samples prepared in the rotary kiln surpassed the samples prepared in the muffle furnace and even surpassed the compressive strengths of the control mixes. These results can be seen in Figure 58. It can therefore be seen that the preparation of the river sediments can still be approved upon.

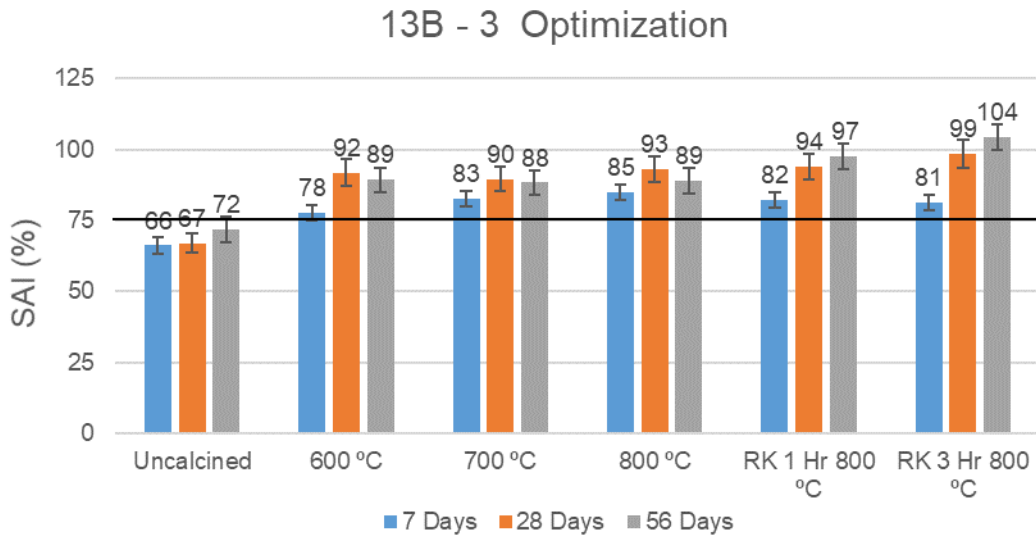


**FIGURE 58. GRAPH. SAMPLE 13B-3 STRENGTH OPTIMIZATION.**

It can be seen through the results that, despite the low purity of the river sediments, relatively high strengths can still be achieved. Additionally, certain

durability properties such as ASR mitigation can still match the performance of high purity metakaolin. It can be determined from this that low purity does not necessarily guarantee low performance. In addition, such river sediments do not need to go through the process of purification which will greatly aid in reducing the cost of the final product.

## **CHAPTER 6. R<sup>3</sup> TEST METHOD**

One of the original objectives in the proposal of this research project included an investigation of the R<sup>3</sup> test method. This stands for the rapid, relevant, and reliable test method. Traditional test methods measure pozzolanic reactivity indirectly and are highly influenced by variations in cement and aggregate. For example, any powder can pass the strength activity index, which is the only measurement of pozzolanic reactivity required in ASTM C618, so long as it is finely divided enough. Evidence for this can be seen in Figure 48 where the raw river sediments pass the minimum SAI limit. Ruben Snellings and the RILEM group introduced the R<sup>3</sup> test method in order to remove such influences.

### **R<sup>3</sup> TEST METHOD EXPERIMENTAL PROCESS**

The R<sup>3</sup> method was created as a method to directly test the pozzolanic reactivity of SCMs (Avet, Snellings, Diaz, Haha, & Scrivener, 2016). Traditional test methods indirectly determine pozzolanic reactivity, which can vary greatly, based on the type of cement or sand used. The R<sup>3</sup> method works independently of these parameters and may be more reliable across various laboratories. With the R<sup>3</sup> test, the potential SCM is blended with an excessive amount of calcium

hydroxide and water. This mixture is also blended with a small amount of potassium hydroxide, potassium sulfate, and calcite in order to speed up the pozzolanic reaction. These samples are then stored in airtight containers at 40 °C until testing. When tested, the top 5mm is removed from the sample in order to account for carbonation of the sample. These samples are ground and dried at 40 °C overnight before passing them through a No. 8 sieve. These materials can now be tested for bound water content, calcium hydroxide content, and for heat evolution.

In order to test the efficacy of this test method the river sediment samples were prepared at 800 °C as described in section 5.2.2. Given that this is a newly introduced test method there are no current limits on any of the test methods that will be introduced. However, by comparing these values to nonreactive quartz and to the commercial metakaolin, we can infer the level of pozzolanic reactivity.

## **BOUND WATER**

The bound water test is meant to indirectly measure the quantity of C-S-H gel in the samples (Avet, Snellings, Diaz, Haha, & Scrivener, 2016). Once the sample is prepared in accordance with section 5.6.1, samples are then placed in a muffle furnace and heated up to 350 °C and held for 2 hours or until constant mass is reached. The percent mass drop is then recorded and determined to be

the quantity of water bound by the C-S-H gel. The bound water for the heat-treated river sediments and the commercially available metakaolin is determined at 7, 28, and 56 days. It can be seen in Figure 59 that the bound water for the sediment samples increase over time and achieves 40-60% of the bound water content in comparison to the commercially available metakaolin. This range is larger than the kaolinite content of the river sediments as seen in Table 14. This may imply that the muscovite, diatoms, and fine amorphous silica is reacting, or it may imply that the R<sup>3</sup> test method overestimates the reactivity of pozzolans.

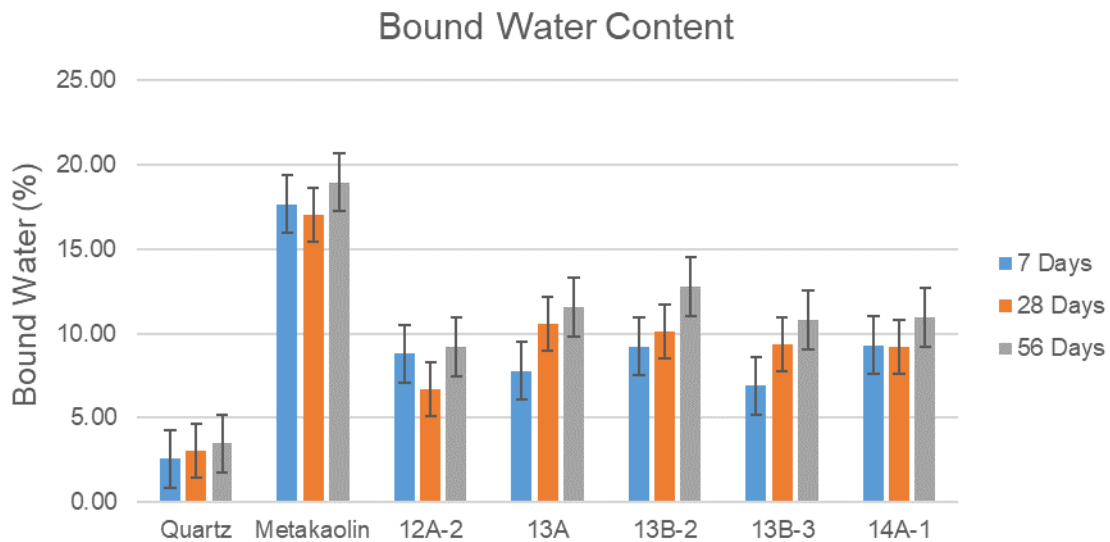


**FIGURE 59. GRAPH. BOUND WATER CONTENT OF HEAT-TREATED RIVER SEDIMENT.**

## ISOTHERMAL CALORIMETRY

Isothermal calorimetry can be determined to measure the pozzolanic activity of the paste, created with the R<sup>3</sup> method, over time. In this scenario, the paste is loaded into a calorimeter and held at 40 °C for seven days with de-ionized water used as a reference. These materials were tested for the heat-treated river sediment and with the commercially available metakaolin. These values are recorded in their normalized and cumulative forms in Figure 60 and Figure 61. In these experiments the metakaolin reaches 1100 J/g while the river sediment reaches 400-500 J/g. This implies that the river sediment achieves a pozzolanic reactivity of 35-45% of the value of the commercially available metakaolin. These values are slightly larger than the overall kaolinite content of the river sediments. Additionally, this test overall is the most similar to the calcium hydroxide consumption of blended cement pastes.

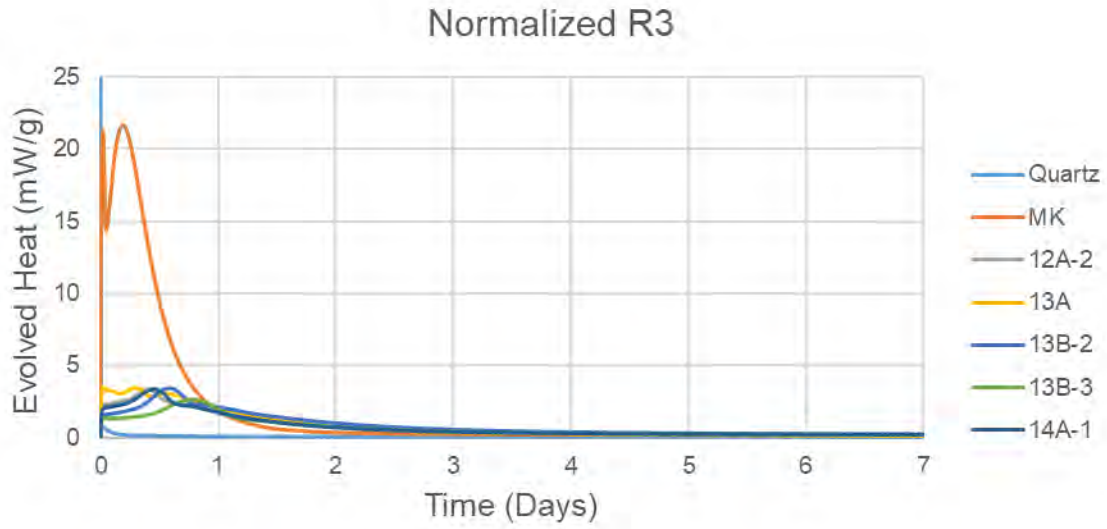


**FIGURE 60. GRAPH. NORMALIZED HEAT EVOLVED FOR R<sup>3</sup> PASTES.**

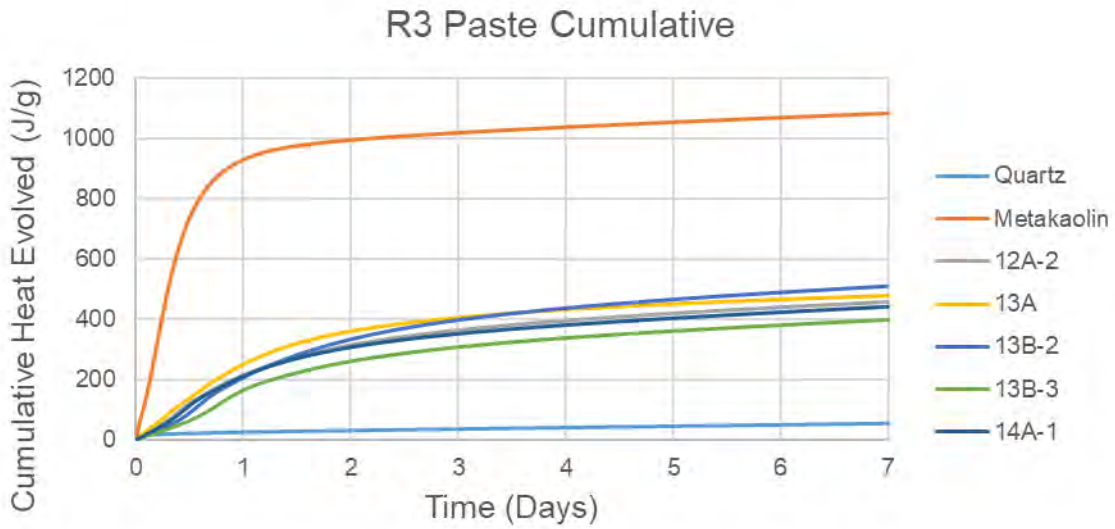


**FIGURE 61. GRAPH. CUMULATIVE HEAT EVOLVED R<sup>3</sup> PASTES.**

## CALCIUM HYDROXIDE CONSUMPTION

Additionally, these R<sup>3</sup> pastes were also fed into a thermogravimetric analyzer in order to determine the calcium hydroxide consumed by the SCM as described in section 5.4.2. It should be noted that TGA is not a standard test for the R3 test method but was determined anyway. The results for this can be seen in Figure 62. It can be seen that the tested SCMs (i.e. river sediment) consume a relatively constant amount of calcium hydroxide over time. Results show that the river sediment consumes approximately 20% calcium hydroxide and the metakaolin consumes 30-35% calcium hydroxide. This implies that the sediment samples are approximately 50-70% as reactive in comparison to the commercially available metakaolin.

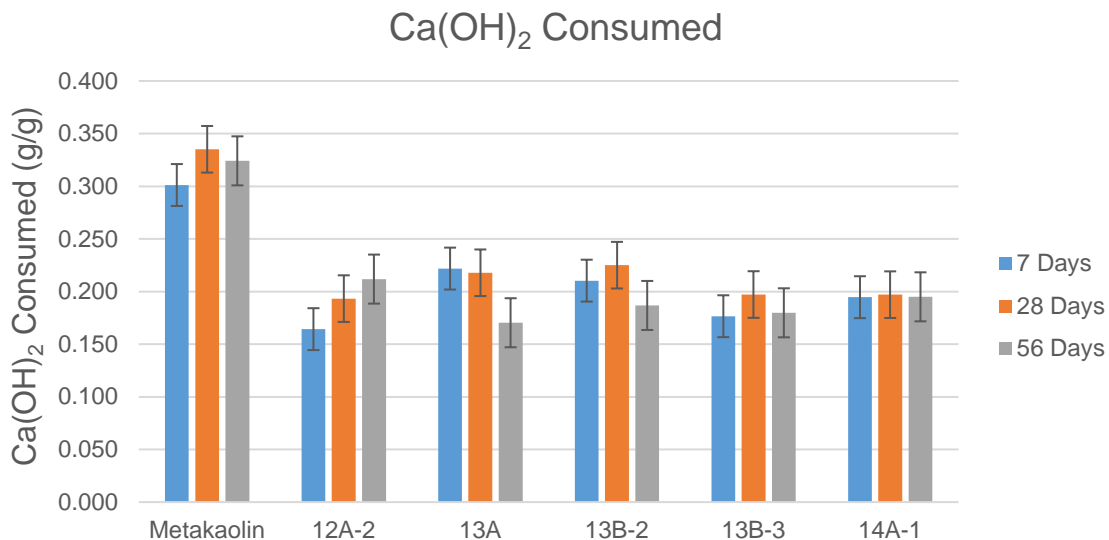


**FIGURE 62. GRAPH. CALCIUM HYDROXIDE CONSUMED IN R<sup>3</sup> PASTES.**

## CORRELATIONS AND PERFORMANCE OF R<sup>3</sup> METHOD

In order to determine whether the R<sup>3</sup> test method is an acceptable test method, these results are correlated to results taken from the cement-based tests. The most direct test method that can be used is the calcium hydroxide consumption of blended cement pastes seen in section 5.4.2. These results are correlated to the results for the R<sup>3</sup> method in Figure 63-Figure 65. The fitted linear trend line possesses an R<sup>2</sup> of 0.75-0.95 for all of the correlations, implying a good relation between the R<sup>3</sup> test method and traditional tests. However, it can also be seen that the R<sup>3</sup> test methods tend to overestimate results in comparison to traditional test methods. This is likely caused by the abundance of calcium hydroxide available in the R<sup>3</sup> method. While this is not necessarily a significant problem, it does mean that this method has the tendency to overestimate the performance of the tested SCM. This problem is more noticeable for more highly reactive SCMs, like pure metakaolin. This property of SCMs should be kept in mind for future testing with this test method. These R<sup>3</sup> test methods may be useful for GDOT testing when comparing the pozzolanic reactivity of potential SCMs; however, they should not be used to replace existing test methods (Li, et al.).

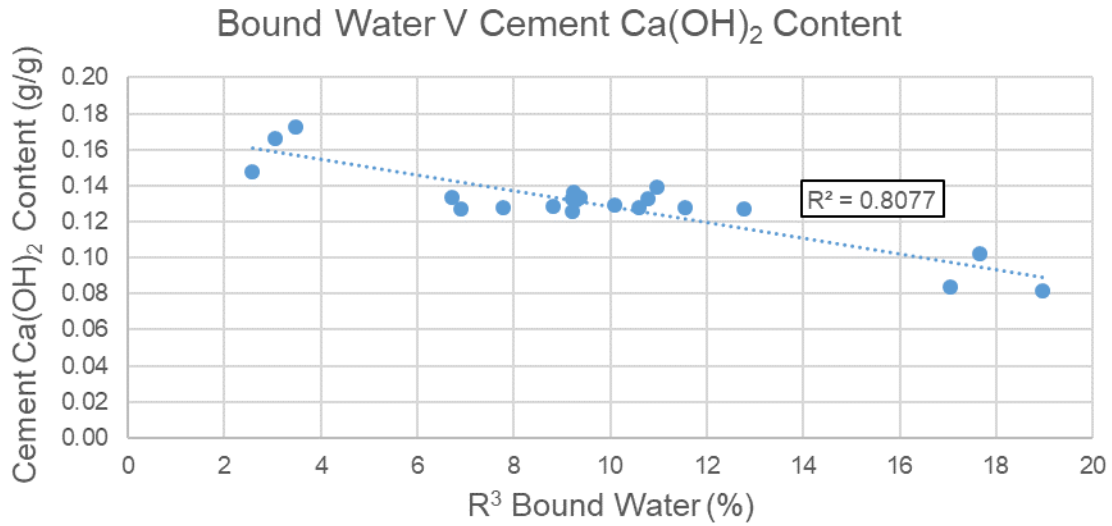


**FIGURE 63. GRAPH. CORRELATION FOR CH CONSUMPTION OF CEMENT PASTE AND BOUND WATER IN THE R<sup>3</sup> PASTE.**

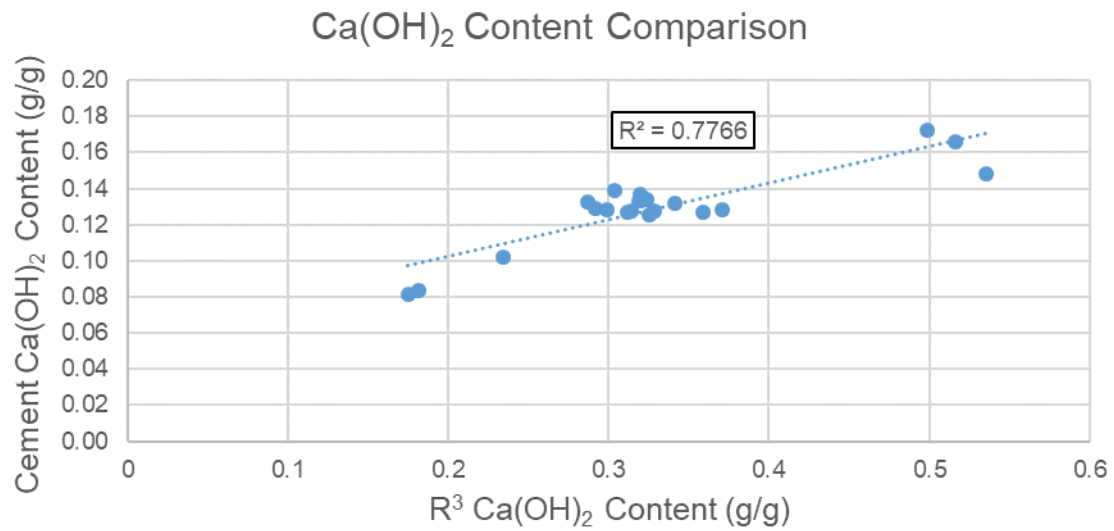


**FIGURE 64. GRAPH. CORRELATION BETWEEN CH CONTENT OF BLENDED CEMENT PASTE AND CH CONTENT OF R<sup>3</sup> PASTE.**

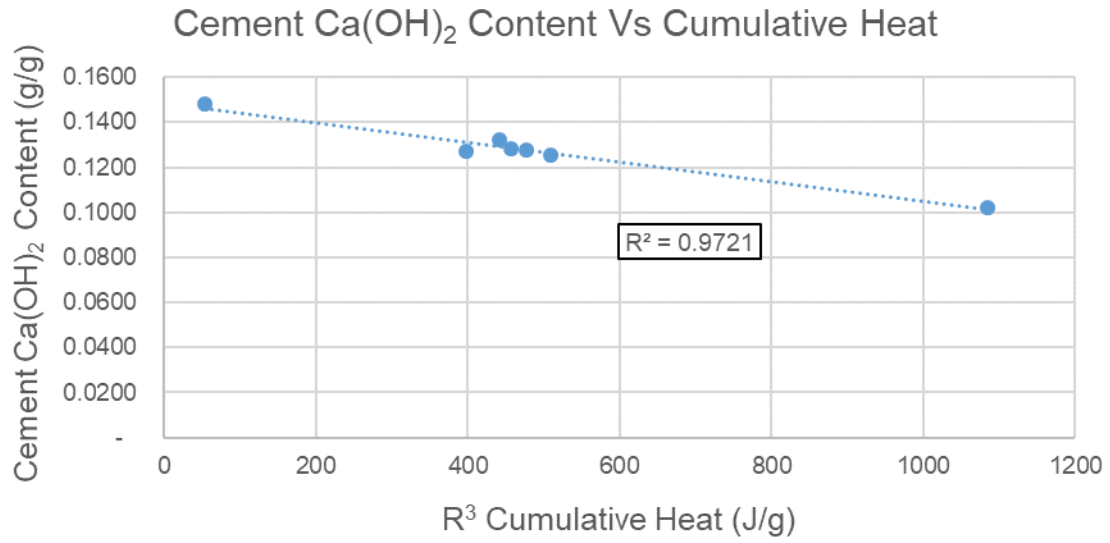


**FIGURE 65. GRAPH. CORRELATION BETWEEN CH CONSUMED FOR BLENDED CEMENT PASTE AND CUMULATIVE HEAT OF THE R<sup>3</sup> PASTE.**

## **CHAPTER 7. APPLICATION AS A CEMENT FEEDSTOCK**

The previous structural applications discussed require a specific mineralogical or elemental composition. In order to properly utilize the full quantity of material stored a more flexible application is needed. If the river sediment is utilized as a cement feedstock, then the overall composition of the material can be changed to compensate for variation in its mineralogical/elemental composition. The biggest issue that may be present in this is associated with heavy metal contaminations. This chapter will primarily involve investigating the quantity of sediment that could be utilized in the feedstock and if possible contaminants will be properly bound.

### **CEMENT PRODUCTION**

A five-step process can generally describe the production of ordinary portland cement (Oss & Padovani, Cement Manufacture and The Environment, 2002). The first step is the proportioning of the raw material feedstock. Feedstock is primarily composed of limestone, shale, sand, clay, and iron oxide. These materials are proportioned so that the final product is composed of one of the

classifications of OPC in accordance with ASTM C150 (C150, 2020). The second step is to grind and blend the raw material feedstock until the material is homogenous. The third step has these raw materials fed into a rotary kiln, which gradually heats up the feedstock to ~1500 °C. This is where the material is converted to what we call cement “clinker” which are glassy balls about 3-25 mm in size. Once the material is cooled down, it is then ground down to a specific surface area of 260-430 m<sup>2</sup>/kg. This material is composed of four primary elements: Tri-calcium silicate (C<sub>3</sub>S in cement shorthand), di-calcium silicate (C<sub>2</sub>S), tri-calcium aluminate (C<sub>3</sub>A), and tetra-calcium aluminoferrite (C<sub>4</sub>AF). Of these materials, C<sub>3</sub>S and C<sub>2</sub>S react with water to form C-S-H gel and calcium hydroxide; as such, they provide most of the compressive strength in a concrete mix. C<sub>4</sub>AF provides no strength but lowers the melting temperature of the raw feedstock. C<sub>3</sub>A reacts very quickly and releases a lot of heat but primarily helps with early age stiffening (Oss & Padovani, 2003). Sometimes the C<sub>3</sub>A will react too quickly and create a “flash set” which stiffens the concrete so quickly that there is no time to place the concrete. To counteract this, the final step in the OPC production process is to grind gypsum into the clinker material. The gypsum slows down the overall reaction of the C<sub>3</sub>A, which prevents the onset of flash setting. A description of this overall process can be seen in Figure 66.

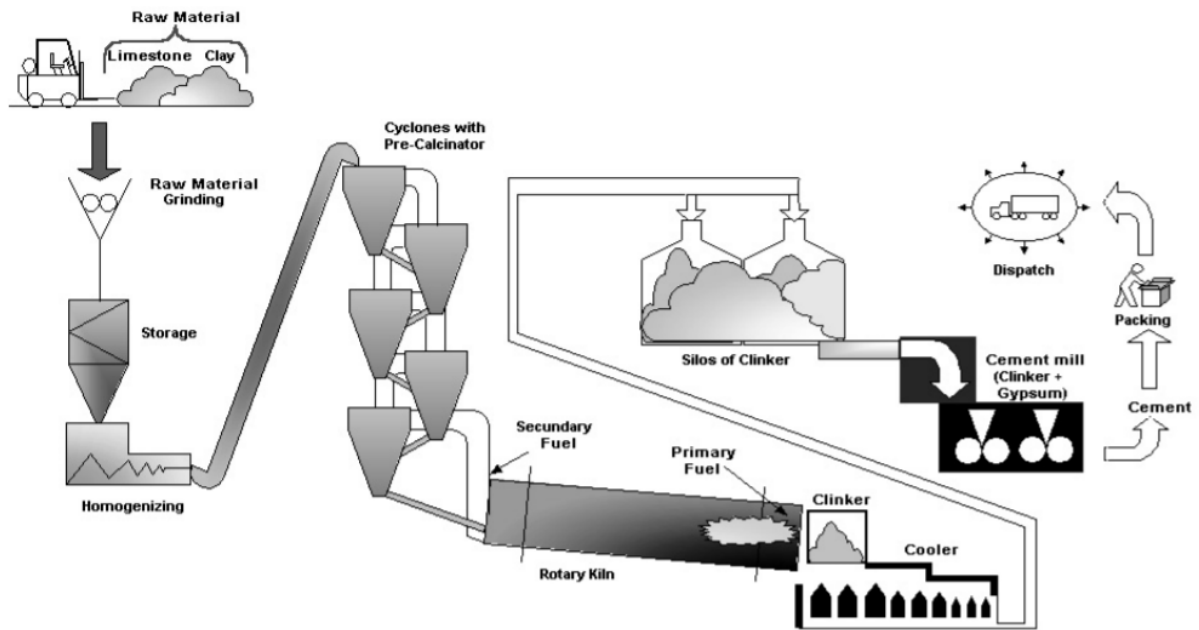


**FIGURE 66. ILLUSTRATION. STAGES OF THE ORDINARY PORTLAND CEMENT PRODUCTION PROCESS (CARPIO, JUNIOR, COELHO, & SILVA, 2008).**

## LITERATURE REVIEW

River harbor sediments have been successfully used as a feedstock for cement production by other researchers in the past. Baptise Anger successfully used dredged river sediments to produce Type I/II cements (Anger, Moulin, Commence, They, & Levacher, 2019). These sediments contain little calcium and are primarily composed of sand and clay. Due to this, the river sediment composes 20-30% of the cement feedstock, with the rest of the material composed of limestone. Due to the similar composition of the Savannah River sediment, the

feedstock for this material should be relatively similar. G. Aouad produced a similar Type I/II cement from a polluted river sediment sourced from the Harlem River in the New York/New Jersey Harbor (Aouad, Laboudigue, Gineys, & Abriak, 2012). The feedstock was composed of approximately 25% river sediment and the final product performed very similarly to traditionally produced Type I/II cement. Jennifer Dalton used river sediments polluted with high levels of heavy metals and chlorides (Dalton, et al., 2004). These sediments were used to replace up to 12% of the feedstock material and successfully produced Type I/II cement. The final product successfully binds or oxidizes the heavy metal and chloride content of the raw river sediment during hydration. Saha Dauji investigates a variety of ways to beneficially utilize contaminated river sediments from the Indiana Harbor Canal. This includes its use in pavements, lightweight aggregate, brick production, and finally as a cement production feedstock. In these tests, the Type I/II cements are successfully produced with a 3-6% replacement in the raw feedstock. The final product is not affected by the high levels of chloride in the original river sediment.

Through these investigations, it is seen that river harbor sediments have successfully been utilized to produce ordinary portland cements. Typically, additional feedstock of limestone, alumina, and/or iron oxide is needed depending on the exact composition of the river sediment. Additionally, it was seen in these experiments that the final product successfully binds or oxidizes heavy metal and chloride contents in the raw materials. As such, the exact composition of the sediment is not vital for whether it can be used in cement production. The other components of the feedstock simply need to be altered as needed.

## CEMENT FEEDSTOCK WITH SAVANNAH SEDIMENT

The main goal of this section is to predict what exact composition the cement feedstock produced from Savannah River sediment might be. In order to determine this, the exact chemical oxide composition of the overall river sediment needs to be determined. These values were unfortunately not determined; the XRF completed in chapter 5 was performed on the sediment fines. The mineralogical composition of the sediment (seen in chapter 2) can be used to predict the elemental composition of the overall sediment. In that chapter, the mineralogy of the river sediments were completed using X-Ray Diffraction with the overall mineralogy seen in Table 15.

**TABLE 15. X-RAY DIFFRACTION OF RIVER SEDIMENT SAMPLES.**

Wt. %	XRD of Overall Dredge						
	12A-1	13A	13B-1	13B-2	14A-1	14B-1	14B-2
Quartz	74	68	83	40	92	68	34
Kaolinite	0	20	0	0	0	11	0
Cristobalite	0	1	1	0	0	1	0
Orthoclase	0	11	0	7	0	0	0
Muscovite	15	0	0	52	7	15	62
Calcite	0	0	5	0	1	2	2
Montmorillonite	11	0	12	0	0	0	0
Dolomite	0	0	0	0	0	2	2

Standard elemental compositions of each of these materials were collected from online databases. The elemental composition of the overall river sediment was predicted using the rule of mixtures between the mineralogy and the oxide

composition of those mineralogy's. The results of those predictions are shown in Table 16.

**TABLE 16. PREDICTED CHEMICAL OXIDE COMPOSITION OF RIVER SEDIMENTS.**

Wt. %	Predicted Oxide Composition for Overall Dredge						
	12A-1	13A	13B-1	13B-2	14A-1	14B-1	14B-2
SiO <sub>2</sub>	88.7	86.5	92.4	69.2	95.3	81.8	63.3
Al <sub>2</sub> O <sub>3</sub>	7.1	10.9	2.3	18.8	2.4	10.0	20.9
Fe <sub>2</sub> O <sub>3</sub>	0.9	0.1	0.3	2.1	0.3	0.7	2.5
CaO	0.3	0.0	5.3	0.0	1.0	3.5	3.5
SO <sub>3</sub>	0.0	0.0	0.0	0.0	0.0	0.0	0.0
K <sub>2</sub> O	1.7	1.5	0.1	6.6	0.8	1.6	6.8
TiO <sub>2</sub>	0.0	0.3	0.0	0.1	0.0	0.2	0.1
MgO	0.6	0.0	0.7	0.1	0.0	0.5	0.6
P <sub>2</sub> O <sub>5</sub>	0.0	0.0	0.0	0.0	0.0	0.0	0.0
Na <sub>2</sub> O	0.1	0.2	0.0	0.5	0.0	0.1	0.4
Na <sub>2</sub> O <sub>e</sub>	1.2	1.2	0.1	4.8	0.5	1.2	4.8

These predicted chemical oxide compositions are similar in nature to the compositions possessed by the samples used in the research conducted by Anger (2019). Due to the high sand content in these sediments, they will be utilized as the primary source of silica in the cement. Limestone can be used as the primary source of calcium in the material. The alumina content of the dredge material is not large enough to provide for what is required in Type I/II cement. To compensate, a small amount of bauxite can be blended in as well. Finally, small amounts of iron oxide can be blended in as well to provide for required iron contents. It should be noted that the method used to predict the chemical composition of the river sediment does not account for all of the iron content in the material. As such, the iron oxide content required in the feedstock may be variable. These feedstock materials will be used to predict what feedstock composition

would be required to produce a standard Type I/II portland cement. The results of this feedstock composition can be seen in Table 17.

**TABLE 17. PREDICTED CEMENT FEEDSTOCK COMPOSITION.**

Predicted Feedstock Composition							
Wt. %	12A-1	13A	13B-1	13B-2	14A-1	14B-1	14B-2
Limestone	71.90	71.38	72.43	68.00	72.89	70.58	66.50
Bauxite	2.69	2.63	2.76	2.17	2.82	2.52	1.97
Iron Oxide	2.52	2.66	2.66	2.05	2.68	2.51	1.86
Dredge Material	22.89	23.32	22.15	27.78	21.60	24.39	29.67

Through this, we can see that the feedstock material is composed of approximately 70% limestone by weight. Approximately 2% bauxite and iron oxide is required to provide proper alumina and iron contents. The dredge material composes 20-30% of the overall cement feedstock, similar to the composition completed by Baptise Anger. The total mass of the cement feedstock composition should decrease by approximately 35%. This is primarily due to the decomposition of limestone into calcium oxide and carbon dioxide, as well as the decomposition of clays in the dredge material.

It should be noted that bauxite shouldn't be utilized in large scale production due to the cost. This was utilized in this situation for simplicity; it would be more practical to utilize a purer clay to make up the alumina content though this would require a smaller quantity of river sediment.

## CHAPTER 8. LIFE CYCLE ANALYSIS

### INTRODUCTION – LCA

Life cycle analysis and assessment (LCA) is a methodology used to qualify and quantify the environmental impact of a product over its entire life. It is also referred to as cradle-to-grave assessment because it sums the impacts from the creation of the input products through to the disposal of the end products. LCA is performed by quantifying the inputs as well as the outputs for all product phases and determining the effects of the cumulative inventory on the environment. The product's phases include raw material extraction, production, distribution use, and disposal and recycling (Figure 68). Since LCA enables the estimation of the environmental impacts associated from all product phases, it allows decision makers to select the product, the path or the procedure that is more environmentally preferable.

#### Goal and Scope

LCA is typically conducted in four phases: description of goal and scope, life cycle inventory (LCI), life cycle impact assessment (LCIA), and interpretation (Figure 67). In the first step, the goal of the study should identify the specific

purpose of the study, as well as the intended audience. The scope of the study should include the best definition of the functional units to be compared, clearly state the system boundaries, and define the limits for including inputs and outputs. System boundaries are used to outline the extent of data to be analyzed in this study. Three orders of analysis are normally considered in LCA analysis: 1<sup>st</sup> order, which includes only production of material and transport; 2<sup>nd</sup> order, which includes all life cycle processes included but no capital goods; and 3<sup>rd</sup> order, which is the same as the 2<sup>nd</sup> order with capital goods included.

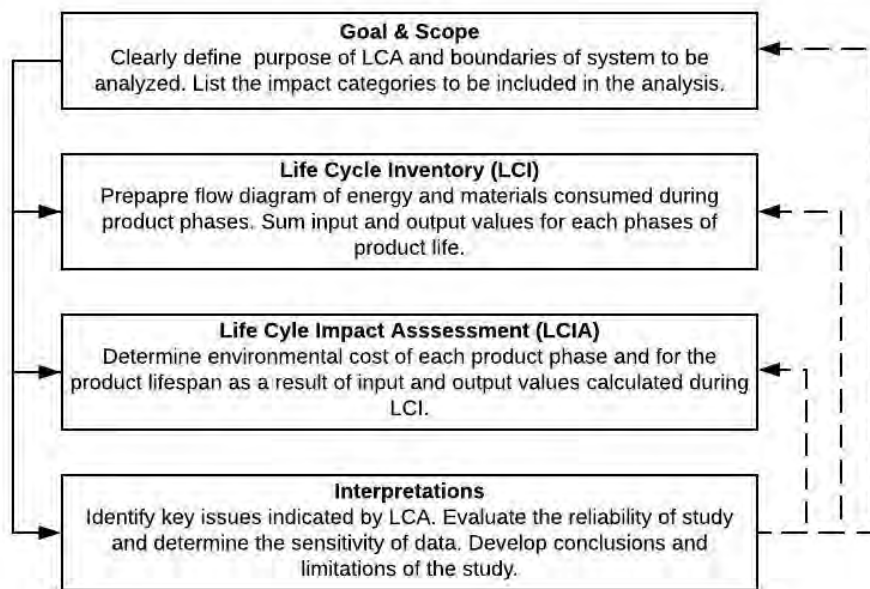


**FIGURE 67. ILLUSTRATION. LIFE CYCLE FLOWCHART AND DEFINITIONS OF THE FOUR MAIN PHASES.**

Compiling an LCI is the second step of performing an LCA and includes defining the process chain that occurs within the system boundaries and determining the inputs and outputs required/generated for each process.

Developing a complex LCI is simplified by the use of background data. Background data includes information compiled and made widely available by the LCA industry that describes common processes. Background data are available in the form of an LCI database and usually come as part of any LCA software. When using background data, it is important that the provided process adequately resembles the process it is intended to represent. Results of the LCI can be used to compare two processes. This type of comparison is called loading. Additionally, in this step, the process chain that occurs within the system boundaries are defined and the inputs as well as the outputs for each process are determined.

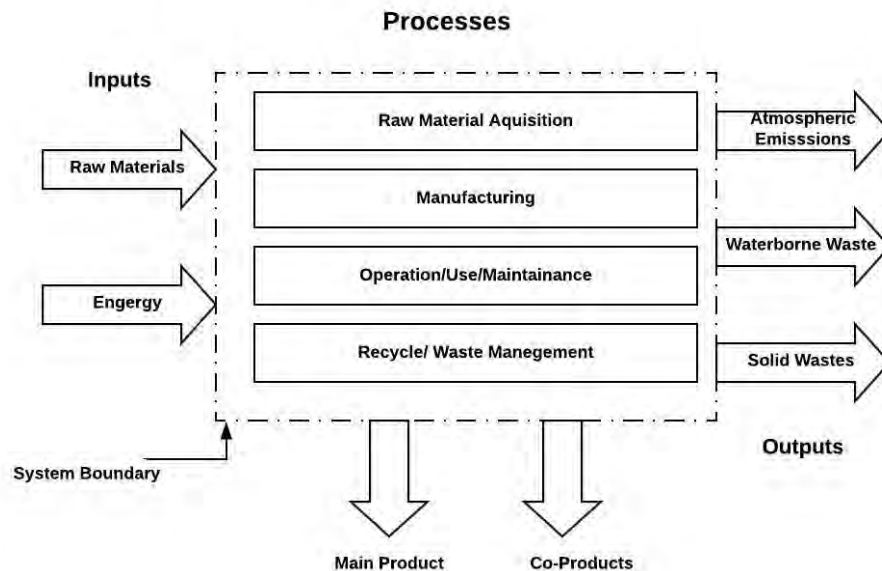


**FIGURE 68. ILLUSTRATION. MAIN STAGES, TYPICAL INFLOWS AND OUTFLOWS IN LIFE CYCLE ASSESSMENT.**

In the third step, the environments associated with the LCI are evaluated, which is subject to the scientific understanding of how the materials and energy assumptions have an impact on the environment. The last step of the process

involves drawing conclusions and listing the limitations based on the results from all three previous steps. The following section describes the steps used for analysis in this study.

## **LCA ANALYSIS**

**Goal:** For this project, we are tasked with estimating the life cycle environmental impacts of products derived from the dredged material from Savannah Harbor.

**Scope:** The analysis includes the raw material excavation, transportation, material placement, and compaction or manufacturing phases of life cycle. The functional unit is chosen to be the utilization of the dredged materials from a 3000 m<sup>3</sup> embankment, and the impact of interest is chosen to be global warming potential (GWP). GWP is presented in terms of equivalent mass of CO<sub>2</sub>. The 100-yr GWP considered in this study includes CO<sub>2</sub> (1), methane (30), Nitrous Oxide (298).

**Methods:** The LCA proposed in this study is a cradle-to-grave model based on USEPS TRACI methodology, ISO 14040 and 14044 standards. The system boundaries are drawn as big as possible, and all necessary processes associated with beneficial use of dredged materials are included: extraction of materials, and treatment of dredged material, and transportation. In this analysis, the impacts from equipment manufacturing, transport, and maintenance will be ignored. Any end-life impact, including demolition and abandonment will also be ignored.

## System Boundaries

The system does not include energy and materials required for production of the machinery and equipment used. Figure 69 and Figure 70 shows the flow chart and system boundaries for both the non-structural fill and supplementary cementitious materials.

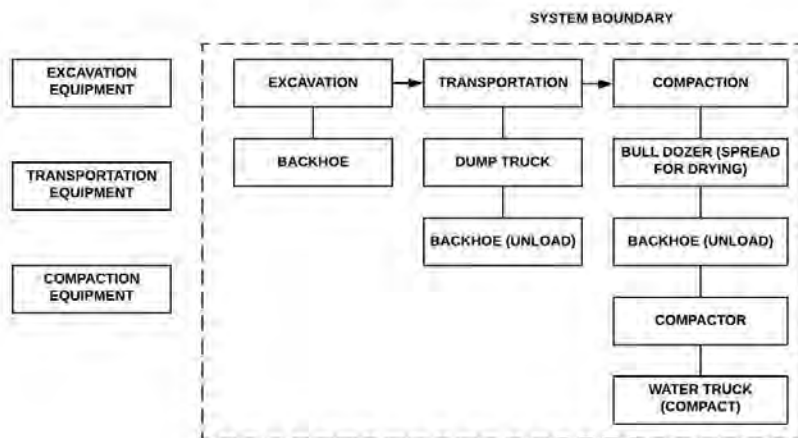


**FIGURE 69. ILLUSTRATION. THE FLOW OF WORK: THE LIFE CYCLE OF NON-STRUCTURE FILL BROKEN INTO THREE MAIN STAGES: EXCAVATION, TRANSPORTATION, AND COMPACTION.**

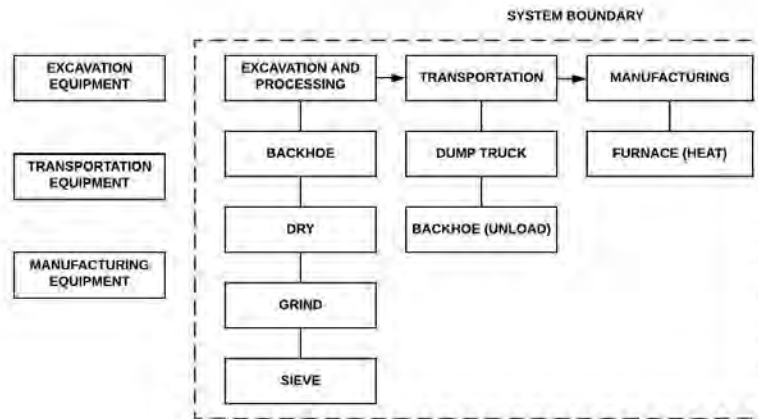


**Figure 70. Illustration. The Flow of Work: The life cycle of supplementary cementitious material is broken into three main stages: excavation & processing, transportation, and manufacturing.**

## Analysis

The standard capacities of the equipment and machinery used for this project were obtained from online databases applicable for LCA analysis. Based on the assumptions of the horsepower and the distance for the trip (31.07 miles [50 km] for a single trip), the total fuel consumption in terms of diesel fuel was calculated from a spreadsheet provided by California Air Resources board (CARB). The spreadsheet provided a quick estimation of the fuel use as well as the emissions for the equipment in a specific year. The results are very close to those from the official inventory model developed by CARB. The diesel production, including the amount of emission and the GWP, is shown in Table 18. Table 19 and Table 20 show the life cycle analysis in terms of non-structural fill and the supplementary cementitious material, respectively. After being excavated from the

site, the soil will be transported to the fill site using a dump truck and then compacted to a water content of 15%.

**TABLE 18. DIESEL FUEL PRODUCTION PER 1kg FUEL (ADAPTED FROM GABI DATABASE).**

<b>Diesel Fuel Production ( per 1kg fuel produced )</b>			
	Flow	Quantity	Unit
Inputs	Primary energy use	57.7	MJ
outputs	Carbon Dioxide	0.527	kg CO <sub>2</sub>
	Methane (fossil)	0.00255	kg CH <sub>4</sub>
	Nitrous Oxide	0.0000225	kg N <sub>2</sub> O
	Global warming potential	0.609	kg CO <sub>2</sub> eq

**TABLE 19. LIFE CYCLE ANALYSIS OF NON-STRUCTURAL FILL IN TERMS OF GWP.**

Life Cycle Phase	Equipment Type	Fuel Type	Operating Time ( hr )	Hourly Fuel Use (gal/hr)	Total Fuel Use (gal)	Total Fuel Use (kg)	Total GWP (kg CO <sub>2</sub> EQ)
<b>Equipment Use ( aka Fuel Consumption )</b>	Backhoe (Excavation)	Diesel	20.00	1.7	34	128.7	770.9
	Dump Truck (Transport)	Diesel	600	7.8	4708	17821.7	76585
	Backhoe (Unload)	Diesel	20.00	1.7	34	128.7	1562
	Bulldozer (Spread for Drying)	Diesel	15.63	9.8	153	579.2	1562
	Compactor (Compact)	Diesel	23.08	2.3	53	200.6	770.9
	Water Truck (Compact)	Diesel	80	2.3	184	696.5	4048

**TABLE 20. LIFE CYCLE ANALYSIS OF SCM IN TERMS OF GWP.**

Life Cycle Phase	Equipment Type	Fuel Type	Operating Time ( hr )	Hourly Fuel Use (gal/hr)	Total Fuel Use (gal)	Total Fuel Use (kg)	Total GWP (kg CO <sub>2</sub> EQ)
Equipment Use ( aka Fuel Consumption )	Excavation (Backhoe)	Diesel	20	1.7	34	129	771
	Dry, Grinding, Sieving	Diesel	300	2.0	600	2271	13604
	Loading (Backhoe)	Diesel	6	2.3	10	39	245
	Transport (Dump Truck)	Diesel	80	2.3	184	697	22976
	Heat	Diesel	----	----	-----	22910	13963

After excavation from the site, the dredged material will be dried, ground and separated on site using a No. 200 sieve to limit the volume of material transported. After being transported, the dredged material will be heated up to 800 °C for one hour. The total amount of fuel for heating and the GWP associated were computed given the specific heat of silicate (0.68 j/kg/degree), the amount of fine materials and the heat provided by 1 kg of diesel.

**Conclusion for analysis:** In terms of global warming potentials, the use of non-structural fill produces 85,299 kg CO<sub>2</sub> eq. while the use of supplementary cementitious material produces 51,558 kg CO<sub>2</sub> eq. Utilizing Savannah River sediment as a non-structural fill and as a supplementary cementitious material are promising beneficial use options.

## CHAPTER 9. RECCOMENDATIONS AND CONCLUSIONS

This research considered both relatively low (e.g., fill, fine aggregate) and high economic value (e.g., cement, SCMs, LECA) reuse options for Savannah River sediment and demonstrated that some productive reuse strategy can be identified for the large majority of the Savannah River sediments. The most suitable application for a sediment source will depend on its elemental, mineralogical, or physical properties. This chapter provides guidance on determining the most suitable strategy for reuse, including a decision tree based upon technical information obtained in this study. Additionally, a relatively new process for evaluation of SCMs – the R3 method – was assessed and recommendations for its implementation prospects are made. Life cycle assessments were also studied to determine environmental and economic benefits for the production of these applications. Further recommendations are made suggesting future work that should be conducted.

## **RECOMENDATIONS**

### **Structural/Non-Structural Fill**

The chemical, physical and morphological properties of dredged sediments from Savannah River were investigated in order to evaluate their potential beneficial use in large-scale geotechnical engineering applications. The engineering tests included particle size distribution, Atterberg limits, specific gravity, standard compaction tests, TOC, LOI, TGA, XRD and SEM.

The test results indicated that CH and SC dredge are promising materials in non-structural fill geotechnical applications while SP and SP-SM can be used as structural fill.

### **Fine Aggregates**

While the river sediment tested (13B-1) meets requirements for alkali aggregate reactivity (ASTM C1260), there are far too many organics in this sample for it to be used as a fine aggregate in concrete mixes. In fact, the majority of the sediments collected contain far too many fines and organics for the samples to be viable. Such samples would need to be beneficiated to remove such materials. As such, utilizing river sediments as a fine aggregate in concrete is not recommended.

The degree of beneficiation this material would need to go through for it to meet standards is too great to be practical or profitable.

## **Lightweight Expanded Clay Aggregates**

Sediments, so long as there is a large enough quantity of finely ground clay, have been successfully processed into lightweight aggregates. Sediments with as low as 20% clay were successfully processed into LWA. Additionally, sediment samples can be processed into lightweight expanded clay aggregates (LECA), which are distinguished by their expanded porous core. Such sediments must possess an elemental composition of 48-80% SiO<sub>2</sub>, 8-25% Al<sub>2</sub>O<sub>3</sub>, and 5-25% miscellaneous elements in order for them to be processed into LECA. LECA can be utilized in a wider degree of applications, and possesses similar production requirements. Therefore, LECA possesses a higher economic value option compared to ordinary LWA. As such, it is suggested that the elemental composition of the sediment should first be determined (via XRF). If the material meets requirements, then the sediment should be processed into LECA. These sediments possess the same production process as ordinary LWA with the exception of the required composition measurements, so the cost of production should be similar. Additionally, sediments may pass the required elemental composition if coarser elements are sieved with the removed elements being used

for cement feedstock. However, this would increase processing costs due to sieving and may require multiple iterations so that the material passes requirements.

### **Supplementary Cementitious Materials**

All of the sediments tested perform similarly as a supplementary cementitious material, although sediments with more kaolinite tend to perform better. Additionally, all but one of the sediments tested pass ASTM C618 standards for class N pozzolans. The exception, with one sample failing fineness requirements, can be solved with additional grinding. While these materials successfully pass standards, performance as an SCM correlates with kaolinite content. As such, when deciding if a sediment source will be processed into an SCM, the quantity of kaolinite in the sediment is a primary factor, with >40% kaolin by mass recommended for this application. Also, if a dredge resource is processed for a different application (e.g., screened to remove sand for fine aggregate) and the residual has a >40% kaolinite, that portion of the sediment can be processed into an SCM.

This study explored various thermal processing strategies, examining hold times, cooling regimes, and ultimate temperatures during calcining. From this, the recommended thermal processing to produce an SCM is calcination in a rotary kiln at 800 °C for 3 hours.

Of the potential applications discussed, processing sediments into SCMs is one of the more energy intensive options, due to the requirements for screening and thermal treatment. As such, this application should only be used when a high quality SCM is present. A higher potential profit may be obtained due to the color change of the sediment upon calcination as seen in Figure 12 (Pg. 17), which may allow for marketing of colored cementitious materials, including cement and concrete.

### **SCM Assessment through the R<sup>3</sup> Method**

The R<sup>3</sup> experimental process can be utilized as a method for assessing the pozzolanic reactivity of potential SCMs. This test method is most useful for comparing the reactivity of SCMs to pre-existing references. Through this, the presence of pozzolanic reactivity can be definitively confirmed. However, the R<sup>3</sup> test method should not be used as a replacement for existing performance test methods such as the strength activity index and other durability-based tests. The R<sup>3</sup> test is useful for supplementing pre-existing measurements for pozzolanic

reactivity, such as TGA and isothermal calorimetry. The R<sup>3</sup> method may be most useful for determining the viability of using a river sediment as an SCM by comparing their reactivity to pure metakaolin. Through this it may be assumed that a river sediment may be used if it possesses a pozzolanic reactivity of >40% in comparison to the pure metakaolin.

### **Cement Feedstock**

Because several promising avenues were discovered that could consume high volumes of sediment to produce a range of marketable products, less emphasis was placed on experimental validation for use in cement feedstock which is regarded as a relatively smaller volume reuse avenue. However, river sediment similar to that in this study has been demonstrated in prior research for use in cement feedstock. Even sediments polluted with heavy metals and high concentrations of chlorides have been successfully demonstrated for use in this application. Based on the mineralogy of the sediment, approximately 20-30% of the cement feedstock may be composed from sediment, with the remaining fraction consisting primarily of limestone and smaller amounts of sand, clay and other sources of iron oxide. Since most sediments can be utilized as a cement feedstock, any compositions not suitable for processing into LECA or into SCMs

should be utilized as a cement feedstock. Additionally, any fractions rejected for uses in other applications can be processed as cement feedstock as well. This would imply that processing the river sediment into cement feedstock might be the option with the highest capacity for reducing the stored sediment.

## **Life Cycle Analysis**

Dredged material is attributed with some environmental benefits and LCA is a good tool to assess the impacts associated with it. The existing results found in the literature have not demonstrated a comprehensive economic, social and environmental analysis in the beneficial reuse of dredged material. Given the economic and environmental impacts from LCA, each application that appearing promising and sustainable will be further discussed with relevant industry professions to facilitate upscaling of the application, in order to promote the sustainable and environmentally responsible utilization of dredged materials.

A comprehensive life cycle flow chart was constructed, as shown in *Figure 71*. Although the economic analysis has not be fully updated, three issues are immediately clear. Firstly, the transportation cost would be a big concern when reducing accumulations of dredged material by making it possible to either the non-structural filler sites or the cementitious material firms. Secondly, how to process the dredged material efficiently for the entire dredged material deposition site

seems very challenging, as there exists tremendous volume of material. Thirdly, what process could we take for the dewatering of the dredged material, so that it could be done more economically.

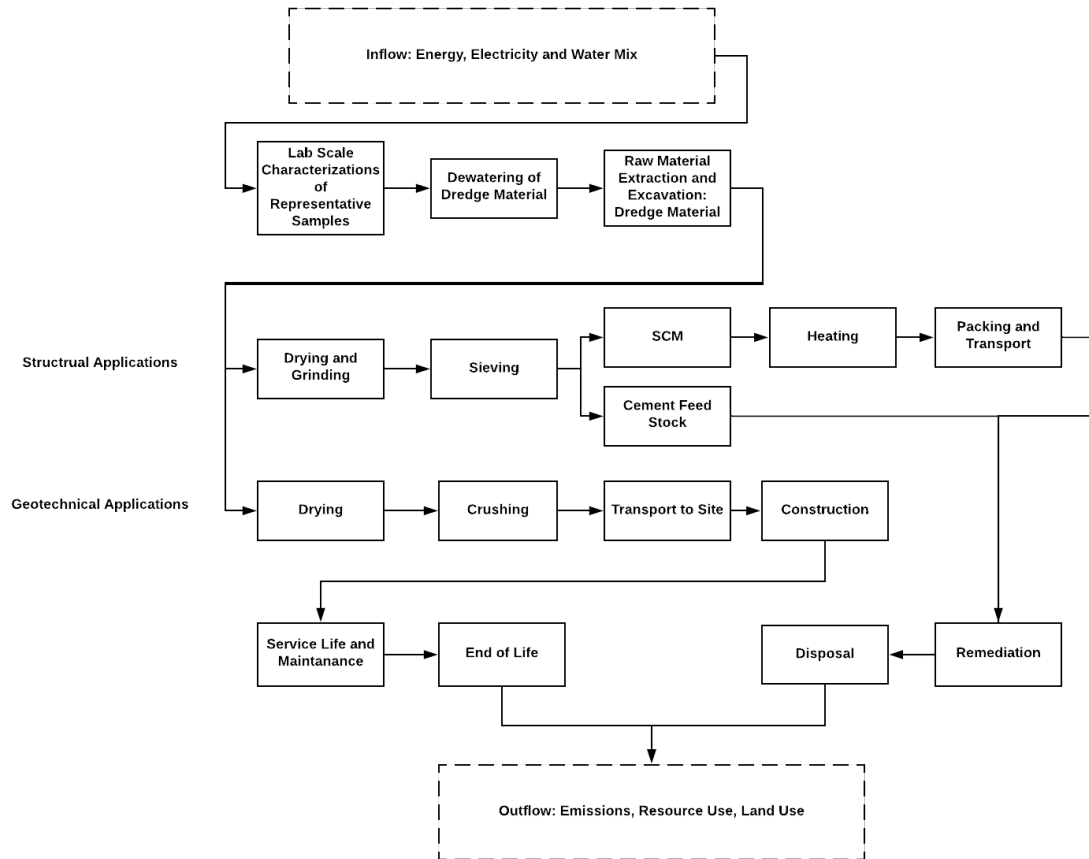


**FIGURE 71. ILLUSTRATION. COMPREHENSIVE LIFE CYCLE FLOW CHART FOR SEDIMENT APPLICATIONS.**

## **Beneficial Use Decision Making Process**

To outline the process for determining suitable reuse options for sediment, a technical decision tree was constructed for geotechnical and structural applications (Figure 72). Cementitious materials tend to be ideal for binding heavy metals, either due to oxidation during the heat treatment process or after hydration. As such, any sediment with an unacceptable quantity of heavy metal contamination should be processed into an application related to cementitious materials. Soils containing larger quantities of coarsely grained materials tend to be stronger and therefore more useful for fill applications.

Further detail into deciding the sediment applications can be seen in Figure 72. While producing sediments into LECA can oxidize some degree of heavy metal contaminants, there may still be a chance of leaching if used in geotechnical applications. As such, LECA produced with heavy metal contaminated sediments should only be used in concrete mixes, as cement hydration is an effective method for binding such contaminants. This technical decision tree was created with the purpose of categorizing the sediments into areas of best potential performance. It does not account for economic or environmental benefits but may be adjusted in the future to account for those effects.

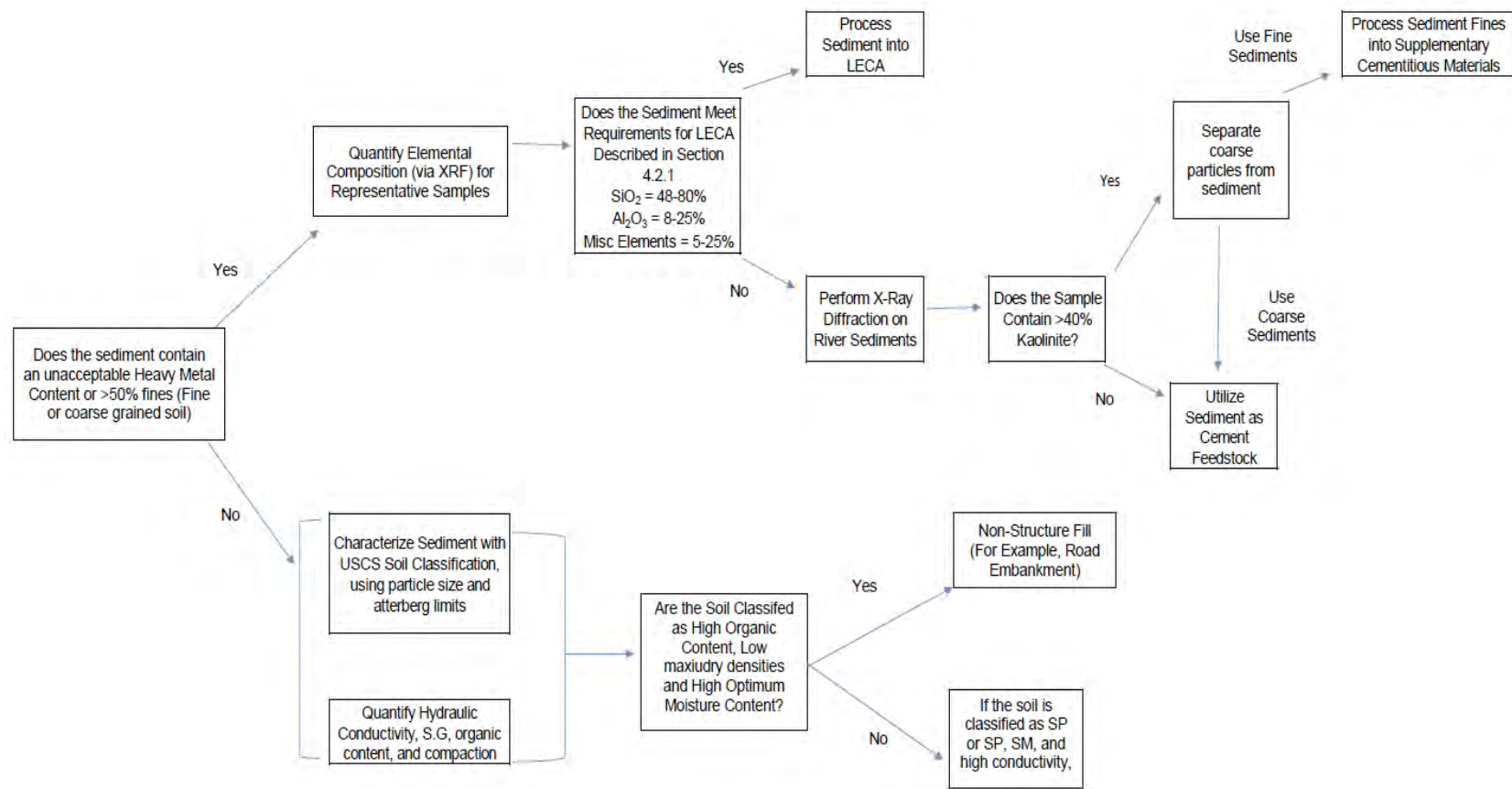


**FIGURE 72. ILLUSTRATION. TECHNICAL DECISION TREE FOR SEDIMENT APPLICATION**

## FUTURE WORK

While the lightweight expanded clay aggregates created meet requirements for density, not enough samples were created in order to test bulk density or compressive strength. It is suggested that further research be conducted utilizing a pelletizer and rotary kiln to produce LECA at a larger scale. In this way, LECA can be used to produce lightweight concrete and can be tested for compressive strength. LECA created from Savannah River sediments can then be compared to ASTM C33 for structural lightweight aggregates.

While the heat-treated river sediments successfully passed standards listed for ASTM C618 for class N pozzolans, they do not perform as well as they could have. In particular, these materials were coarse enough that they do not provide any particle packing or nucleation effect benefits. Further investigations could be made on the effects of grinding these materials. It would be particularly useful to grind the sediments to particle size ranges close to that of commercially available metakaolin (1-10  $\mu\text{m}$ ) in order to investigate how they compare.

Investigations into the utilization of river sediments as cement feedstock confirms that it is possible to do so. Additionally, contaminants of heavy metals and chlorides do not significantly affect the final product as these elements are either entrapped in the cement or oxidized. Experimental work into actually producing these materials into portland cements were not conducted due to a lack of access to a rotary kiln for the majority of this period. Further investigations into

the viability of cement produced from river sediments should be conducted. These cements can then be compared to ASTM C150 in order to determine which type of cement they are.

## **CONCLUSIONS**

The beneficial use of dredge material in large geotechnical applications, structural fill and non-structural fill is among one of the most environmentally sound and technically feasible options. Our study discovered that all eight dredged sediments sampled could be utilized as fill materials, with sediments classified as CH and SC applied to non-structural fill and sediments classified as SP and SP-SM applied to structural fill, diverting dredge from disposal for higher-level use. Future geotechnical research can also investigate the potential of combining the dredge sediments (CH) with other materials to form a useful and usable composite material, for example, landfill liner material.

Only one sediment was tested for use as a fine aggregate as it contained a large quantity of coarse soil. While this sediment passed requirements for the alkali aggregate reaction (ASTM C1260) it ultimately did not pass requirements for use as a fine aggregate in concrete mixes due to an excessive quantity of organics. This is an issue that was present in all samples, and most samples contained an unacceptable quantity of fines. As such, sediments could only be used as a fine

aggregate with a large degree of beneficiation or screening. Therefore, using the sediments as a fine aggregate source is impractical.

It was discovered that sediments could be processed into lightweight aggregates so long as the sediment contains a sufficient clay content (>20% was successful in this case). Additionally, sediments can be processed into lightweight expanded clay aggregates (characterized by the presence of an expanded porous core) so long as they possess an elemental composition of 48-80% SiO<sub>2</sub>, 8-25% Al<sub>2</sub>O<sub>3</sub>, and 5-25% miscellaneous elements. An ideal heat treatment process was determined based on the presence/absence of the expanded core. Both LWA and LECA were successfully produced and possessed an S.G of ~1, which meets density requirements for lightweight aggregates. Further investigations are needed in order to determine if these produced LWA meet strength requirements for structural lightweight concrete.

All (5) sediments tested were successfully processed into SCMs with the exception of one sample which failed fineness requirements. An ideal calcination process was determined using the strength activity index, in which heat treatment in a rotary kiln at 800 °C for 3 hours was determined to be the most ideal. These sediments performed well in terms of the strength activity index (85-95%) and in the mitigation of the alkali aggregate reaction. Through these tests, as well as with traditional pozzolanic reactivity tests (TGA/Isothermal Calorimetry), it was determined that the performance of such SCM is primarily dependent on the kaolinite content of the overall material sediment. Through this it was determined

that a kaolinite content of >40% is generally necessary for a decent quality natural pozzolan.

The relatively new R<sup>3</sup> test method was investigated to determine a material's pozzolanic reactivity. Sediments tested with isothermal calorimetry report similar relative levels of reactivity as traditional methods to measure pozzolanic reactivity (TGA/Isothermal Calorimetry). Bound water and calcium hydroxide consumption tests tended to overestimate the reactivity of tested sediments, likely due to the abundance of calcium hydroxide present. The R<sup>3</sup> test method may be a useful test for comparing different SCMs but should not be used as a replacement for traditional tests.

Through a literature review it was determined that any sediments can be used as a cement feedstock so long as the overall feedstock composition is adjusted to account for different mineralogical compositions. These cement feedstocks are capable of containing 20-30% sediments. The resulting cements should be capable of oxidizing or binding heavy metal or chloride contaminants. Further work should be done to actually produce such cements and measure their resulting performance.

In this study, LCA investigates the environmental burdens of a range of potential new approaches for the beneficial use of dredged sediments and also enables comparisons between the different options. The LCA results underline the potential impacts of the different options in terms of the amount of energy and resources required. The results indicate that beneficial uses as non-structural fill

and supplementary cementitious materials can be considered as promising alternative solutions.

A comprehensive decision-making process was developed with the purpose of determining which sediments should be used in specific applications. Utilizing this decision tree should allow for the complete use of all sediments stored in the Savannah River's confined disposal areas. This will allow for potential profitability when using the currently stored sediments and with sediments dredged in the future.

## APPENDIX A.

Certain graphs and figures were not included in the main text body for a variety of reasons. This section will report such figures and why they were not included in the main body of the report.

The first graph can be seen in Figure 73, which reports TGA of raw sediment samples. This analysis was conducted prior to the x-ray diffraction scans seen in section 5.3. Using TGA would allow for certain elements to be easily identified. This figure was not included in the main body of text as the same results were reported in the x-ray diffraction analysis.

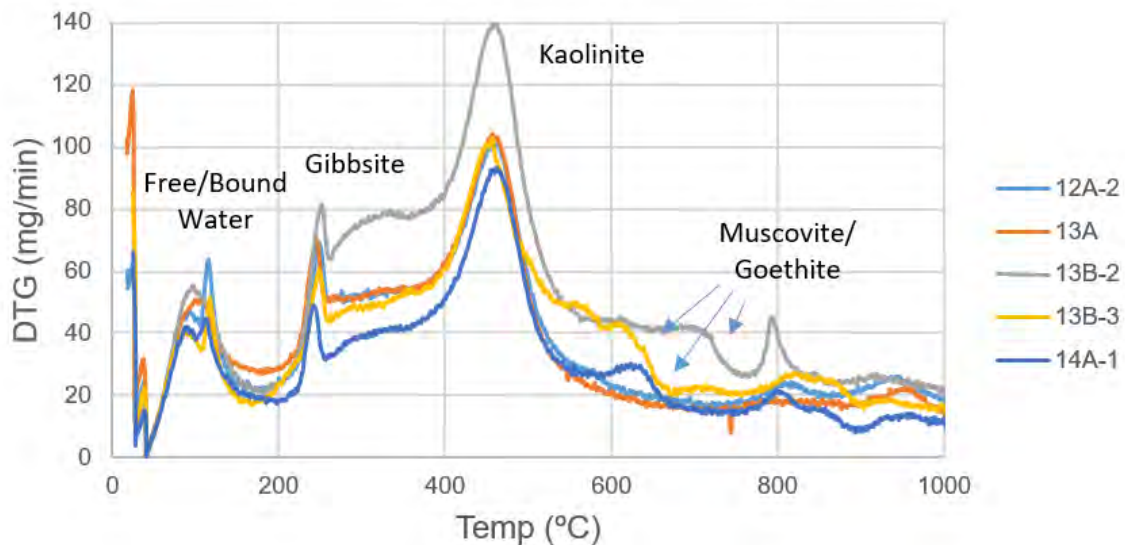


**FIGURE 73. GRAPH. RAW SEDIMENT TGA ANALYSIS.**

The raw data for the x-ray diffraction scans in section 5.3 were also not included in the main body of text. Scans for the raw samples can be seen in Figure

74 to Figure 78 and the scans for the calcined samples can be seen in Figure 79 to Figure 83. These scans were not included, as the number of figures required would interrupt the flow of the document.

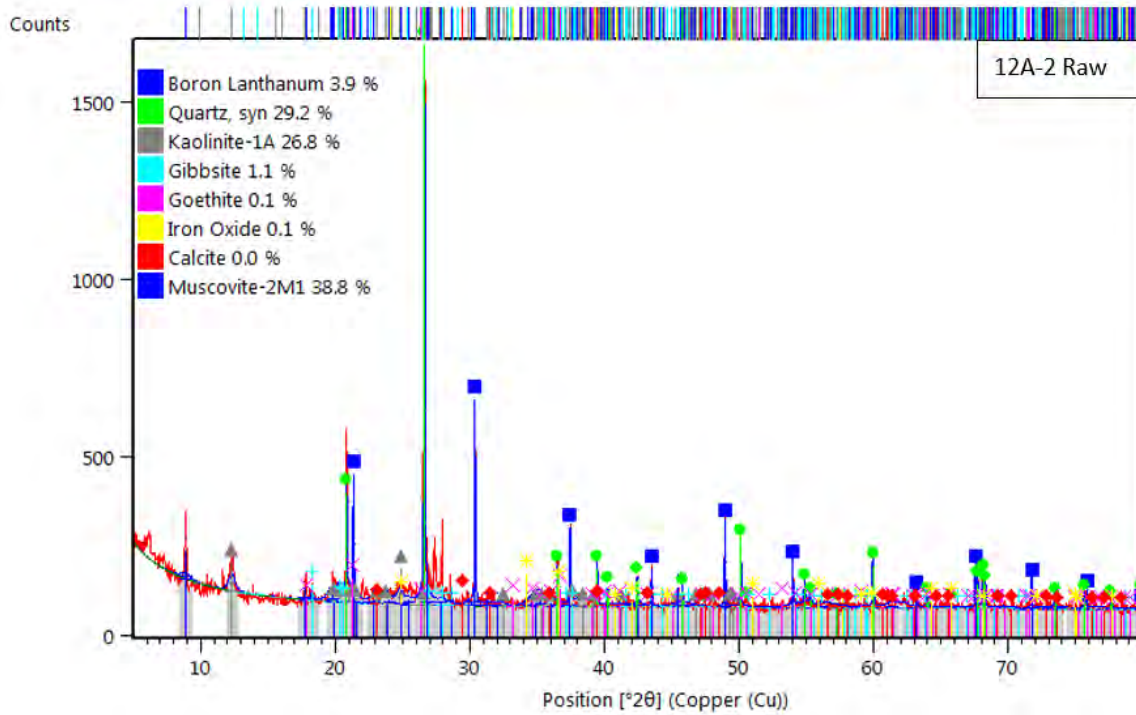


**FIGURE 74. GRAPH. RAW XRD SCANS FOR SAMPLE 12A-2 RAW.**

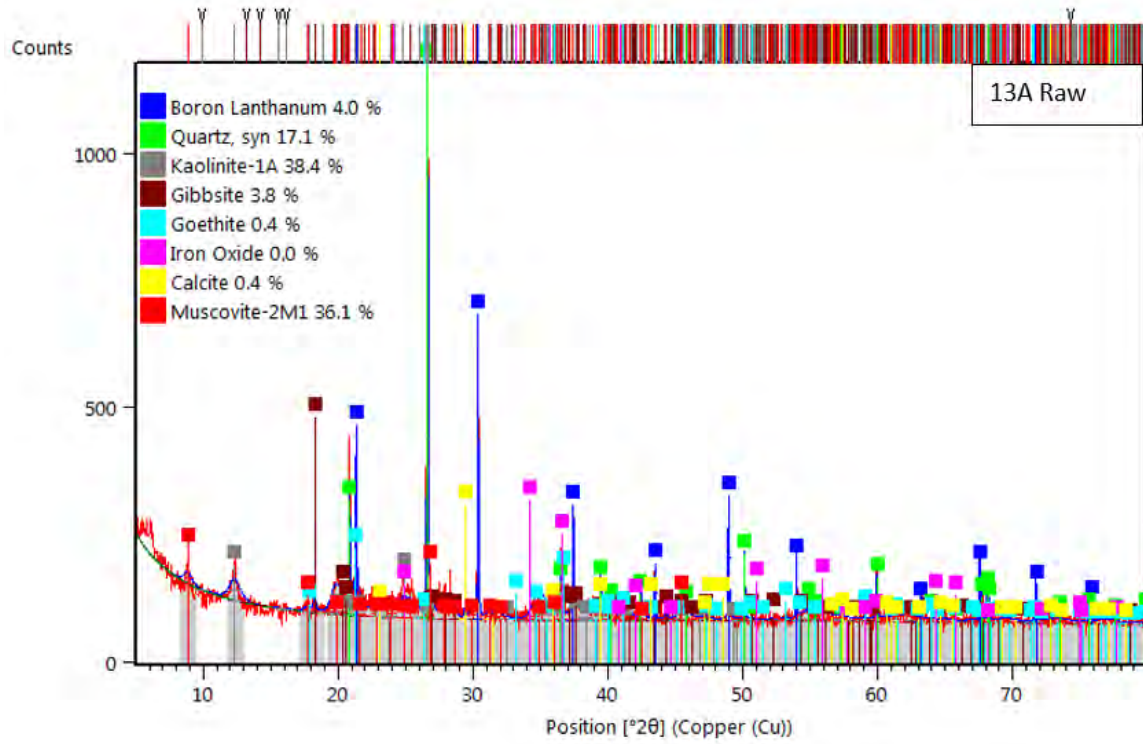


**FIGURE 75. GRAPH. RAW XRD SCAN FOR SAMPLE 13A RAW.**

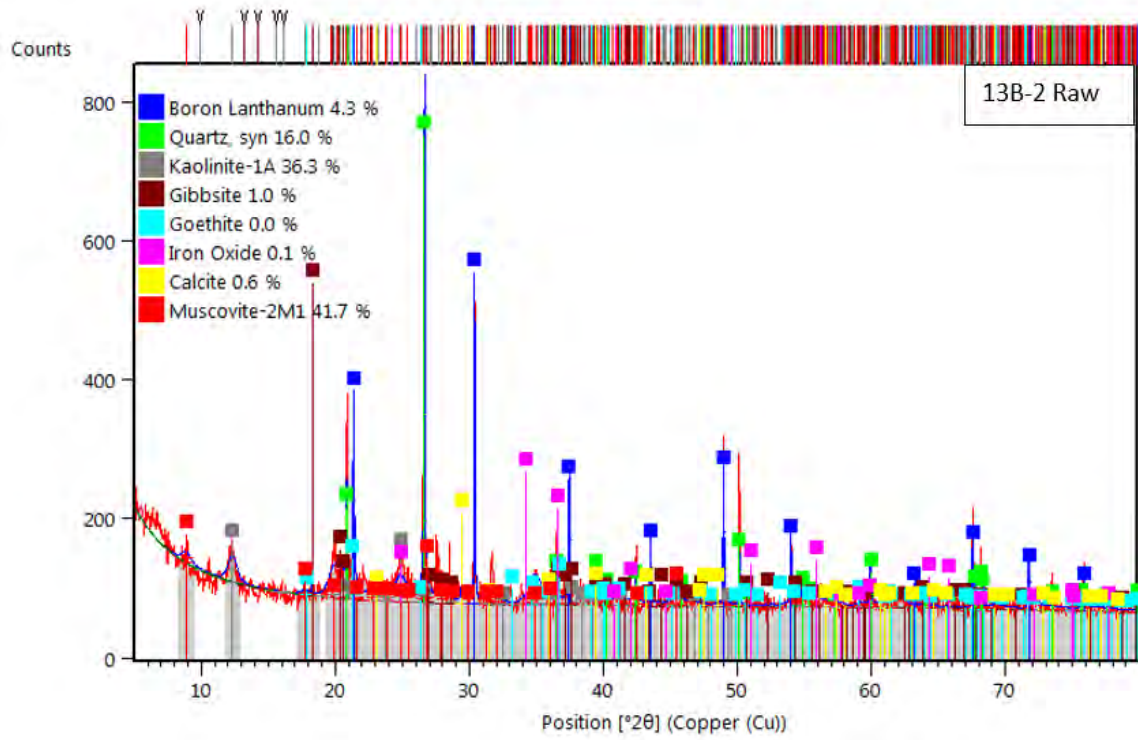


**FIGURE 76. GRAPH. RAW XRD SCAN FOR SAMPLE 13B-2 RAW.**

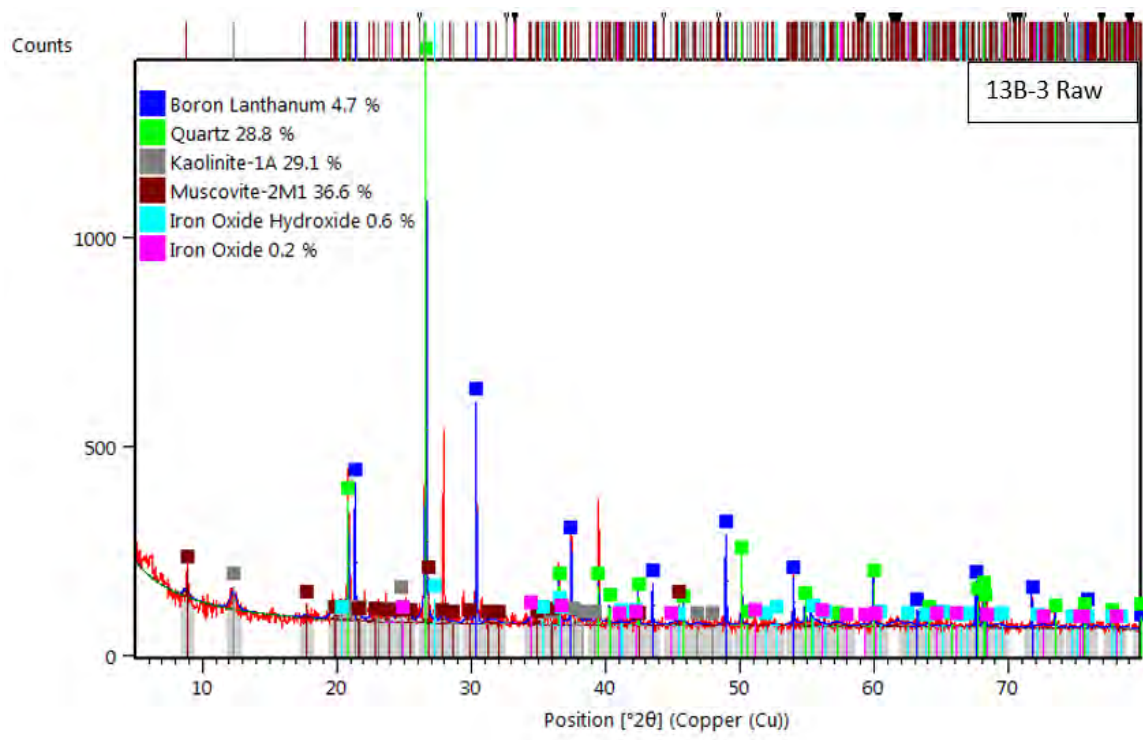


**FIGURE 77. GRAPH. RAW XRD SCAN FOR SAMPLE 13B-3 RAW.**

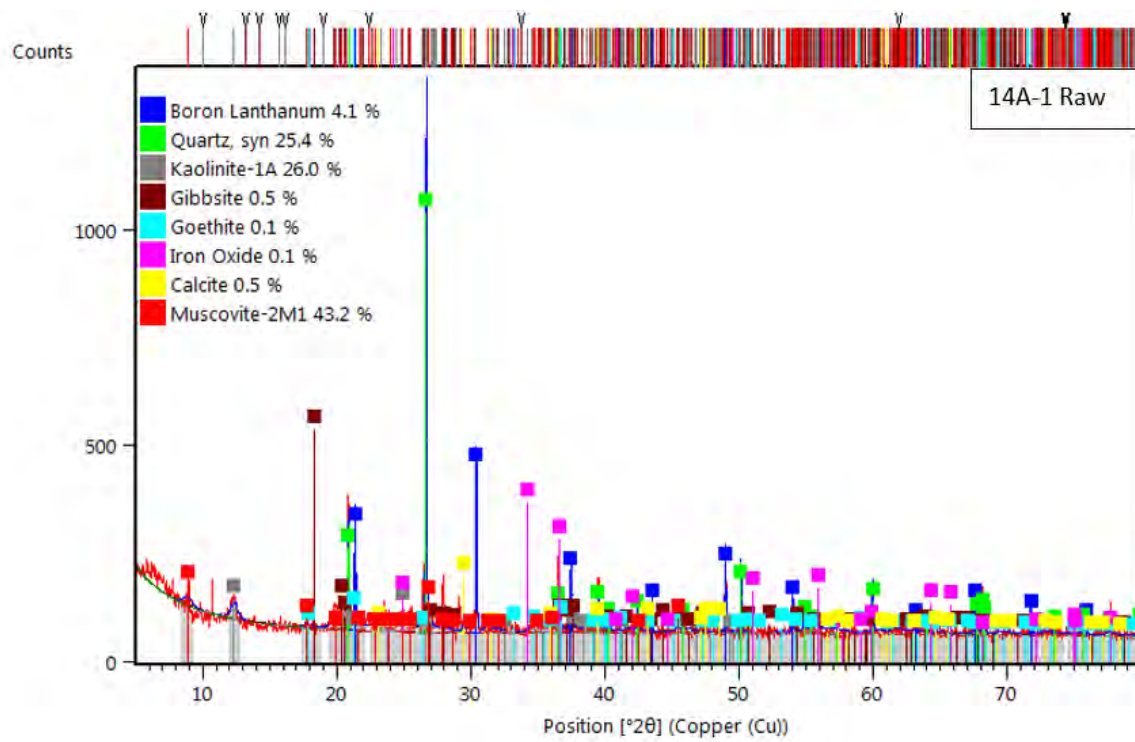


**FIGURE 78. GRAPH. RAW XRD SCAN FOR SAMPLE 14A-1 RAW.**

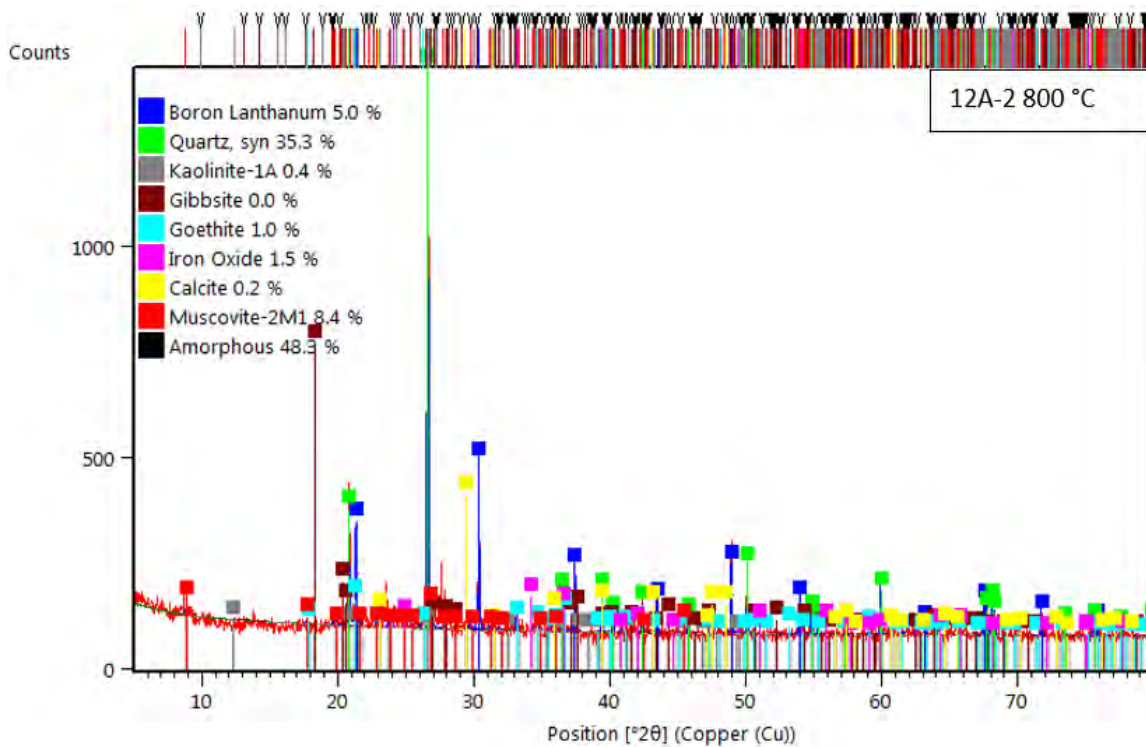


**FIGURE 79. GRAPH. RAW XRD SCAN FOR SAMPLE 12A-2 800 °C.**

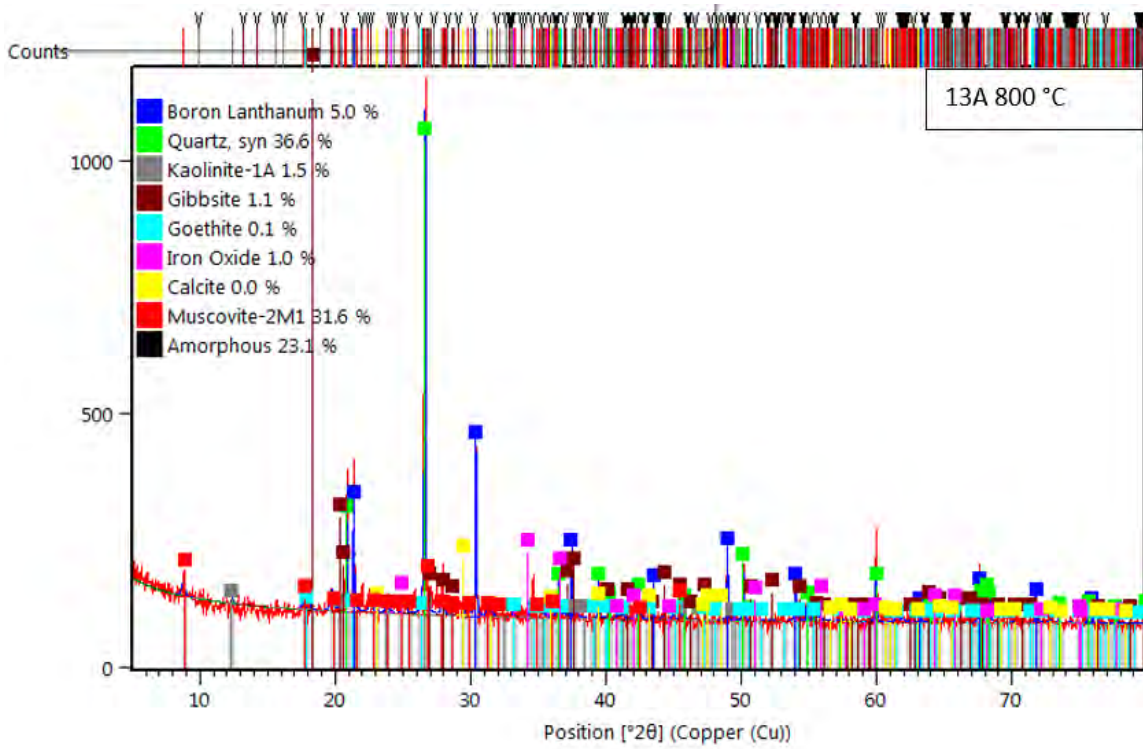


**FIGURE 80. GRAPH. RAW XRD SCAN FOR SAMPLE 13A 800 °C**

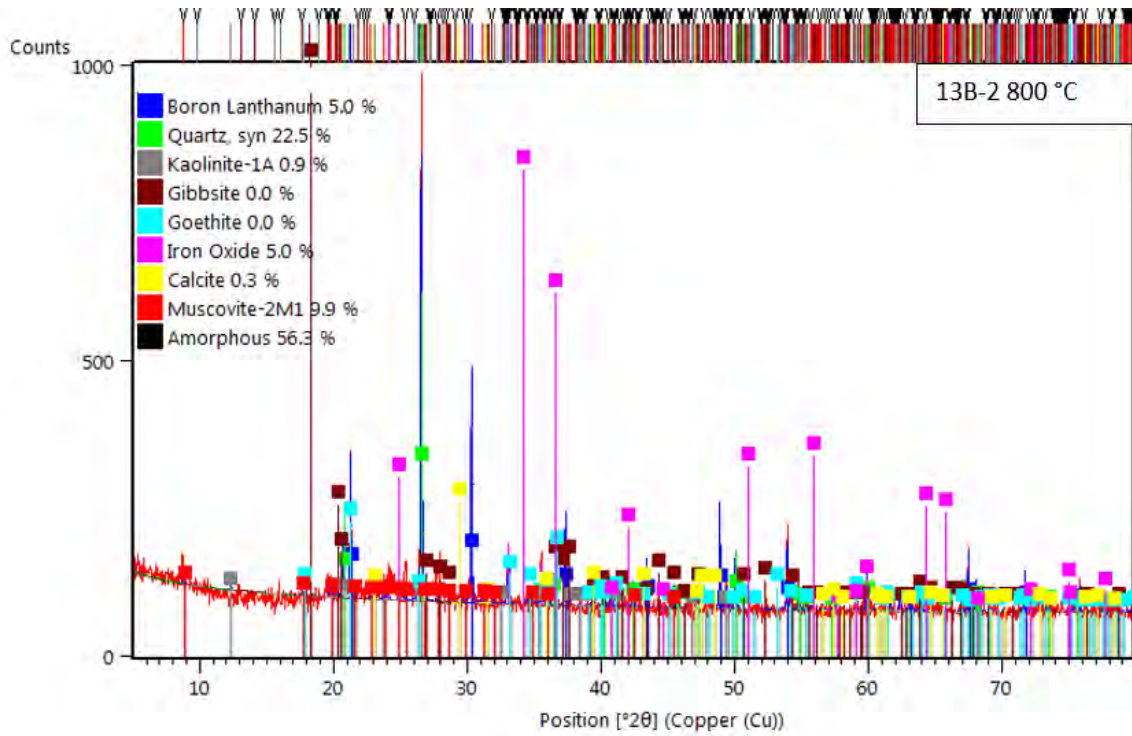
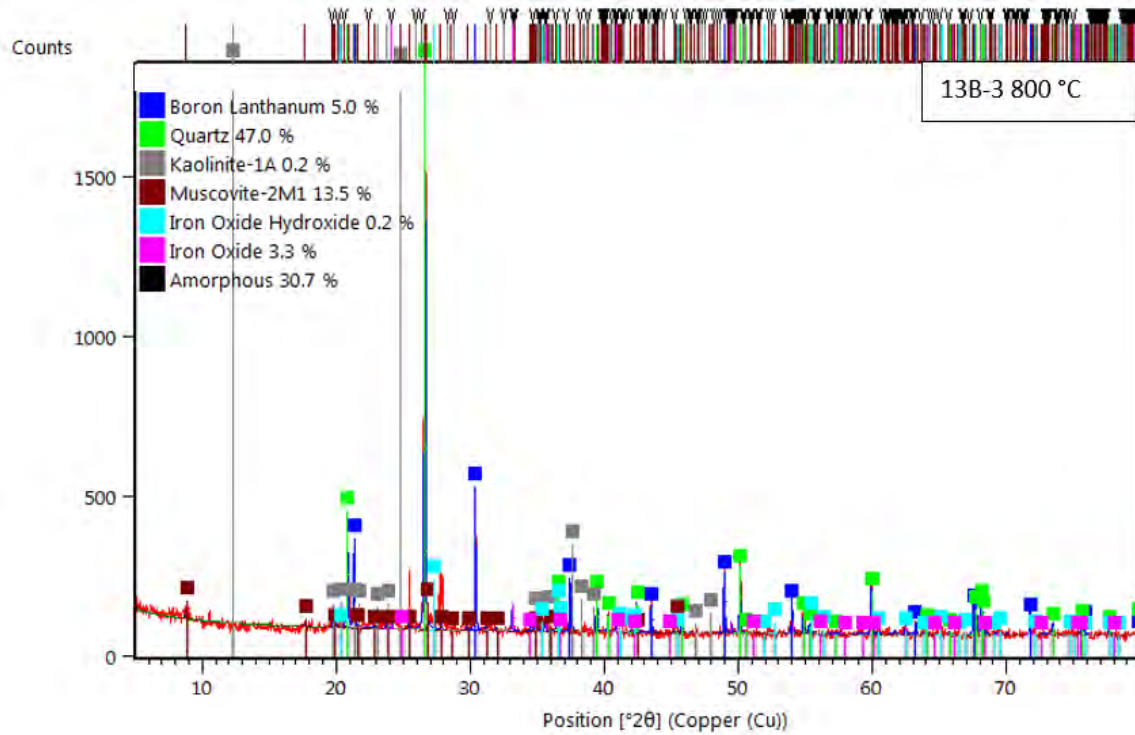
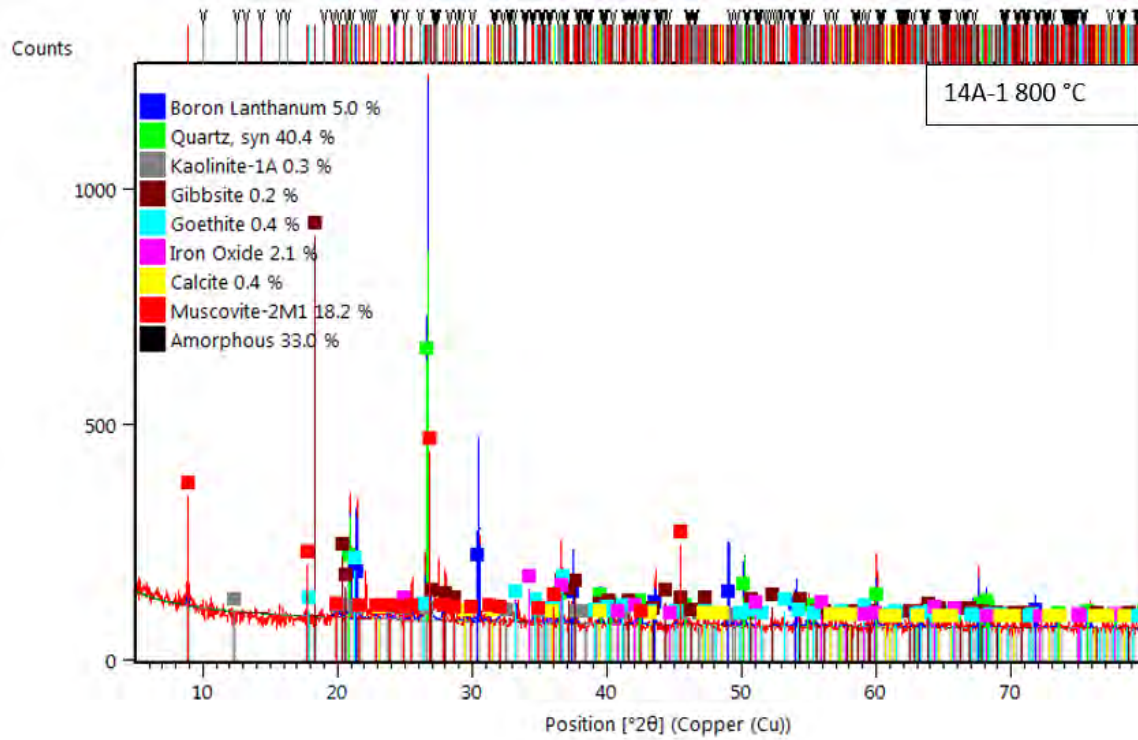


FIGURE 81. GRAPH. RAW XRD SCAN FOR SAMPLE 13B-2 800 °C.



**FIGURE 82. GRAPH. RAW XRD SCAN FOR SAMPLE 13B-3 800 °C.**



**FIGURE 83. GRAPH. RAW XRD SCAN FOR SAMPLE 14A-1 800 °C.**

## **ACKNOWLEDGEMENTS**

The research team is grateful for GDOT personnel that provided valuable assistance during the course of this study: Mr. Trey Daniell, Waterways Program Manager; Mr. Brennan A. Roney, Research Engineer; Mr. Binh Bui, Research Implementation Manager; Ms. Supriya Kamatkar, Assistant Office Head; and Mr. Gary Wood, Technical Services Manager.

The opinions and conclusions expressed herein are those of the authors and do not represent the opinions, conclusions, policies, standards, or specifications of GDOT or of other cooperating organizations.

The authors would like to thank the following graduate and undergraduate students for assistance in advising and collecting data in this research: Mr. William Cole Spencer, Miss Clara Bouret, Miss Heyinn Rho, and Miss Kimberly Hernandez.

The authors express their gratitude to all contributors for their assistance during the completion of this research project.

## REFERENCES

- A, P., & De Rose, J. (2018). Application of Light Expanded Clay Aggregate as Replacement of Coarse Aggregate in Concrete Pavement. *International Journal of Engineering and Technology*, 1-4.
- Alizadeh, R., & Beaudoin, J. (2009). Nanostructure and Engineering Propertis of basic and modified Calcium-Silicate-Hydrate Systems. *University of Ottawa (PhD Thesis)*, 1-251.
- Anger, B., Moulin, I., Commence, J.-P., They, F., & Levacher, D. (2019). Fine-grained reservoir sediments: an intersejing alternative raw material for portland cement clinker production. *European Journal of Environmental and Civil Engineering*, 957-970.
- Aouad, G., Laboudigue, A., Gineys, N., & Abriak, N. (2012). Dredged sediments used as novel supply of raw material to produce Portland cement clinker. *Cement and Concrete Composites*, 788-793.
- Arulrajah, A., Maghoolpilehrood, F., Disfani, M., & Horpibulsuk, S. (2014). Spent coffee grounds as a non-structural embankment fill material: engineering and environmental considerations. *Journal of cleaner production*, 181-186.
- Avet, F., Snellings, R., Diaz, A., Haha, M., & Scrivener, K. (2016). Development of a new rapid, relevant and reliable (R3) test method to evaluate the pozzolanic reactivity of calcined kaolinitic clays. *Cement and Concrete Research*, 1-11.
- Baxter, C., King, J., Silva, A., Page, M., & Calabretta, V. (2005). Site Characterization of dredged sediments and evaluation of beneficial uses. *Recycled Materials in Geotechnics*, 150-161.
- Bernal, S. (2017). Characterization of supplementary cementitious materials by thermal analysis. *Materials and Structures*, 1-13.
- Berodier, E., & Scrivener, K. (2014). Understanding the Filler Effect on the Nucleation and Growth of C-S-H. *The American Ceramic Society*, 3764-3773.
- Bogas, J. A., Gomes, A., & Pereira, M. (2012). Self-compacting lightweight concrete produced with expanded clay aggregate. *Construction and Building Materials*, 1013-1022.
- Boughton, B. (2007). Evaluation of shredder residue as cement manufacturing feedstock. *Resources, Conservation and Recycling*, 621-642.
- Bunderen, C., Snellings, R., Horckmans, L., Dockx, J., Vandekeybus, J., Vandewalle, L., & Cizer, O. (2018). Concrete with Flash-Calcined Dredging Sediments as a Novel Supplementary Cementitious Material. *Springer International Publishing*, 109-116.

- C109, A. (2020). Standard Test Method for Compressive Strength of Hydraulic Cement Mortars (Using 2-in. or [50-mm] Cube Specimens). *American Society for Testing and Materials*, DOI: 10.1520/C0109\_C0109M-20A.
- C1260, A. (2014). Standard Test Method for Potential Alkali Reactivity of Aggregates (Mortar-Bar Method). *American Society for Testing and Materials*, DOI: 10.1520/C1260-14.
- C136, A. (2020). Standard Test Method for Sieve Analysis of Fine and Coarse Aggregates. *American Society for Testing and Materials*, DOI:10.1520/C0136\_C0136M-19.
- C142, A. (2017). Standard Test method for Clay Lumps and Friable Particles in Aggregates. *American Society for Testing and Materials*, DOI: 10.1520/C0142\_C0142M-17.
- C150, A. (2020). Standard Specification for Portland Cement. *American Society of Testing and Materials*, 1-9.
- C1567, A. (2013). Standard Test Method for Determining the Potential Alkali-Silica Reactivity of Combinations of Cementitious Materials and Aggregate (Accelerated Mortar-Bar Method). *American Society of Testing and Materials*, DOI: 10.1520/C1567-13.
- C1679, A. (2017). Standard Practice for Measuring Hydration Kinetics of Hydraulic Cementitious Mixtures Using Isothermal Calorimetry. *American Society of Testing and Materials*, DOI: 10.1520/C1679-17.
- C1778, A. (2020). Standard Guide for Reducing the Risk of Deleterious Alkali-Aggregate Reaction in Concrete. *American Society of Testing and Materials*, DOI: 10.1520/C1778-19B.
- C33, A. (2018). Standard Specification for Concrete Aggregates. *American Society for Testing and Materials*, DOI: 10.1520/C0033\_C0033M-18.
- C330, A. (2017). Standard Specification for Lightweight Aggregates for Structural Concrete. *American Society for Testing and Materials*, DOI: 10.1520/C0330\_C0330M-17A.
- C40, A. (2020). Standard Test Method for Organic Impurities in Fine Aggregates for Concrete. *American Society for Testing and Materials*, DOI: 10.1520/C0040\_C0040M-20.
- C618, A. (2019). Standard Specification for Coal Fly Ash and Raw or Calcined Natural Pozzolan for Use in Concrete. *American Society for Testing and Materials*, DOI: 10.1520/C0618-19.
- Carpio, R., Junior, F., Coelho, L., & Silva, R. (2008). Alternative Fuels Mixture in Cement Industry Kilns Employing Particle Swarm Optimization Algorithm. *Journal of the Brazilian Society of Mechanical Sciences and Engineering*, 335-340.
- Dalton, J., Gardner, K., Seager, T., Weime, M., Spear, J., & Magee, B. (2004). Properties of Portland Cement made from contaminated sediments. *Resources, Conservation and Recycling*, 227-241.
- Dauji, S. (2017). Disposal of Sediments for Sustainability: A Review. *International Journal of Economy, Energy and Environment*, 96-103.

- Dullien, F. (1992). *Porous Media: Fluid Transport and Pore Structure (2nd Edition)*. Waterloo, Canada: Academic Press.
- E1131, A. (2014). Standard Test Method for Compositional Analysis by Thermogravimetry. *American Society of Testing and Materials*, DOI: 10.1520/E1131-08R14.
- Engineers, U. A. (2012). Final General Re-Evaluation Report & Environmental Impact Statement for the Savannah Harbor Expansion Project (SHEP): Chatham County, Georgia, and Jasper County, South Carolina.
- Fernandez, R., Martirena, F., & Scrivener, K. (2011). The origin of pozzolanic activity of calcined clay minerals: A comparison between kaolinite, illite, and montmorillonite. *Cement and Concrete Research*, 113-122.
- Frias, M., de Rojas, S., & Cabrera, J. (2000). The effect that the pozzolanic reaction of metakaolin has on the heat evolution in metakaolin-cement mortars. *Cement and Concrete Research*, 209-216.
- Grim, R., & Bradley, W. (1948). Rehydration and Dehydration of the Clay Minerals. *American Mineralogist*, 50-59.
- Hamouche, F., & Zentar, R. (2020). Effects of Organic Matter on Mechanical Properties of Dredged Sediments for Beneficial Use in Road Construction. *Environmental Technology*, 296-308.
- He, C., Bjarne, O., & Makovicky, E. (1995). Pozzolanic Reactions of Six Principal Clay Minerals: Activation, Reactivity Assessments and Technological Effects. *Cement and Concrete Research*, 1691-1702.
- He, C., Makovicky, E., & Osbaeck, B. (1995). Thermal stability and pozzolanic activity of calcined illite. *Applied Clay Science*, 337-354.
- Hollanders, S., Adriaens, R., Skibsted, J., Cizer, O., & Elsen, J. (2016). Pozzolanic reactivity of pure calcined clays. *Applied Clay Science*, 552-560.
- Hollanders, S., Adriaens, R., Skibsted, J., Cizer, O., & Elsen, J. (2016). Pozzolanic Reactivity of pure calcined clays. *Applied Clay Science*, 552-560.
- Holm, T., & Valsangkar, A. (1993). Lightweight Aggregate Soil Mechanics: Properties and Applications. *Transportation Research Record*, 7-14.
- Hu, J., Ge, Z., & Wang, K. (2014). Influence of cement fineness and water-to-cement ratio on mortar early-age heat of hydration and set times. *Construction and Building Materials*, 657-663.
- Hung, M.-F., & Hwang, C.-L. (2007). Study of fine sediments for making lightweight aggregate. *Waste Management and Research*, 449-456.
- Junakova, N., Junak, J., & Balintova, M. (2015). Reservoir sediment as a secondary raw material in concrete production. *Clean Technology and Environmental Policy*, 1161-1169.

- Li, X., Snellings, R., Antoni, M., Alderete, N., Haha, M., Bishnoi, S., . . . Cyr, M. (n.d.). Reactivity Tests for Supplementary Cementitious Materials: RILEM RC 267-TRM phase 1.
- Madloul, N., Saidur, R., Rahim, N., & Kamalisarvestani, M. (2013). An overview of energy savings measurements for cement industries. *Renewable and Sustainable Energy Reviews*, 18-29.
- Malkawi, A., Alawneh, A., & Abu-Safaqah, O. (1999). Effects of Organic Matter on the Physical and the Physicochemical Properties of an Illitic Soil. *Applied Clay Science*, 257-278.
- Marsters, J., & Christian, H. (1990). Hydraulic Conductivity of Diatomaceous Sediment from the Peru Continental Margin Obtained during ODP Leg 112. In *Suess, E., von Huene, R., et al. Proc. ODP, Init. Repts*, 633-638.
- Mehta, P. (1987). *Natural Pozzolans: Supplementary cementing materials*. Athens, Greece: Proc., Int. Symp. on Advances in Concrete Technology.
- Mezencevova, A., Yeboah, N., Burns, S., & Kahn, L. &. (2012). Utilization of Savannah Harbor River Sediment as the Primary Raw Material in Production of Fired Brick. *Journal of Environmental Management*, 128-136.
- Oss, H., & Padovani, A. (2002). Cement Manufacture and The Environment. *Journal of Industrial Ecology*, 89-105.
- Oss, H., & Padovani, A. (2003). Cement Manufacture and the Environment: Part II: Environmental Challenges and Opportunities. *Journal of Industrial Ecology*, 93-126.
- Patel-Predd, P. (2007). Dredged sediments in cement. *Environmental Science and Technology*, 3795.
- Rashad, A. (2018). Lightweight expanded clay aggregate as a building material overview. *Construction and Building Materials*, 757-775.
- Riley, C. (1950). Relation of Chemical Properties to the Bloating of Clays. *Journal of The American Ceramic Society*, 121-128.
- Rivera, O., Pavez, O., Kao, J., & Nazer, A. (2016). Metallurgical Characterization of kaolin from Atacama, Chile. *International Engineering Journal: Metallurgy and Materials*, 473-478.
- Sarfo-Ansah, J., Atiemo, E., Boakye, K., Adjei, D., & Adjaottor, A. (2014). Calcined Clay Pozzolan as an Admixture to Mitigate the Alkali-Silica Reaction in Concrete. *Journal of Materials Science and Chemical Engineering*, 20-26.
- Sierra, E., Miller, S., Sakulich, A., MacKenzie, K., & Barsoum, M. (2010). Pozzolan Activity of Diatomaceous Earth. *The American Ceramic Society*, 3406-3410.
- Snellings, R., Cizer, O., Horckmans, L., Pawel, D., Dierckx, P., Nielson, P., . . . Vandewalle, L. (2016). Properties and pozzolanic reactivity of flash calcined dredging sediments. *Applied Clay Science*, 35-39.

- Snellings, R., Horckmans, L., Bunderen, C., Vandewalle, L., & Cizer, O. (2017). Flash-Calcined dredging sediment blended cements: effect on cement hydration and properties. *Materials and Structures*, 1-12.
- Sperinck, S., Raiteri, P., Marks, N., & Wright, K. (2010). Dehydroxylation of kaolinite to metakaolin - a molecular dynamics study. *Journal of Materials Chemistry*, 2118-2125.
- Taylor-Lange, S., Lamon, E., Riding, K., & Juinger, M. (2015). Calcined kaolinite-bentoniteclay blends as supplementary cementitious materials. *Applied Clay Science*, 84-93.
- USACE, U. A. (2012). Savannah Harbor Expansion Project: Dredged Material Management Plan Updated.
- Uson, A., Lopez-Sabiron, A., Ferreira, G., & Sastresa, E. (2013). Uses of alternative fuels and raw materials in the cement industry as sustainable waste management options. *Renewable and Sustainable Energy Reviews*, 242-260.
- Van Oss, H. G., & Padovani, A. (2002). Cement Manufacture and the Environment: Part I: Chemistry and Technology. *Journal of Industrial Ecology*, 89-105.
- Van Oss, H., & Padovani, A. (2003). Cement Manufacture and the Environment: Part II: Environmental Challenges and Opportunities. *Journal of Industrial Ecology*, 93-126.
- Vijayalakshmi, R., & Ramanagopal, S. (2018). Structural Concrete using Expanded Clay Aggregate: A Review. *Indian Journal of Science and Technology*, 1-12.
- Wei, Y.-L., Yang, j.-C., lin, Y.-Y., Chuang, S.-Y., & Wang, H. P. (2008). Recycling of harbor sediment as lightweight aggregate. *Marine Pollution Bulletin*, 867-872.
- Yeboah, N., Mezencevova, A., Phillips, J., Burns, S., & Kurtis, K. (2011). Investigating the potential for producing fired bricks from Savannah Harbor Dredged Sediment. *In Geo-Frontiers 2011: Advances in Geotechnical Engineering*, 1245-1254.
- Yu, H., Yin, J. S., Likos, W., & Edil, T. (2016). Engineering properties of dredged materials stabilized with fly ash. *In 4th International Conference on Sustainable Construction Materials and Technologies*.